National Library of Canada
Canadian Theses Service
Ottawa, Canada
K1A 0N4

Bibliothèque nationale du Canada
Services des thèses canadiennes

CANADIAN THESES

THÈSES CANADIENNES

NOTICE

The quality of this microfiche is heavily dependent upon the quality of the original thesis submitted for microfilming. Every effort has been made to ensure the highest quality of reproduction possible.

If pages are missing, contact the university which granted the degree.

Some pages may have indistinct print especially if the original pages were typed with a poor typewriter ribbon or if the university sent us an inferior photocopy.

Previously copyrighted materials (journal articles, published tests, etc.) are not filmed.

Reproduction in full or in part of this film is governed by the Canadian Copyright Act, R.S.C. 1970, c. C-30. Please read the authorization forms which accompany this thesis.

AVIS

La qualité de cette microfiche dépend grandement de la qualité de la thèse soumise au microfilmage. Nous avons tout fait pour assurer une qualité supérieure de reproduction.

S'il manque des pages, veuillez communiquer avec l'université qui a conféré le grade.

La qualité d'impression de certaines pages peut laisser à désirer, surtout si les pages originales ont été dactylographiées à l'aide d'un ruban usé ou si l'université nous a fait parvenir une photocopie de qualité inférieure.

Les documents qui font déjà l'objet d'un droit d'auteur (articles de revue, examens publiés, etc.) ne sont pas microfilmés.

La reproduction, même partielle, de ce microfilm est soumise à la Loi canadienne sur le droit d'auteur, SRC 1970, c. C-30. Veuillez prendre connaissance des formules d'autorisation qui accompagnent cette thèse.

THIS DISSERTATION HAS BEEN MICROFILMED EXACTLY AS RECEIVED

LA THÈSE A ÉTÉ MICROFILMÉE TELLE QUE NOUS L'AVONS REÇUE

NL 339 (r. 86/01)

Canada

National Library of Canada
Bibliothèque nationale du Canada

0-315-23373-7

179

Canadian Theses Division
Division des thèses canadiennes

Ottawa, Canada
K1A 0N4

PERMISSION TO MICROFILM — AUTORISATION DE MICROFILMER

• Please print or type — Écrire en lettres moulées ou dactylographier

Full Name of Author — Nom complet de l'auteur

Larry William Kostiuk

Date of Birth — Date de naissance

August 18, 1961

Country of Birth — Lieu de naissance

Canada

Permanent Address — Résidence fixe

P.O. Box 510
Pine Point, NWT
X0E 0W0

Title of Thesis — Titre de la thèse

Energy Flows in an Insulated Masonry Structure

University — Université

University of Alberta

Degree for which thesis was presented — Grade pour lequel cette thèse fut présentée

Master of Science

Year this degree conferred — Année d'obtention de ce grade

1985

Name of Supervisor — Nom du directeur de thèse

J. D. Dale

Permission is hereby granted to the NATIONAL LIBRARY OF CANADA to microfilm this thesis and to lend or sell copies of the film.

The author reserves other publication rights, and neither the thesis nor extensive extracts from it may be printed or otherwise reproduced without the author's written permission.

L'autorisation est, par la présente, accordée à la BIBLIOTHÈQUE NATIONALE DU CANADA de microfilmer cette thèse et de prêter ou de vendre des exemplaires du film.

L'auteur se réserve les autres droits de publication; ni la thèse ni de longs extraits de celle-ci ne doivent être imprimés ou autrement reproduits sans l'autorisation écrite de l'auteur.

Date

Sept 19, 1985

Signature

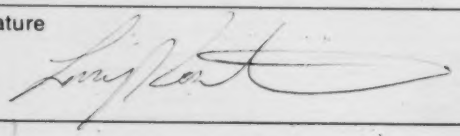

NL-91 (4/77)

THE UNIVERSITY OF ALBERTA

ENERGY FLOWS IN AN INSULATED MASONRY STRUCTURE

BY

© LARRY WILLIAM KOSTIUK

A THESIS

SUBMITTED TO THE FACULTY OF GRADUATE STUDIES AND RESEARCH IN PARTIAL FULFILMENT OF THE REQUIREMENTS FOR THE DEGREE OF MASTER OF SCIENCE

DEPARTMENT OF MECHANICAL ENGINEERING

EDMONTON, ALBERTA

FALL 1985

THE UNIVERSITY OF ALBERTA

RELEASE FORM

NAME OF AUTHOR: LARRY WILLIAM KOSTIUK

TITLE OF THESIS: ENERGY FLOWS IN AN INSULATED MASONRY STRUCTURE

DEGREE: MASTER OF SCIENCE

YEAR THIS DEGREE GRANTED: FALL 1985

Permission is hereby granted to THE UNIVERSITY OF ALBERTA LIBRARY to reproduce single copies of this thesis and to lend or sell such copies for private, scholarly, or scientific research purposes only.

The author reserves other publication rights, and neither the thesis nor extensive extracts from it may be printed or otherwise reproduced without the author's written permission.

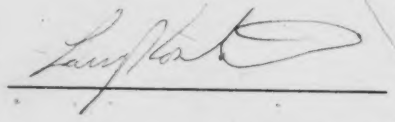

Permanent Address:

P.O. Box 510

Pine Point, NWT

X0E 0W0

DATED Sept. 19, 1985

THE UNIVERSITY OF ALBERTA

FACULTY OF GRADUATE STUDIES AND RESEARCH

The undersigned certify that they have read, and recommend to the Faculty of Graduate Studies and Research for acceptance, a thesis entitled ENERGY FLOWS IN AN INSULATED MASONRY STRUCTURE submitted by LARRY WILLIAM KOSTIUK in partial fulfilment of the requirements for the degree of MASTER OF SCIENCE.

J.D. Dale
(Supervisor)

Gerald W. Sodler

Marleigh

Date: Sept 19, 1985

ABSTRACT

A two year experimental and analytical study of the energy flows in a insulated masonry structure in a northern climate was undertaken. The experimental part of the study involved the testing of a single storey, uninhabited, electrically heated masonry module, 7400 x 6800 mm in plan, with full height double wythe walls and concrete basements. The insulation used in 90% of the wall area was polyurethane foam, the remaining 10% was insulated with vermiculite. For comparison, a convectional wood frame module of similar dimensions on the same site was also tested. During the first heating season the only difference between the two modules was their above grade walls. For the second heating season, two south facing windows were installed in the masonry module, and no modifications were made to the wood frame module.

During the first heating season the heat transmission losses of the masonry module were 81% of the wood frame module. The addition of the south facing windows increased the relative heat transmission losses of the masonry module 3%, to 84% of the wood frame module. The natural air infiltration rates of the masonry module were 60%, and 75%, of the wood frame module for the first and second heating seasons, respectively.

The thermal resistance of the walls and ceiling of the masonry module were measured, and were in good agreement

with resistances calculated using one dimensional steady state heat transfer theory. The measured thermal resistance of the walls indicated that the conductivity of the polyurethane is that of an unaged foam. There was no measurable aging of the polyurethane over the two years of this study.

The influence of the metal ties in the walls were modelled with the finite element method. Results for a simplified wall model showed that the wall's thermal resistance should be lowered by 10%. This result could not be confirmed experimentally.

The use of masonry was found to have a significant effect on the time lag of the heat transfer through the walls, but during cool down there was no energy recovery from the masonry back to the air in the module's interior.

ACKNOWLEDGEMENTS

The author wishes to express his sincere appreciation for the invaluable advice, guidance and supervision rendered by Dr. J.D. Dale and M.Y. Ackerman in the preparation of this thesis.

Financial support for this project was provided jointly by the Alberta Masonry Institute and the Alberta/Canada Energy Resource Research Fund (A/CERRF). A/CERRF is a joint program of the Federal and Alberta governments which is administered by Alberta Energy and Natural Resources. Materials for the construction of the masonry module were provided by I-XL Industries Ltd., and Consolidated Concrete Ltd., Masonry and Building Materials Division. The Support of the Alberta Masonry Institute, A/CERRF, and I-XL Industries Ltd. is gratefully acknowledged.

TABLE OF CONTENTS

CHAPTER		PAGE
1.	INTRODUCTION	1
	1.1 Construction Details of the Masonry Module	7
	1.2 Data Acquisition System	14
	1.2.1 Measurement Details of the Masonry Module	18
2.	LONG TERM THERMAL PERFORMANCE OF MASONRY MODULE	22
	2.1 Predicted Long Term Energy Loss	24
	2.1.1 ASHRAE Prediction	25
	2.1.2 Detailed Prediction for Masonry Walls	29
	2.2 Long Term Experimental Results	46
	2.2.1 Total and Relative Energy Consumption	46
	2.2.2 Measured Component Resistance	56
	2.2.3 Measured Air Infiltration	70
3.	SHORT TERM THERMAL BEHAVIOR OF MASONRY MODULE	77
	3.1 Steady Periodic Heat Transfer	77
	3.2 Short Term Experimental Results	82
	3.2.1 Response of Masonry Walls	82
	3.2.2 Short Term Effect of South Facing Windows	93
	3.2.3 Temperature Decay Test	97
4.	CONCLUSIONS	108

REFERENCES 113
APPENDIX A Construction Details of Reference Module 115

APPENDIX B Environmental and Module Measurements 117

APPENDIX C ASHRAE Prediction 124

APPENDIX D Finite Element Model of Simplified Wall Section 136

APPENDIX E Steady Periodic Heat Conduction through a Composite Slab 160

LIST OF TABLES

		PAGE
1.1	Nominal Insulating Values for Modules	5
1.2	Construction Details for the Modules	6
1.3A	Specifications - Module 1 - Masonry Module (SI units)	15
1.3B	Specifications - Module 1 - Masonry Module (English units)	16
2.1	Summary of ASHRAE Predicted Overall Transmission Coefficients (not including air infiltration)	27
2.2	ASHRAE Predicted Percent Contribution of Heating Load (not including air infiltration)	30
2.3	Predicted Heat Transfer Through Simplified Wall Section With and Without Metal Tie	43
2.4	Predicted Overall Transmission Coefficients for Modules 1 and 5 (not including air infiltration)	45
2.5	Comparison of Measured and Predicted UA values for Modules 1 and 5 (not including air infiltration)	57
2.6	Comparison of Measured and Predicted Relative UA for Module 1 (not including air infiltration)	58
2.7	Measured and Predicted Thermal Resistances for Components of Module 1	64
3.1	Measured UA and Q_f for Modules during March 1984	101
3.2	Measured Time Constants for Modules with Flue Pipes Open	103
3.3	Measured Effective Capacitances at 1/2 Hour of Temperature Decay	105
A.1	Specifications - Module 5 - Reference Module (SI units)	115
A.2	Specifications - Module 5 - Reference Module (English units)	116

C.1 Resistance Calculation for Zone A of Wall Section by ASHRAE's "Zone Method" 128

C.2 Summary of ASHRAE Predicted Overall Transmission Coefficients (not including air infiltration) 135

D.1 Material Properties used in Finite Element Model 138

D.2 Measured and Predicted Temperatures Within the Styrofoam Wall 143

LIST OF FIGURES

		PAGE
1.1	Alberta Home Heating Research Facility	3
1.2	Masonry Module	8
1.3	Cross Section of Double Wythe Wall	10
1.4	Positioning of Internal Wall Thermocouples	20
1.5	Location of Heat Flux Transducers and Thermocouples	21
2.1	Finite Element Mesh for Simplified Wall Section	38
2.2	Selected Isotherms around Metal Tie	40
2.3	Areas Associated with Surface Elements	41
2.4	Electrical Energy Consumption for Modules 1 and 5 for the 1983-4 Heating Season	47
2.5	Electrical Energy Consumption for Modules 1 and 5 for the 1984-5 Heating Season	48
2.6	Relative Overall Transmission Coefficient (UA) for Module 1	51
2.7	Heat Transmission Losses for Modules 1 and 5 for the 1983-4 Heating Season	53
2.8	Heat Transmission Losses for Modules 1 and 5 for the 1984-5 Heating Season	54
2.9	Relative Heat Transmission Losses for Module 1	55
2.10	Overall Heat Transfer Coefficients for North Wall of Module 1	60
2.11	Monthly Measured Thermal Resistance of the North Polyurethane Wall Section and the Above Grade Walls of Module 5	61
2.12	Overall Heat Transfer Coeffiecient for the Ceiling of Module 1	62
2.13	Overall Heat Transfer Coefficient for West Wall of Module 1	63

2.14 Heat Transfer Coefficient for Air Gap, Wallboard, and Interior Air Film of North Wall of Module 1 67

2.15 Positioning of Metal Ties Relative to Heat Flux Transducer on West Wall 69

2.16 Air Infiltration Rates for Modules 1 and 5 for the 1983-4 Heating Season 71

2.17 Air Infiltration Rates for Modules 1 and 5 for the 1984-5 Heating Season 72

2.18 Relative Air Infiltration Rate for Module 1 74

3.1 Steady Periodic Heat Conduction through a Finite Slab 79

3.2 Potential and Actual Heat Flux Response to Steady Periodic Heat Conduction 80

3.3 Internal Wall Temperatures for North Polyurethane Wall Section 83

3.4 Internal Wall Temperatures for North Vermiculite Wall Section 84

3.5 Internal Wall Temperatures for South Polyurethane Wall Section 86

3.6 Wall Heat Flux for April 12-13, 1984 88

3.7 Measured Power Consumption for Module 1 for April 12-13, 1984 91

3.8 Measured Power Consumption for Module 5 for April 12-13, 1984 92

3.9 Measured Power Consumption for Module 1 for March 31 - April 1, 1985 95

3.10 Measured Power Consumption for Module 5 for March 31 - April 1, 1985 96

3.11 Electrical Analogy of Modules during Temperature Decay Tests 98

3.12 Typical Temperature Decay Test 102

3.13 Internal Wall Temperatures during Temperature Decay Test 107

B.1 Ground Probe Thermocouple Location 118

B.2 Air Infiltration Measurement System Schematic 123

C.1 Wall Cross Section for "Zone Method" Calculation 127

C.2 Basement of Module 1 131

D.1 Cross Section of Experimental Wall 141

E.1 Steady Periodic Heat Conduction in a Composite Slab 161

LIST OF PHOTOGRAPHIC PLATES

		PAGE
1.1	Photograph of Double Wythe Wall During Construction	11
1.2	Photograph of Masonry Module - 1983-4 Heating Season	12
1.3	Photograph of Masonry Module - 1984-5 Heating Season	13

NOMENCLATURE

Notation

A	Area (m^2)
A,B,C,D	Complex Constants
C	Specific Heat Capacity ($kJ/kg \cdot {}^oC$)
C	Electrical Capacitance (F)
dT/dx	Temperature Gradient ($^oC/m$)
h	Surface Conductances ($W/m^2 \cdot {}^oC$)
k	Thermal Conductivity ($W/m \cdot {}^oC$)
L	Length (m)
$\ln\left[\frac{T(t) - T_\infty - Q_f/UA}{T_o - T_\infty - Q_f/UA}\right]$	non-dimensional temperature difference
q	Heat Flux (W/m^2)
Q	Rate of Heat Transfer (W)
Q_v	Flow Rate (m^3/s)
Q_f	Circulation Fan Power (W)
R	Thermal Resistance ($^oC \cdot m^2/W$)
R	Electrical Resistance (Ω)
t	time (s)
T	Temperature (^oC)
U	Thermal Transmittance ($W/m^2 \cdot {}^oC$)
UA	Overall Transmission Coefficient ($W/^oC$)
V	Volume (m^3)
V	Electrical Potential (V)
w	Angular Frequency (1/s)
x	coordinate direction

α	$k/\rho C$ - Thermal Diffusivity (m^2/s)
ΔT	Temperature Difference (^oC)
ρ	Density (kg/m^3)
ρVC	Effective Thermal Capacitance ($J/^oC$)
$\rho VC/UA$	Time Constant (s)

Subscripts.

e	Exterior
i	Interior
m	Mean or Average Value
o	Initial
poly	Polyurethane
verm	Vermiculite
∞	Ambient

CHAPTER 1

INTRODUCTION

In the 1970's rising energy costs brought an awareness of the need for energy conservation. A review of the sectors of energy consumption in Canada shows that almost 20% of all the energy consumed goes towards residential heating (1)* . The potential for energy savings from home heating is therefore large, and of national priority when faced with potential future energy supply problems.

Concerns about the amount of energy used in residential buildings led to many suggestions for the modification of existing housing design. These suggestions varied widely, from simply upgrading insulation levels, to more elaborate schemes involving passive and/or active solar heating. A major problem existed as little or no quantitative data was available for proper evaluation of many of these schemes. Compounding the problem for Canada was that little research had been done in a northern climate.

One building design of interest involves the use of large quantities of masonry in the above grade walls of a structure. This type of house design is capable of storing relatively large quantities of energy in its above grade

---

* numbers in parenthesis indicate references

walls. This work will summarize the results of a two year investigation conducted at the Alberta Home Heating Research Facility (AHHRF) into the thermal performance of a masonry structure.

The objective of this study was to better understand the above grade envelope losses of a residential masonry structure in a northern climate. Primary concerns were with :

1) the overall thermal performance of the masonry structure relative to a more conventional wood framed structure
2) the influence of the thermal mass on the above grade transmission losses
3) the air-tightness of a masonry structure
4) the thermal performance of the foamed-in-place insulation
5) the effects of adding south facing windows

Before going into details about the masonry module, a brief description of the entire Facility may be useful. Since 1979 the AHHRF has been used to study the envelope losses from both conventional and non-conventional demonstration modules. The AHHRF is an experimental research facility consisting of six single storey modules, each 7400 x 6800 mm in plan, with full height walls and concrete basements. As shown in Figure 1.1 these uninhabited modules are located in a single east-west row on

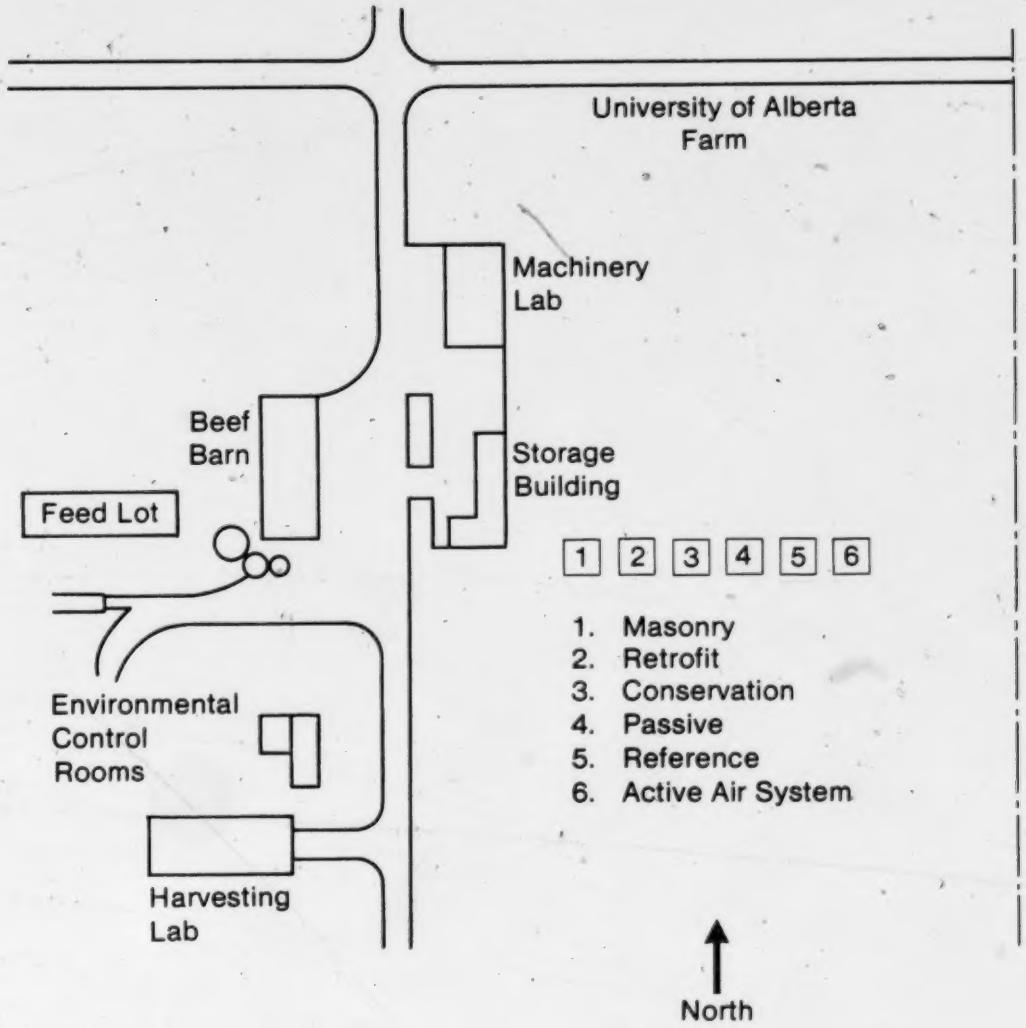

Figure 1.1 Alberta Home Heating Research Facility

the University of Alberta Farm, near Ellerslie, Alberta. Each module was designed with a conservation and heating strategy different from the other modules:

Module 1 : Masonry module - contains a large amount of structural mass inside the wall's main insulating layer.

Module 2 : Retrofit module - constructed with very low levels of insulation in the ceiling and walls, and none in the basement. The module's insulation levels are slowly being upgraded to determine the effectiveness of retrofitting a structure.

Module 3 : Conservation module - represents the extreme limit of insulation levels in the ceiling, walls, and basement.

Module 4 Passive module - has two very large south facing windows, and a substantial amount of thermal mass inside the module.

Module 5 : Reference module - construction is typical of post - 1975 wood framed residential houses.

Module 6 : Active Air module - similar to Module 5, except module is fitted with an active air solar collector system.

The insulation values for each of the modules are listed in Table 1.1, and other construction details relevant to the modules' performance are listed in Table 1.2. Complete construction details for the Facility have been reported previously (2).

Table 1.1 Nominal Insulation Values for Modules (RSI, (R English))

Module	Ceiling	Walls	Basements
1. Masonry	2.11 (12)	2.59 (14.7)[a] 1.06 (6.0)[b]	1.76 (10) to 610 mm[c]
2. Retrofit	5.63 (32)	1.41 (8)	none
3. Conservation	14.08 (80)	7.04 (40)	3.52 (20) full height
4. Passive	7.04 (40)	3.52 (20)	1.76 (10) to 610 mm[c]
5. Reference	2.11 (12)	1.76 (10)	1.76 (10) to 610 mm[c]
6. Active Air	5.63 (32)	1.76 (10)	1.76 (10) to 610 mm[c]

(a) Polyurethane section (90% of wall area), based on conductivity of fully aged foamed-in-place polyurethane from ASHRAE Fundamentals 1981.

(b) Vermiculite section (10% of wall area).

(c) Depth below grade.

Table 1.2 Construction Details for the Modules

Module	Flue Diameter (mm)	Air-Vapor Barrier Thickness (mm)	Total Double Glazed Windows (% floor area)	South Facing Windows (% floor area)
Masonry	152	.152	13.6,[a] 20.6[b]	0,[a] 6.9[b]
Retrofit	152	.102	11.9	0
Conservation	none	.152	13.7	11.3
Passive	152	.152	25.0	22.6
Reference	152	.102	11.9	0
Active Air	152	.102	11.9	0

(a) 1983-4 Heating season

(b) 1984-5 Heating season

The philosophy of the project has been to make annual changes to the modules, and through comparison with an unmodified reference module, quantify the effects of the changes. The reference module used for comparison with the masonry module is Module 5. There were several reasons for selecting Module 5 :

1) Module 5 represents "standard" house construction
2) Module 5 has remained unmodified for five years
3) Differences in construction details between Modules 1 and 5 are limited to the above grade walls, as the basements and ceilings are identical. Construction details of Module 5 are listed in Table A1 (or A2 - English units)

What follows in this Chapter is a detailed description of the masonry module, the modifications made to it between heating seasons, and the data collection system used in monitoring its performance.

1.1 Construction Details of the Masonry Module

The masonry module, shown in elevation in Figure 1.2, has most of the same overall dimensions as the other modules. Common features to all modules are their gable roofs on elevated roof trusses and full concrete basements. The elevated roof trusses permit varying thicknesses of insulation to be installed without structural modifications. The basements extend 1900 mm below grade with weeping tiles

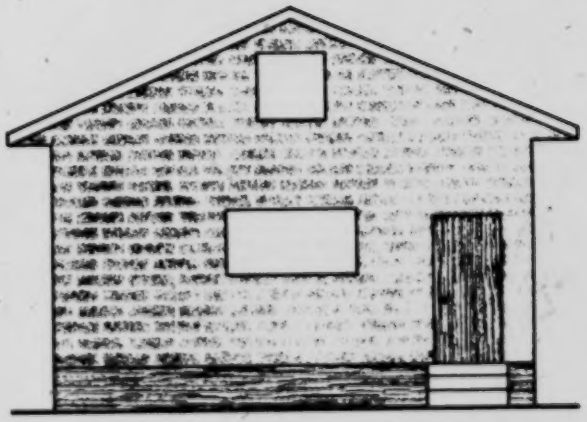

East Elevation

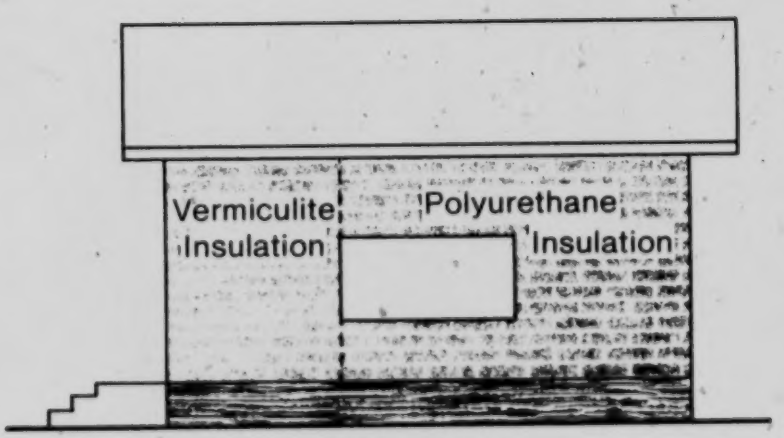

North Elevation

Figure 1.2 Masonry Module

around the perimeter of their foundations. All modules, except Module 3, have a 152 mm class B flue vent terminating 1300 mm above the basement floor. These vents are used to induce pressure distributions similar to those found in residential structures.

The above grade walls of Module 1 are commonly known as a double wythe, or cavity, walls. Figure 1.3 shows the double wythe wall in cross section. This type of wall was selected for study because it contains a significant amount of mass inside its main insulating layer. Two types of insulation were installed in the 64 mm gap between the facing bricks and the load carrying concrete blocks. All east, west, and south walls are solely foamed-in-place polyurethane insulation. One third of the north wall was insulated with poured-in-place vermiculite, as indicated in Figure 1.2. The remainder of the north wall is polyurethane. It should be noted that during construction of the walls, great care was taken to ensure that the wall cavity was kept clear of mortar to avoid thermal bridging. Plate 1.1 is a photograph detailing the walls under construction.

Plate 1.2 is a photograph of the masonry module taken after its construction in the fall of 1983. The masonry module was constructed without south facing windows. During the summer of 1984, two south facing windows were added to the module, as shown in Plate 1.3. The addition of south facing windows were the only structural modification made to

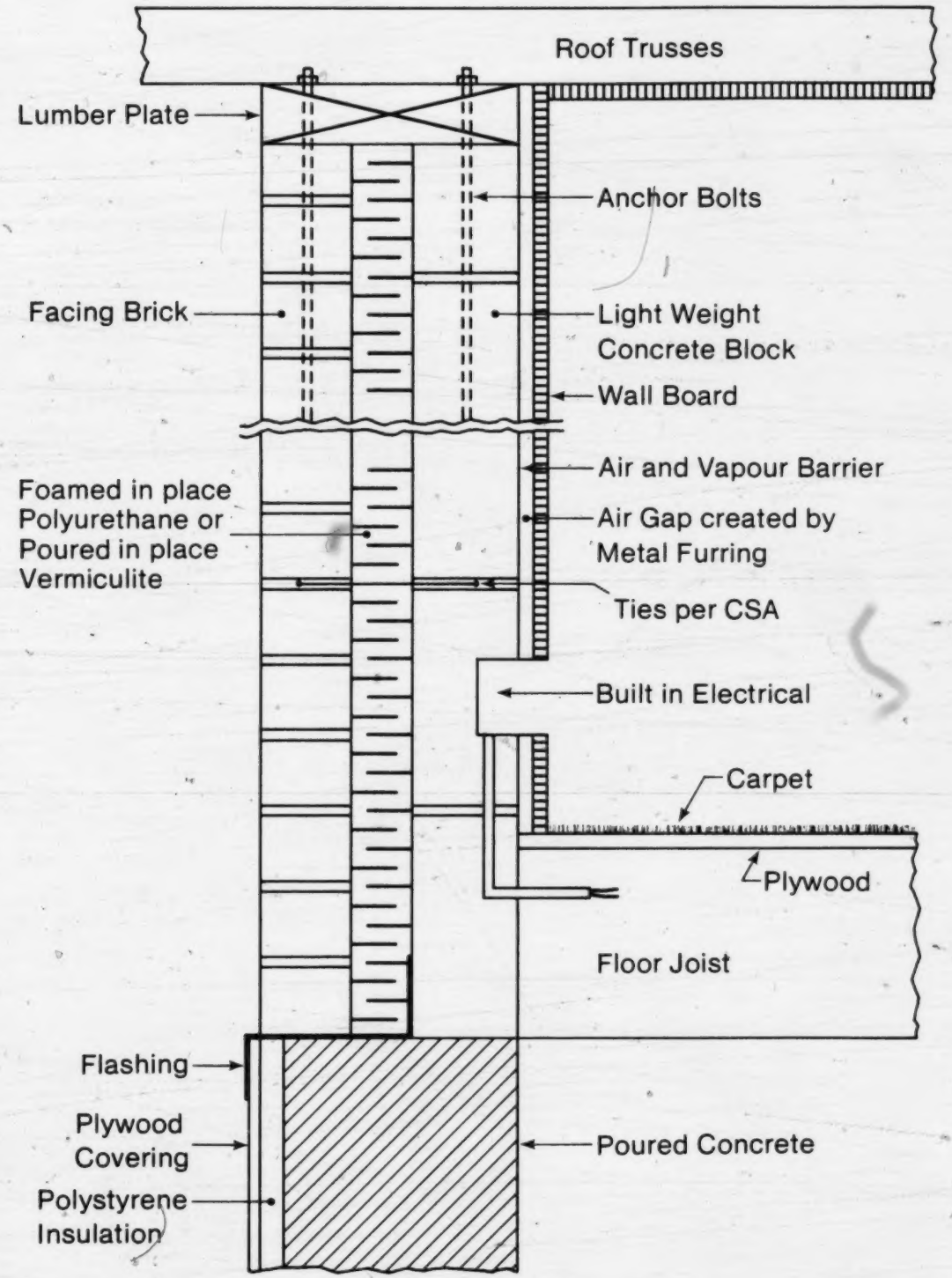

Figure 1.3 Cross Section of Double Wythe Wall

POOR COPY
COPIE DE QUALITEE INFERIEURE

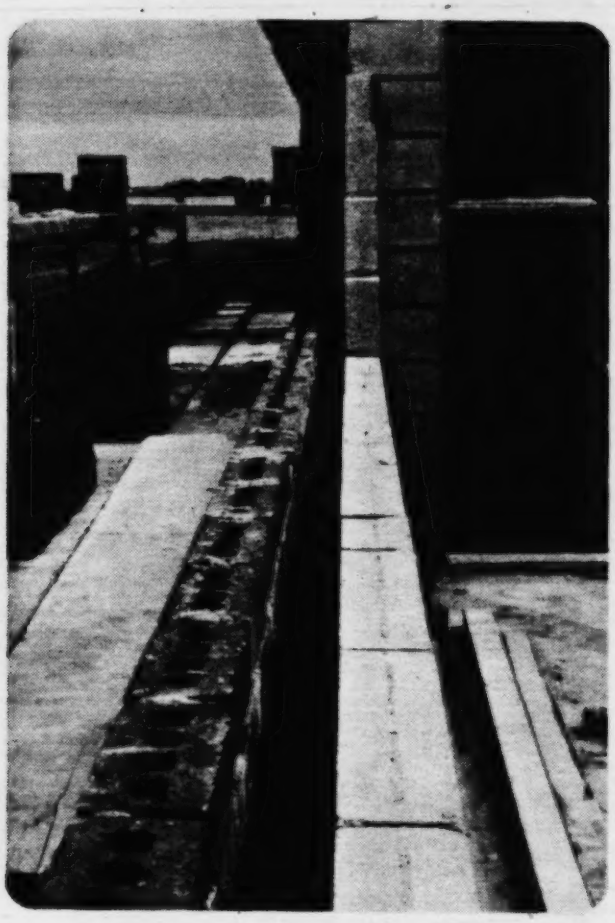

Plate 1.1 Photograph of Double Wythe Wall during Construction

POOR COPY
COPIE DE QUALITEE INFERIEURE

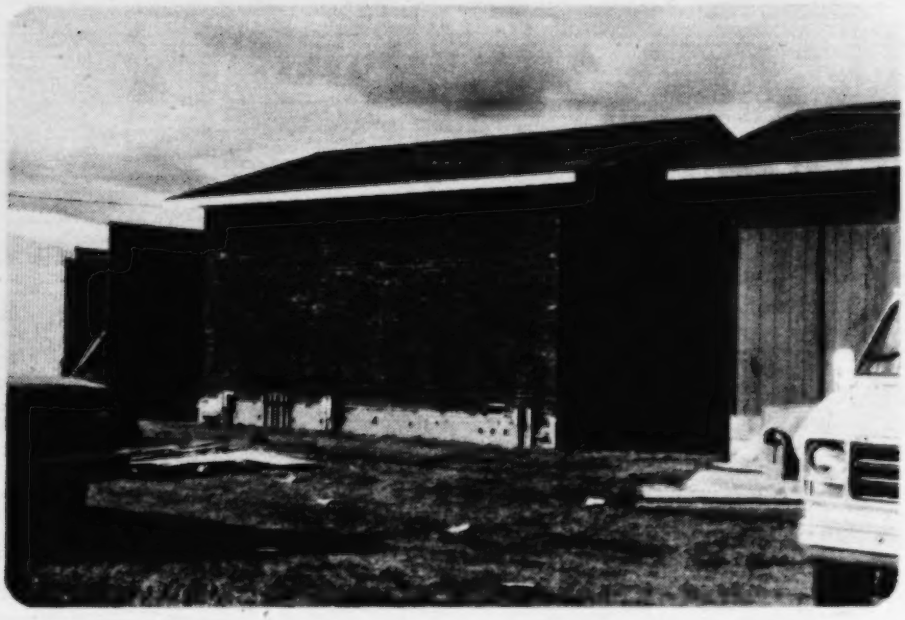

Plate 1.2 Photograph of Masonry Module - 1983-4 Heating Season

POOR COPY
COPIE DE QUALITEE INFERIEURE

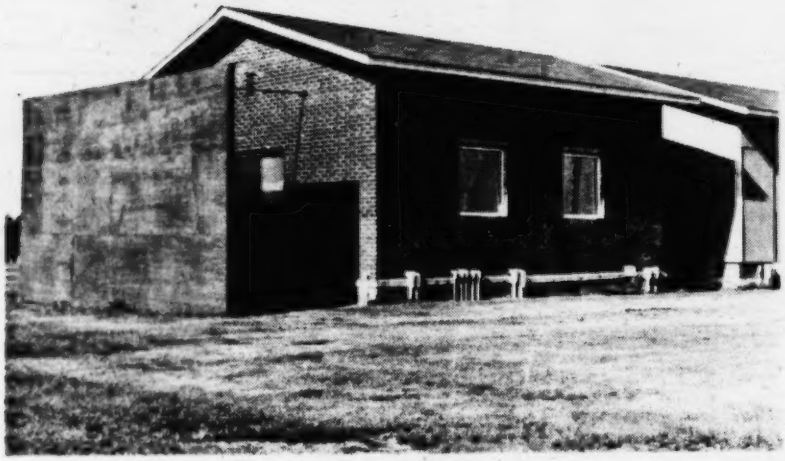

Plate 1.3 Photograph of Masonry Module - 1984-5 Heating Season

the masonry module during this study. The reference module did not have south facing windows in either the 1983-4 or 1984-5 heating seasons. The basic dimensions and construction details of the masonry module are given in Tables 1.3A and 1.3B.

The only other modification made to Module 1 was to install a proportional controller on the heating system during the summer of 1984. This type of controller allowed the heating system to vary the module's energy input as changes in the heating load occurred. The controller eliminated furnace cycling and much of the interior temperature fluctuations, which are normally encountered with an on-off type thermostat. Being able to control and measure the subtle changes in module heating load helps in studying short term phenomena (example - effects of solar gains).

1.2 Data Acquisition System

In order to obtain a good understanding of the thermal behavior of any of the modules, several parameters must be accurately measured and recorded. On site at the Alberta Home Heating Research Facility there are two Hewlett-Packard HP-85 computer based data acquisition systems. One system is used solely to control and monitor natural air infiltration experiments and several related parameters. The second system, the main data acquisition system, records

Table 1.3A

SPECIFICATIONS - MODULE 1 - MASONRY MODULE (SI units)

Exterior Dimensions	6800 x 7400 mm
Interior Dimensions	6250 x 6850 mm
Main Floor Wall Height	2440 mm
Basement: Wall Height	2440 mm
Wall Thickness	200 mm
Floor Thickness	100 mm

Ceiling Construction
- standard truss with 610 mm bobtail
- 38 x 89 mm rafters, 610 mm on center
- fiberglass insulation, RSI = 2.11
- 0.152 mm polyethelene air-vapor barrier
- 13 mm gypsum wallboard

Wall Construction
- 76 mm (nominal) burn clay brick
- 64 mm insulating layer
  (foamed-in-place polyurethane - 90% of wall area
  poured-in-place vermiculite - 10% of wall area)
- 100 mm (nominal) concrete block
- 0.152 mm polyethelene air-vapor barrier
- 25.4 mm air space
- 13 mm gypsum wallboard

Windows
North Wall - 1000 x 1950 mm sealed unit (double glazed)
South Wall - none, 1983-4 ; 2 - 1220 x 1220 mm sealed units, 1984-5
East Wall - 1000 x 1950 mm horizontal slider, aluminum frame
West Wall - 1000 x 1950 mm horizontal slider, aluminum frame

Door
- 910 x 2030 mm solid core fir

Basement Insulation
- 51 mm polystyrene extending 610 mm below grade RSI = 1.76
- 13 mm pressure treated plywood covering

Auxiliary Heating
- 10 kW electric duct heater

Interior Finish
- painted walls
- carpeted floor

Table 1.3B

SPECIFICATIONS - MODULE 1 - MASONRY MODULE (English units)

Exterior Dimensions	22.3 x 24.2 feet
Interior Dimensions	20.5 x 22.5 feet
Main Floor Wall Height	8 feet
Basement : Wall Height	8 feet
Wall Thickness	8 inches
Floor Thickness	4 inches

Ceiling Construction
- standard truss with 2 foot bobtail
- 2 x 4 inch rafters on 24 inch center
- fiberglass insulation, R-12
- 6 mil polyethelene air-vapor barrier
- 1/2 inch gypsum wallboard

Wall Construction
- 3 inch (nominal) burn clay brick
- 2.5 inch insulating layer
  (foamed-in-place polyurethane - 90% of wall area
  poured-in-place vermiculite - 10% of wall area)
- 4 inch (nominal) concrete block
- 6 mil polyethelene air-vapor barrier
- 1 inch air space
- 1/2 inch gypsum wallboard

Windows
- North Wall - 40 x 76 inch sealed unit (double glazed)
- South Wall - none, 1983-4 ; 2 - 48 x 48 inch sealed units, 1984-5
- East Wall - 40 x 76 inch horizontal slider, aluminum frame
- West Wall - 40 x 76 inch horizontal slider, aluminum frame

Door
- 36 x 80 inch

Basement Insulation
- 2 inches polystyrene extending 2 feet below grade, R-10
- 1/2 inch pressure treated plywood insulation covering

Auxiliary Heating
- 10 kW electric duct heater

Interior Finish
- painted walls
- carpeted floor

all module and environmental measurements. The main computer system, through a multiplexer, is capable of accepting multiple inputs from sensors located throughout the Facility. Once every two minutes the logger scans through its more than one hundred channels of inputs, and temporarily stores the signals. At the end of each hour the signals are averaged and transferred to magnetic tape. The magnetic tape is then brought back to the university where the data is transferred to the main frame computer for analysis.

Measurements taken at the Facility include:

1) Environmental Measurements
   - ambient temperature
   - several ground temperatures
   - exterior surface temperature on a south facing wall
   - radiation at various orientations
   - wind speed and direction at 10000 mm height, at two locations

2) Module Measurements
   - electrical energy input
   - interior temperatures
   - component heat fluxes
   - natural air infiltration rates

A detailed description of all the environmental and module measurements taken at the Facility are presented in Appendix B.

1.2.1 Measurement Details of the Masonry Module

The masonry walls; unlike many other building components, do not have their thermal properties dominated by a single material. The combination of similar thicknesses of both masonry and insulation elements, along with the air gap and wallboard, makes the study of the wall's dynamic heat transfer fairly complex. Since the overall thickness of the walls are almost 270 mm, and the insulation and concrete blocks having low thermal diffusivities, the masonry wall's response to changes in ambient conditions will be relatively slow. It is expected to take several hours for changes in exterior temperature to be realized, in terms of heat flux changes, at the modules interior surface. This large delay in wall response limits the usefulness of heat flux measurements in the short term. Therefore, to monitor more clearly the effects of each of the different materials in the wall, several thermocouples were installed inside the wall section.

A total of twelve thermocouples were installed within the walls at three locations. Two sets of thermocouples were located inside the module's north wall - one in the vermiculite section and one in the polyurethane section. The third set was installed inside the module's south wall. At each location three thermocouples were mounted inside the insulating layer. One thermocouple was fixed to the interior side of the facing bricks, one fixed to the exterior side of the concrete blocks, and the third

positioned in approximately the center of the insulation layer. At each location a fourth thermocouple was also mounted to the interior side of the concrete blocks. Figure 1.4 shows the positioning of the thermocouples within the wall, and Figure 1.5 shows their location within the module. Also shown in this latter figure are the locations of the twelve heat flux transducers in the masonry module.

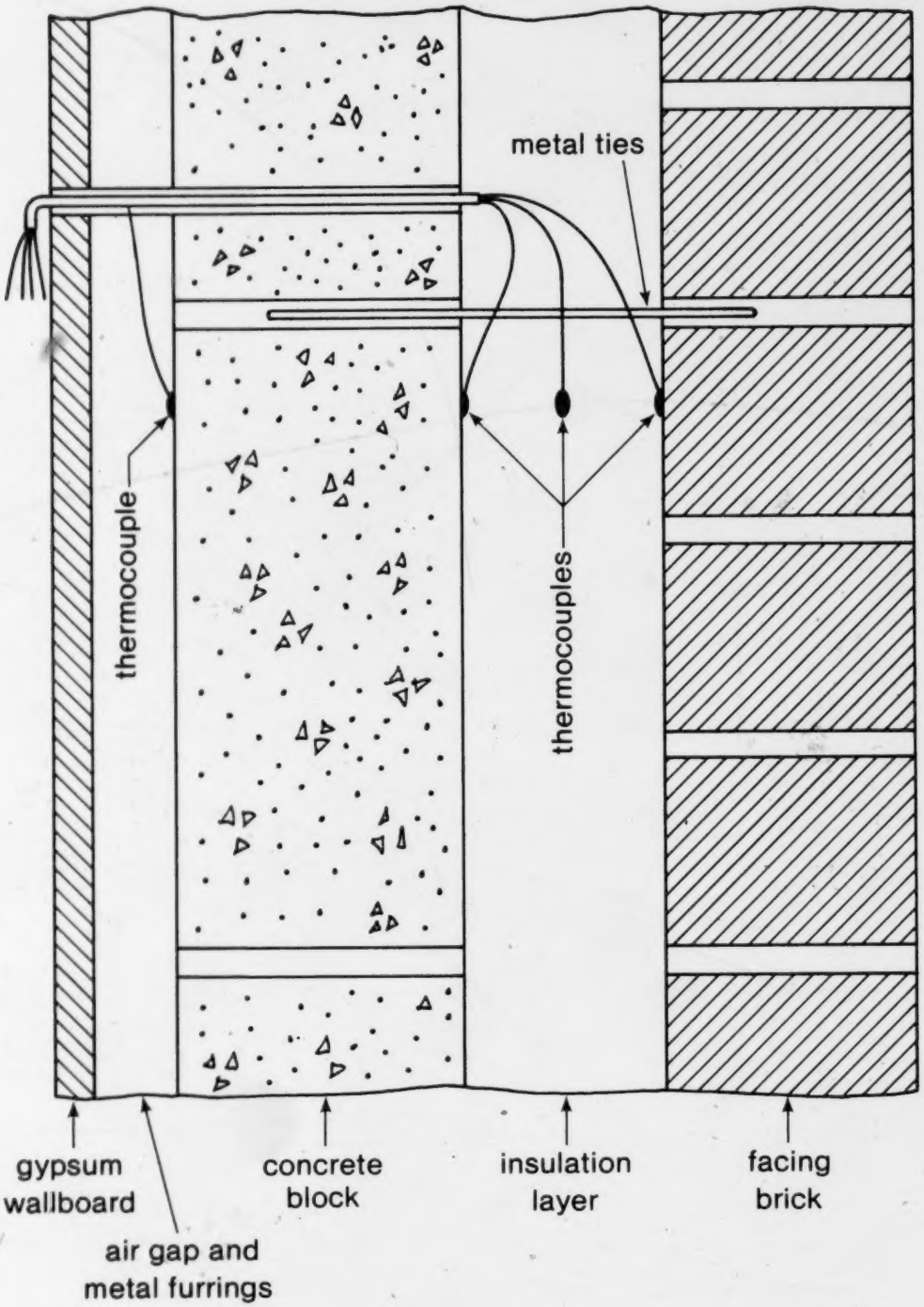

Figure 1.4 Positioning of Internal Wall Thermocouples

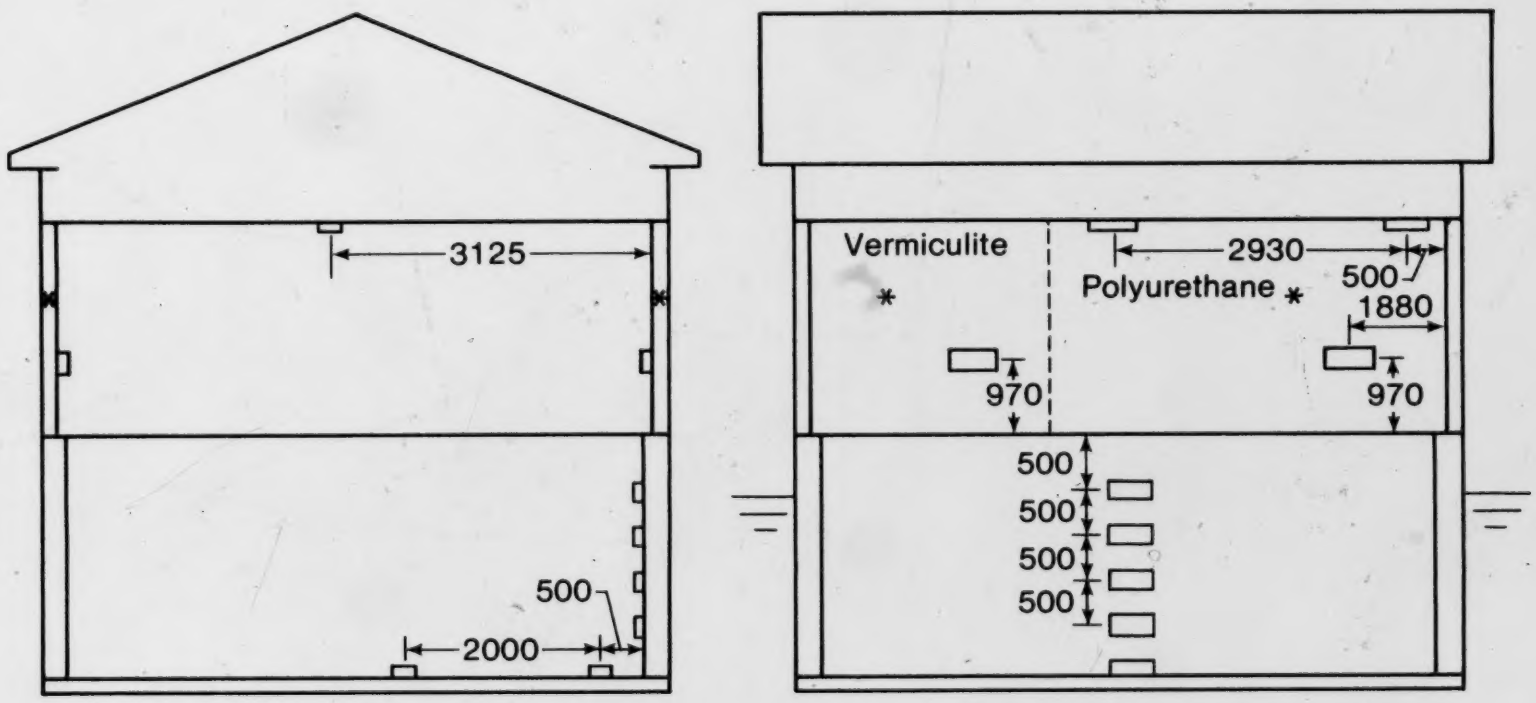

All dimensions in millimeters

* - indicates location of thermocouples inside walls

Figure 1.5 Location of Heat Flux Transducers and Thermocouples

CHAPTER 2

LONG TERM THERMAL PERFORMANCE OF MASONRY MODULE

There are two different approaches that can be taken when analyzing the energy aspects of a structure, one being the "short term" (typically a few hours) and the other the "long term" (typically a few days or longer). This chapter will deal solely with the long term thermal performance of the masonry module.

The concepts of "short term" and "long terms" may seem ambiguous at first, but, in terms of this work, they are given formal definitions. The "short term" approach refers to the transient, or periodic behavior of a structure in response to the changing ambient conditions. The "short term" is then usually confined to events happening within one day. The "long term" approach looks beyond the short term transient behavior of a building, and concentrates only on the overall results. The "long term" can usually avoid the effects of the transients by averaging over a sufficiently long period of time.

Consider for example the heat transfer through a slab, one side of which is held at a constant temperature, and the other side is subject to a harmonically varying temperature. In general, the slab is not only transferring heat but is also temporarily storing (or releasing) energy. When

averaged over one cycle, over the long term, there is no change in internal energy of the slab, and net heat transfer then becomes independent of the cycling temperature. Therefore, the long term often refers to the averaging over a period long enough so that any change in internal energy is negligible compared to the amount of energy transferred. (Further discussion of this approach can be found in (3).) Since changes in internal energy are ignored, the long term performance of a module will appear independent of its thermal capacitance, and dependent just on its thermal resistance.

The first part of this chapter will be a prediction of the long term heat loss from the masonry module. The prediction method used is that presented in the American Society of Heating, Refrigerating, and Air-Conditioning Engineers (ASHRAE) Fundamentals Handbook (4). A more detailed prediction will also be made for the masonry walls, including the use of finite element techniques to deal with the effects of the metal ties that thermally bridge the wall's main insulating layer. The last part of this chapter will present the long term experimental results of the masonry module that were collected over the two heating seasons.

2.1 Predicted Long Term Energy Loss

The approach commonly used in predicting the energy loss from a building is relatively straight forward, but can often be difficult to apply. A building is first divided up into its components, and each component's energy loss is calculated separately. The building's total energy loss is then the sum of the individual component losses.

The above grade portion of a building (walls, ceiling, doors, and windows) have their overall thermal resistance calculated using one dimensional steady state heat transfer theory. The heat transfer through walls and doors is usually simple enough to calculate, but ceilings and windows can be more difficult. The heat transfer through the ceiling can be strongly dependent on the type of roof structure which is on the building. The roof keeps the attic temperature somewhat above ambient temperature, therefore reducing the heat loss through the ceiling. Since windows allow solar radiation to enter directly into a building, the window's net energy transfer can be very difficult to calculate.

The energy loss from the below grade portion of a building is generally more difficult to predict than the above grade portion. Heat loss from the basements are not only to the atmosphere, but also to the deep ground. To complicate the prediction, soil conductivity is hard to estimate since it is highly dependent on its water content.

The final energy loss one would like to predict is the loss due to a buildings natural air infiltration. Air infiltration rates are a function of indoor-outdoor temperature difference , wind speed, wind direction, and the number and type of holes in the building's envelope. Predictions of natural air infiltration rates are often no better than educated guesses. Because the natural air infiltration rates were to be measured in this study no prediction was attempted.

It is obvious that a complete and thorough prediction of a building's energy consumption would be an enormous undertaking. There are simplified methods available that allow a reasonable prediction of energy consumption to be made without extensive calculations. The recognized standard among these simplified methods is presented in the ASHRAE Fundamentals Handbook (4).

2.1.1 ASHRAE Prediction

This section will present the results of the ASHRAE prediction for the masonry and references modules. The calculations involved in the ASHRAE prediction are rather long and tedious. These calculations are presented in Appendix C.

The major difficulty in using the ASHRAE Handbook is accurately estimating the in-situ thermal properties of some building materials. The ASHRAE Handbook contains an extensive listing of building material properties, but it is

sometimes difficult to determine which property applies to a specific situations. In many cases, materials are listed in ASHRAE as having a range of thermal properties, depending upon other related parameters. For example, the conductivity of the foamed-in-place polyurethane insulation that was used in the masonry module can vary between 0.0144 and 0.0317 W/m·°C (4). The actual conductivity of any particular specimen of polyurethane is a function of its density, "age", cell size, surface finish, mean temperature, type of blowing gas used in expanding the foam, and the relative humidity of the air within the foam cells (5,6). Many of these related parameters are difficult to estimate in a non-laboratory situation.

To get around this problem of uncertainty in some of the materials' properties , the ASHRAE prediction was done for the range of those materials' possible properties. Thereby defining an upper and lower bound for the ASHRAE prediction. Shown in Table 2.1 are the results of the ASHRAE prediction for the masonry module (with and without the south facing windows), and for the reference module. The lower bound of the ASHRAE prediction was calculated using the most resistive thermal properties that could be expected for any of the building materials that have uncertainty associated with them. This lower bound of the ASHRAE prediction is shown in brackets in Table 2.1. The upper bound of the ASHRAE prediction was calculated using the building materials' least resistive thermal properties.

Table 2.1
Summary of ASHRAE Predicted Overall Transmission Coefficients (W/°C)
(not including air infiltration)

Component	Module 1 Without South Facing Windows	Module 1 With South Facing Windows	Module 5
Ceiling	19.2	19.2	22.0
Main Walls	23.6[a] (15.4)[a]	22.7[a] (14.9)[a]	32.9
Doors	5.2	5.2	2.0
Windows	18.5	26.8	15.8
Basement Walls	32.4	32.4	35.4[a]
Basement Floor	6.8	6.8	6.8
Total	105.7 (97.5)	113.1 (105.5)	114.9

Note: Values in brackets are the lower bound of ASHRAE prediction, otherwise the value are the upper bound.

(a) Includes joist space

The upper bound of the prediction, as well as component predictions that had no uncertainty associated with their thermal properties are shown as regular entrees in Table 2.1 (that is, not in brackets).

The results of the ASHRAE prediction are in terms of overall transmission coefficients (UA) for all the components of the modules. At the bottom of Table 2.1 are the totals of the transmission coefficients for the two modules. It should be noted that these ASHRAE predictions do not include the heating load from the modules' air infiltration.

The expected heat transfer through any of the components, or from the entire module, can be calculated from Equation 2.1.

$$Q = UA \times \Delta T \qquad (2.1)$$

where: Q - rate of heat transfer (W)

UA - overall transmission coefficient ($W/^oC$)

ΔT - indoor-outdoor temperature (^oC)

The overall transmission coefficient can be related to the overall thermal resistance by

$$R = A / UA \qquad (2.2)$$

where: R - overall thermal resistance ($^oC/W \cdot m^2$)

A - area (m^2)

UA - overall transmission coefficient (W/°C)

The percent contribution of the total predicted heat loss for each of the components in both Modules 1 and 5 is shown in Table 2.2. The distribution of the heating load for both modules shows that the modules' walls are only a small part of their heating energy requirements. With the two modules having identical basements, and very similar ceilings, doors, and windows, their heat overall loss should also be very similar.

2.1.2 Detailed Prediction for Masonry Walls

A review of Table 2.1 shows that the above grade walls of the masonry module is the only component with any uncertainty in its ASHRAE prediction. Some elements within the walls, like the vermiculite, concrete blocks, facing bricks, and wallboard, pose no problem in estimating their thermal properties. Other elements, like the polyurethane, the air gap, and the metal ties, all have some notable uncertainty in their thermal properties.

In this section a closer analysis of the masonry module's walls will be made to remove some of the uncertainty in the ASHRAE prediction.

Polyurethane Foam

By far, the most significant uncertainty in predicting

Table 2.2
ASHRAE Predicted Percent Contribution of Heating Load (%)
(not including air infiltration)

Component	Module 1 Without South Facing Windows		Module 1 With South Facing Windows		Module 5
Ceiling	18.2	(19.7)	17.0	(18.2)	19.1
Main Walls	22.3	(15.8)	20.1	(14.1)	28.6
Doors	4.9	(5.3)	4.6	(4.9)	1.7
Windows	17.5	(19.0)	23.7	(25.4)	13.8
Basement Walls	30.6	(33.2)	28.6	(30.7)	30.8
Basement Floor	6.5	(7.0)	6.0	(6.4)	5.9

Note: Values in brackets are the lower bound of ASHRAE prediction, otherwise the value are the upper bound.

the heat transfer through the masonry walls is estimating the thermal conductivity of the polyurethane foam. The foamed-in-place polyurethane acts as the main insulating layer for 90% of the module's wall area. As pointed out previously there are many factors that can effect the conductivity of the polyurethane foam. The dominate among these factors are the foam's density, the gas used to expand the foam , and the "age" of the foam (5,6).

The foam installed in the masonry module was expanded with the refrigerant R11 to an intended density of 40 kg/m^3. Assuming the actual density of the foam is 40 kg/m^3, the conductivity of the foam can still range between 0.0159 and 0.0226 $W/m \cdot {}^oC$, depending on the age of the foam.

The age of a foam describes how much its thermal properties have deteriorated since it was first foamed, which is not related directly to a foam's chronological age. All polyurethane foams age in a similar manner, but the rate of aging is strongly dependent upon environmental factors (5,6). Initially, the cells of foam are filled almost exclusively with the blowing gas. If the blowing gas has a high molecular weight, like a refrigerant, the thermal conductivity of the foam will be relatively low. Aging of the foam begins as air diffuses inward, and since air's molecular weight is less than that of a refrigerant's, the thermal conductivity of the foam increases. This inward diffusion of air is sometimes called the foam's "primary aging" stage. Primary aging stops when the air inside the

cells reach some equilibrium concentration. Also occurring, but usually at a much slower rate, is the outward diffusion of refrigerant gas. As the refrigerant diffuses outward, called "secondary aging", the thermal conductivity of the foam slowly increases. Aging finally stops when there is only a small percentage of the refrigerant remaining in the cells. Depending on many factors, the complete aging of polyurethane foams can reportedly occur in less than one year, or take more than one hundred years (6).

Certain conditions can accelerate the aging process of polyurethane foams, such as, elevated temperatures, cut specimen (the removal of the outer skin), thin specimen, and high humidity. Most laboratory tests to determine the aging rate of polyurethane foams have been done on 25.4 mm thick cut specimens which have been held at elevated temperatures for specified lengths of time. Very little data is available for the aging of polyurethane foam under the conditions similar to those found in the wall cavity of Module 1. Knox (5) does report that an uncut specimen, at room temperature, did not show any signs of aging over a 720 day period. Noting that the polyurethane used in Module 1 is 64 mm thick, uncut, and has a mean temperature generally below room temperature, then, probably no aging has occurred during this study's test period. The expected conductivity of the foamed-in-place polyurethane is therefore estimated to be 0.0159 W/m·^{o}C.

Air Gap

To provide a conventional interior finish to the masonry module it was necessary to use furrings to mount the wallboard to the concrete blocks. These metal furrings created a 25.4 mm air gap between the concrete blocks and the wallboard. On the exterior side of the air gap, against the concrete blocks, is the wall's air-vapor barrier.

The heat transfer across an air gap is a combination of conduction, convection, and radiation. The approach usually taken in estimating the heat transfer across a plane vertical air space is to divide up the heat transferred into its different modes. The conduction and natural convection is calculated separately from the radiation heat transfer. The rate of heat transfer by conduction and convection is based on experimental results, and the radiation heat transfer is approximated from the solution for two infinite parallel planes (7,8).

As long as the air gap remains a uniform thickness, the conduction/convection component can either be calculated from semi-empirical relationships (9) or approximated from a set of figures (10). There is very good agreement among methods for predicting the heat transfer by conduction and convection.

The radiation heat transfer would be simple to calculate if all the material properties were known. The problem is in calculating the effective emittance between the two surfaces. The emissivity of the wallboard surface,

like many construction materials, can be approximated as 0.9. The emissivity of the polyethelene air-vapor barrier is not known. Picking two extremes for the emissivity of the polyethelene surface as being 0.05 and 0.9, the effective resistance of the air gap, including conduction, convection, and radiation modes of heat transfer, would be 0.655 and 0.173 $m^2 \cdot {}^oC/W$, respectively. This wide range for the effective resistance of the air gap shows the importance of the radiation component of heat transfer. With no other data available to help in the prediction, the mean value of 0.414 $m^2 \cdot {}^oC/W$ is taken as the effective resistance of the air gap.

Effects of the Metal Ties

Metal ties between the inner and outer wythes of the masonry walls are used to transfer all or some of the wind load on the outer wythe to the inner wythe of the wall (11). The steel ties used in the masonry module are 3.2 mm in diameter, and extend approximately half way through both the concrete block and facing brick layers. The positioning of the ties are inside the mortar beds of the bricks and concrete blocks. The ties, spaced 406 mm apart, were laid down in strips on alternate levels of concrete blocks. The concern created is that highly conductive metal ties thermally bridge the main insulating layer of the walls.

The governing relation for one dimensional conduction heat transfer is Fourier's Law,

$$Q = - k A \, dT/dx \qquad (2.3)$$

where: Q - rate of heat transfer (W)

k - thermal conductivity ($W/m \cdot {}^{o}C$)

A - area of heat flow (m^2)

dT/dx - temperature gradient ($^{o}C/m$)

The two physical parameters that are important to the rate of heat transfer are the material's conductivity and area. Calculating the ratio of insulation area to area of metal ties in the masonry walls is approximately 20,000:1. One would normally assume to neglect the ties, except the ratio of conductivity of the steel to the conductivity of polyurethane is just under 3000:1. Treating the steel and polyurethane independently, and applying Fourier's Law, the heat transfer through the steel ties would be approximately 1/7 of the heat transfer through the polyurethane, if the temperature gradients were the same.

In general the heat transfer through the metal ties and insulation will <u>not</u> be one dimensional or independent of each other. ASHRAE does have a method to deal with heat transfer through panels containing metal. The method is referred to as the "zone method", this is the method used in calculating the ASHRAE prediction shown in Table 2.1. The details of the zone method's calculation are shown in Appendix C. The zone method shows an increase in the heat transfer through the polyurethane wall section of 2.2% due

to the steel ties.

There is no analytical solution available to calculate the multidimensional heat transfer around the metal ties. Even a numerical approximation to this problem would be very difficult to calculate because of the heat transfer across the air gap. A numeric solution could be done for a simplified wall section that did not include the air and wallboard layers. The results for this simplified wall section would not be directly applicable to the actual wall section, but would give the order of magnitude of the heat transfer.

The numerical technique used to analyze the temperature field around the metal ties was the finite element method. The finite element method was used so a fine mesh of elements could analyze the temperature field near the tie, and a coarse mesh could be used farther away from the tie. The type of element used to discretize the temperature field within the wall was a two dimensional triangular element. Each element having three nodes, the nodes are located at the vertices of the triangle. At each node there is only one degree of freedom, the field variable temperature. A linear interpolation function was used to approximate the temperature within each element. A complete description of the finite element model is given in Appendix D.

To model the wall section, the assumption was first made that the metal ties were sufficiently isolated from each other that it was only necessary to model the region

around one of the ties. Figure 2.1 shows the mesh of assembled elements used in approximating the temperature field within the wall. Since the heat transfer is the same in all directions around the metal tie, only half of any section taken through the tie needs to be modelled. The entire mesh is made up of 271 elements, and has 159 degrees of freedom.

Before the finite element model was used to predict the temperature field within the masonry walls the computer code was tested on a less complicated wall section. The finite element program was used to predict the temperature field around a copper rod inside of a homogeneous styrofoam wall section. This type of wall section was constructed, instrumented with thermocouples, and tested between two environmental chambers. The results of the finite element model were compared to the actual measured temperatures inside the styrofoam wall. There was reasonably good agreement between these measured and predicted temperatures. The finite element model was considered to be working, and could then be used to predict the heat transfer through the simplified masonry wall. Further description of the testing of the finite element model is presented in Appendix D.

The boundary conditions applied to model the masonry walls were:

1) Interior surface (concrete blocks) - specified temperature of 20°C.

2) Exterior surface (facing bricks) - specified

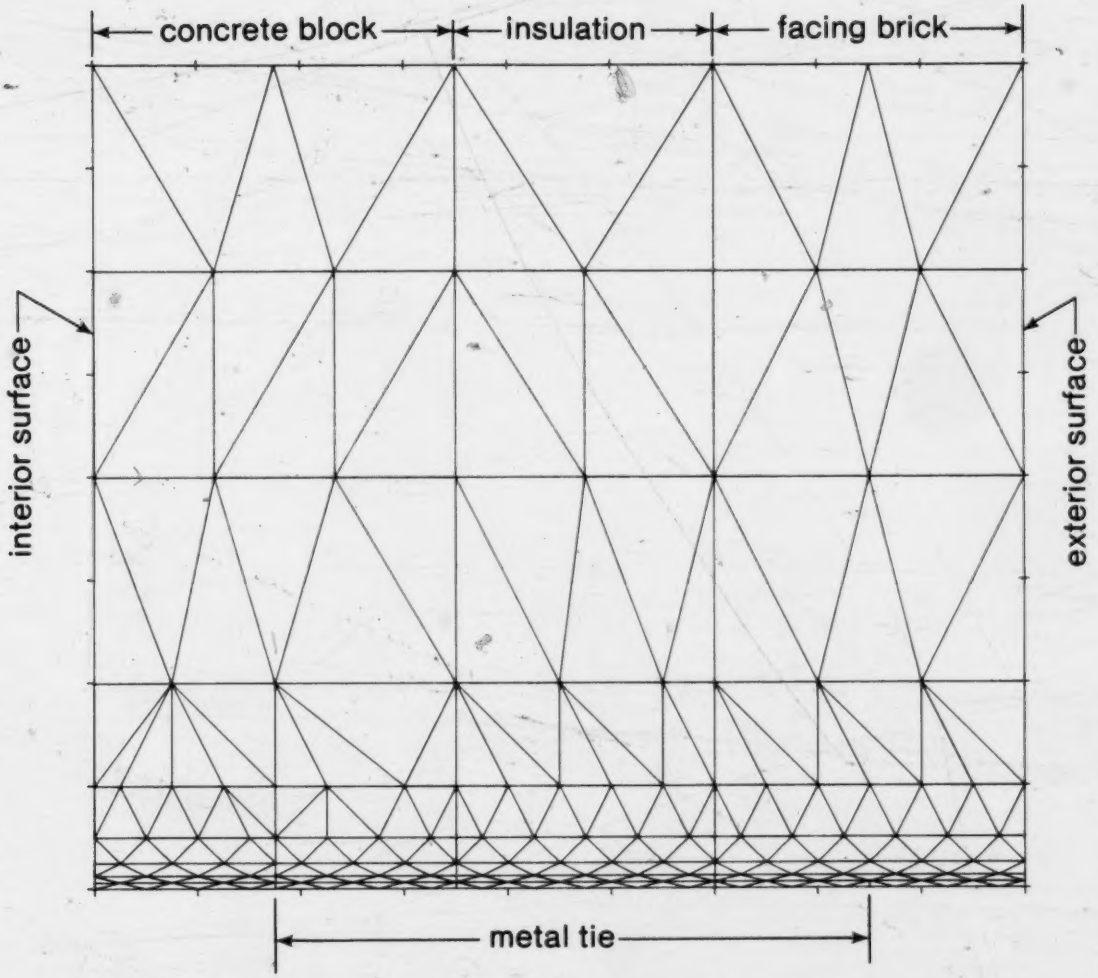

Figure 2.1 Finite Element Mesh for Simplified Wall Section

temperature of 0°C.

3) Axis of symmetry at the metal ties - adiabatic or zero heat flux.

4) Infinite boundary - adiabatic or zero heat flux.

The solution to the finite element model approximates the value of the temperature at each of the 159 nodes. To present these results in a useful manner a plot of selected isotherms are shown in Figure 2.2. Figure 2.2 shows there is significant distortion of what would normally be parallel isotherms if the metal tie were not present. From this distorted temperature field the direction and magnitude of the heat flow can be approximated. The direction of the heat flow is always perpendicular to the isotherms, and the magnitude can be calculated from Equation 2.3 once the temperature gradient is known.

The magnitude of heat transfer that is important to the overall effect of the metal ties is the heat flowing either into, or out of the wall section. The heat transfer is calculated from the temperature gradient in the boundary elements, the area associated with each element, and that element's thermal conductivity (Equation 2.3). Each surface element actually represents a ring, or annulus, concentric around the tie, see Figure 2.3.

Using the node temperatures that are presented in Appendix D the temperature gradient at the interior surface of the concrete blocks were calculated for both cases - with

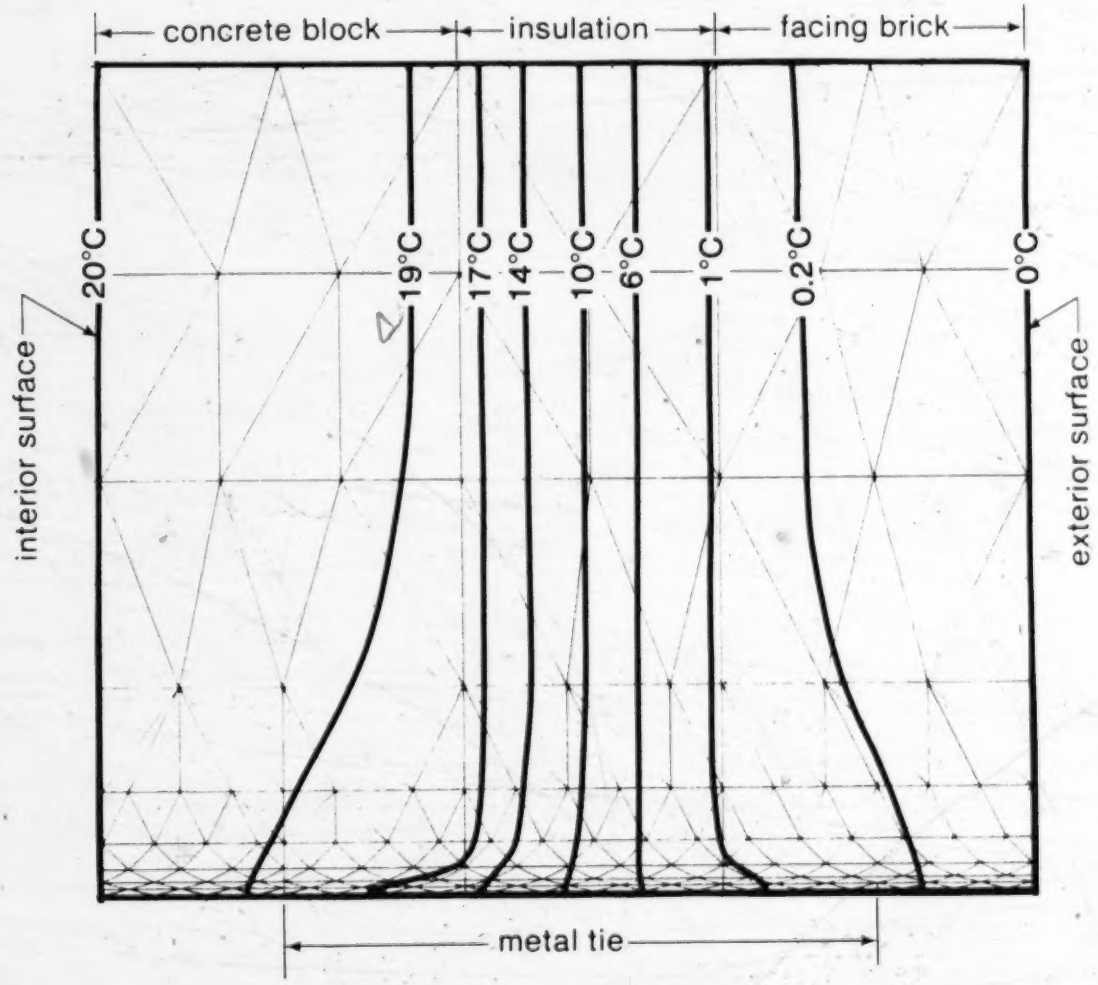

Figure 2.2 Selected Isotherms around Metal Tie

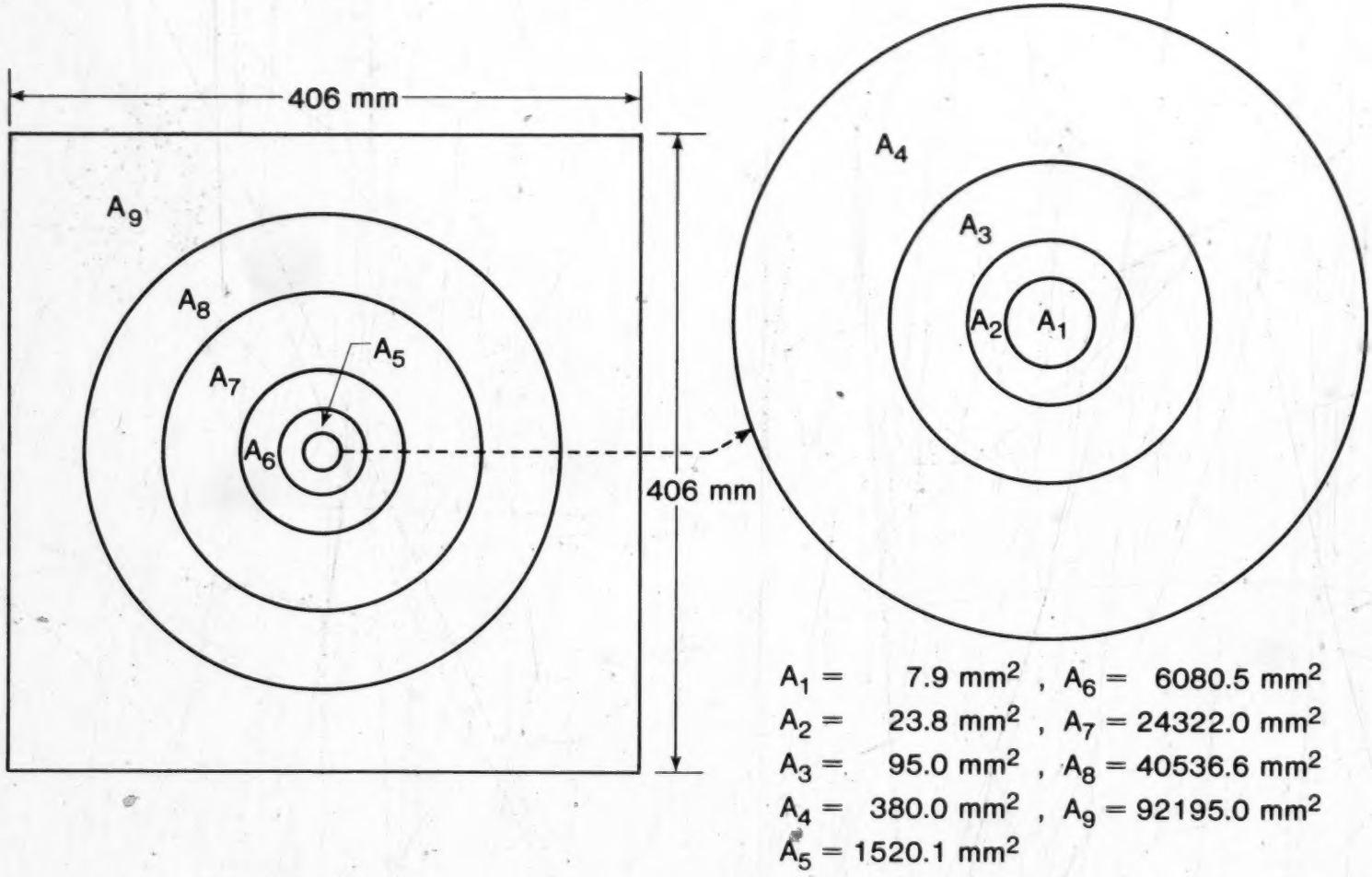

Figure 2.3 Areas Associated with Surface Elements

and without the metal tie in the wall. These temperature gradients are listed in Table 2.3. Multiplying these temperature gradients by the areas represented by the boundary element (Figure 2.3), and summing, gives the totals listed at the bottom of Table 2.3. Comparing these values to Equation 2.3 shows that the rate of heat transfer (Q) can be calculated by multiplying these total values by the material's thermal conductivity (conductivity of concrete blocks = 0.37 W/m·°C). Comparing the rates of heat transfer for the wall section, shown below Table 2.3, with and without the metal ties indicates a 10% increase in heat flux due to the ties.

These results do not relate directly to the wall section in the masonry module since the air gap and wallboard were not included in the finite element model. Without properly being able to deal with the conduction, convection, and radiation across the air gap, it is difficult to estimate the effect of the ties on the actual wall section. Also, both the concrete blocks and the facing bricks were modelled as a continuum, neglecting their internal air spaces. The effect of the ties on the actual wall section would be less than the 10% predicted for the simplified wall section. The ASHRAE zone method prediction of the masonry walls appears to be of the right magnitude, and can be considered a reasonable prediction to the effect of the metal ties.

Table 2.3 Predicted Heat Transfer Through Simplified Wall Section - With and Without Metal Ties

Annulus Number	Area x 10^4, A (m^2)	Without Metal Tie		With Metal Tie	
		$\Delta T/\Delta x$ (°C/m)	$A\frac{\Delta T}{\Delta x} \times 10^4$ (°C·m)	$\Delta T/\Delta x$ (°C/m)	$A\frac{\Delta T}{\Delta x} \times 10^4$ (°C·m)
1	0.0792	12.56	0.9948	20.80	1.6474
2	0.2375	12.56	2.9830	20.80	4.9400
3	0.9501	12.56	11.933	20.87	19.829
4	3.8003	12.56	47.732	20.87	79.312
5	15.201	12.56	190.92	19.21	292.01
6	60.805	12.56	763.71	16.57	1007.5
7	243.22	12.56	3054.8	16.57	4030.2
8	405.37	12.56	5091.4	13.14	5326.6
9	921.95	12.56	11580.	13.14	12114.0
TOTALS			20744		22876

Conductivity of concrete blocks = 0.37 $\frac{W}{m \cdot °C}$

Without steel Q = 0.7675 W

With steel Q = 0.8464 W

In this past section a detailed analysis of the polyurethane foam, air gap, and metal ties has been made to better estimate their thermal properties. Using these detailed estimations, along with the ASHRAE prediction, a single prediction of the masonry module was made. Table 2.4 is a summary of the predicted long term overall transmission coefficients of the masonry and reference modules.

Table 2.4
Predicted Overall Transmission Coefficients
for Modules 1 and 5 (W/°C)
(not including air infiltration)

Component	Module 1 Without South Facing Windows	Module 1 With South Facing Windows	Module 5
Ceiling	19.2	19.2	22.0
Main Walls	16.2[a]	15.6[a]	32.9
Door	5.2	5.2	2.0
Windows	18.5	26.8	15.8
Basement Walls	32.4	32.4	35.4[a]
Basement Floor	6.8	6.8	6.8
TOTAL	98.3	106.0	114.9

(a) Includes joist space

2.2 Long Term Experimental Results

2.2.1 Total and Relative Energy Consumption

The simplest measure of a module's overall thermal performance is its total energy consumption over a heating season. The total energy that is consumed by a module is a function of the severity of the ambient conditions, and the envelope characteristics of that module. The customary measure of the severity of the ambient conditions is the indoor-outdoor temperature difference, expressed in units of heating degree days (HDD). (The heating degree day is a unit, based on temperature difference and time, used normally in estimating energy consumption, and specifying the nominal heating load of a building during the winter. For any one day, when the mean ambient temperature is less than 23°C, the degree days are equal to the number of Celcius degrees difference between mean ambient temperature for the day and the mean room temperature.) It is important that each module have its own HDD calculated separately, since even a slight difference in thermostat set point over an entire heating season can greatly effect the energy consumption of that module.

The cumulative energy consumed by Modules 1 and 5 are plotted against each module's own HDD in Figures 2.4 and 2.5, the 1983-4 and 1984-5 heating seasons, respectively. The slopes of these lines are related to each module's overall transmission coefficient (UA), including

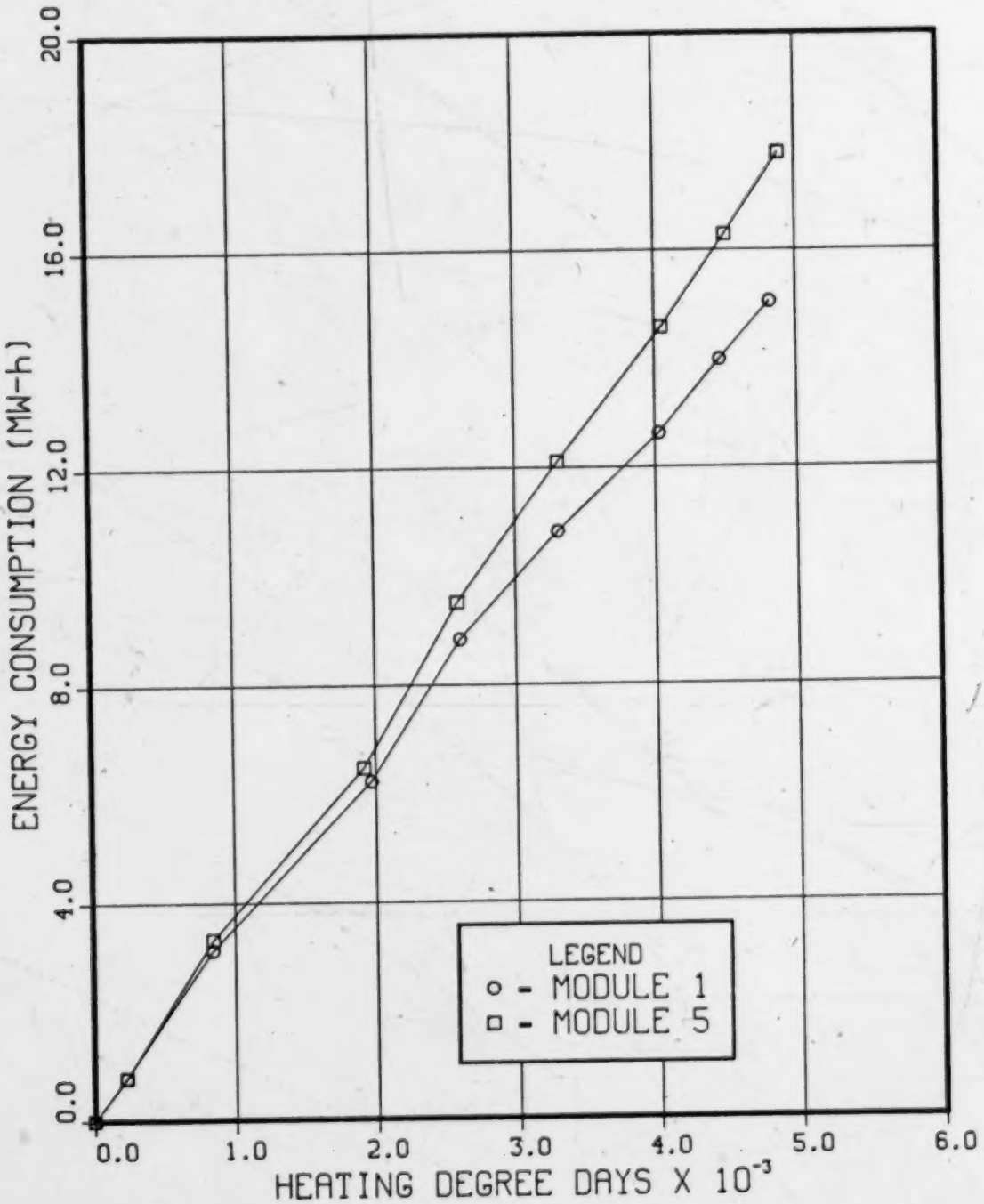

Figure 2.4 Electrical Energy Consumption for Modules 1 and 5 for the 1983-4 Heating Season

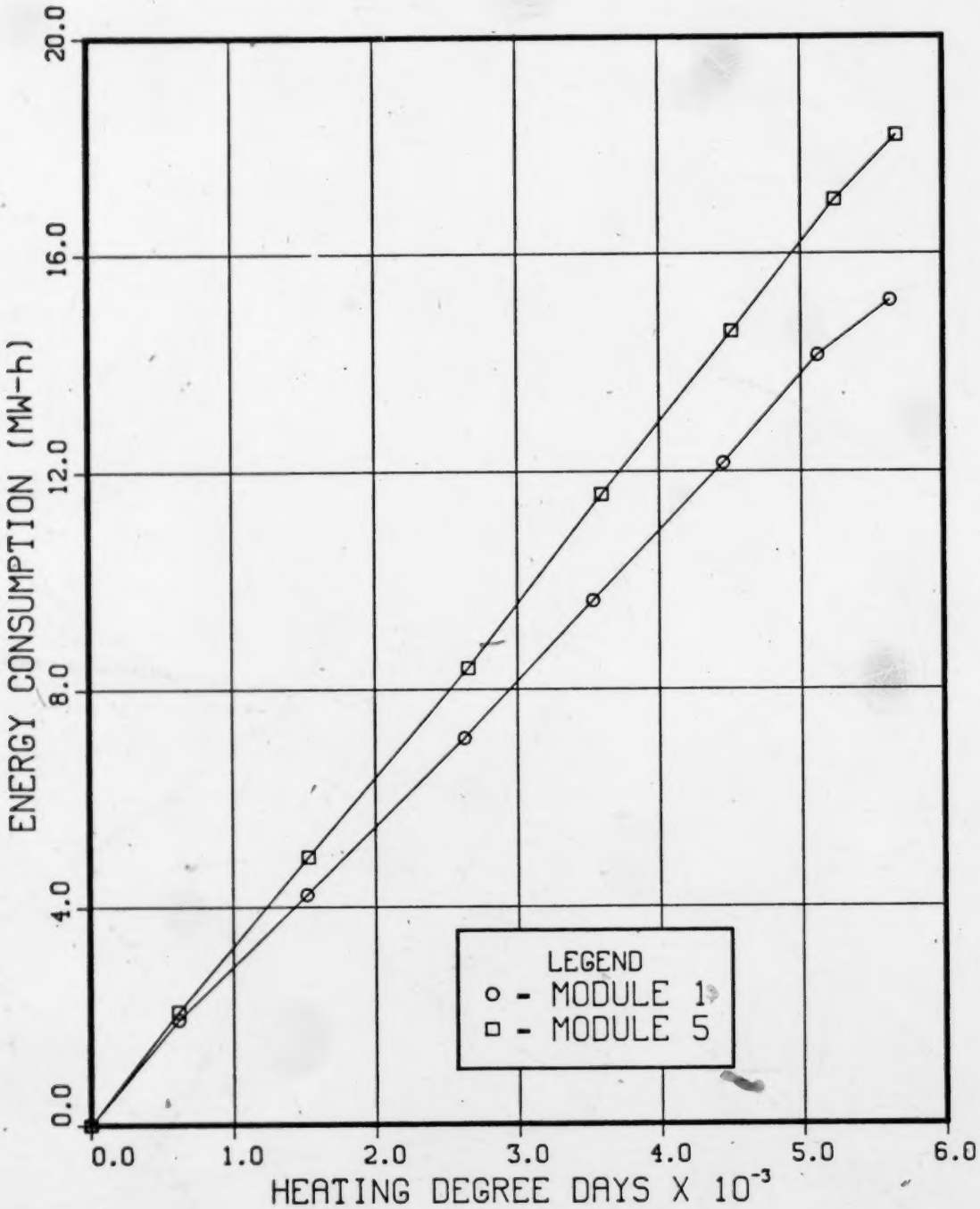

Figure 2.5 Electrical Energy Consumption for Modules 1 and 5 for the 1984-5 Heating Season

air infiltration. The lines in Figures 2.4 and 2.5 have subtle changes in their slopes over the heating season. This would suggest that the overall UA values of the modules are not constants, but change with the time of year. These subtle bends occur because the HDD does not fully describe the severity of the ambient conditions. The measure of HDD ignores variations in ground temperature, solar radiation, and wind velocity, all of which effect the module's energy consumption.

There is a sharp change in overall UA for Module 1 at approximately the 2600 HDD point of the 1983-4 heating season. It was discovered at that time that the makeup air vent in Module 1 had not been properly sealed after the module's construction. Consequently, Module 1 was severely over ventilated for the first three and a half months of its operation. A complete discussion of this part of the module's performance can be found in Section 2.2.3 on air infiltration.

It is common not to be overly concerned with the absolute value of the slopes of the lines in Figures 2.4 and 2.5. As stated before, these lines are subject to influences by ambient conditions that are not included in the measure of HDD (example, ground temperature). Since ambient conditions are the same for all modules, a large degree of seasonal variation in results can be removed by defining a module's "relative position" with respect to the reference module. The "relative position" meaning simply

the ratio of the performance of any of the modules to the performance of Module 5, multiplied by 100. In terms of energy consumption, the "relative position" also implies that any difference in HDD is accounted for between the modules.

Figure 2.6 shows the month by month relative overall transmission coefficient, including air infiltration, for Module 1. At the start of the 1983-4 heating season the relative position of Module 1 was greater than unity. This initially high relative UA for Module 1 was caused by the over ventilation problems mentioned previously. There was a similar debugging problem at the start of the 1984-5 heating season when Module 1's windows were first installed. Considering only the periods when the air infiltration rates were reasonably stable, the relative overall UA for Module 1 was 79% and 83% over the 1983-4 and 1984-5 heating seasons, respectively.

Historically at the AHHRF, the relative UA values for the modules would remain constant when no modifications were made to the modules (12). Therefore, the relative UA of a module could be used to estimate the overall effect of any modifications made to that module. The only modification made to either Module 1 or 5 between heating seasons was the addition of south facing windows to Module 1. Therefore, the addition of the south facing windows to Module 1 can be said to have increased the module's relative energy consumption 4% over the heating season.

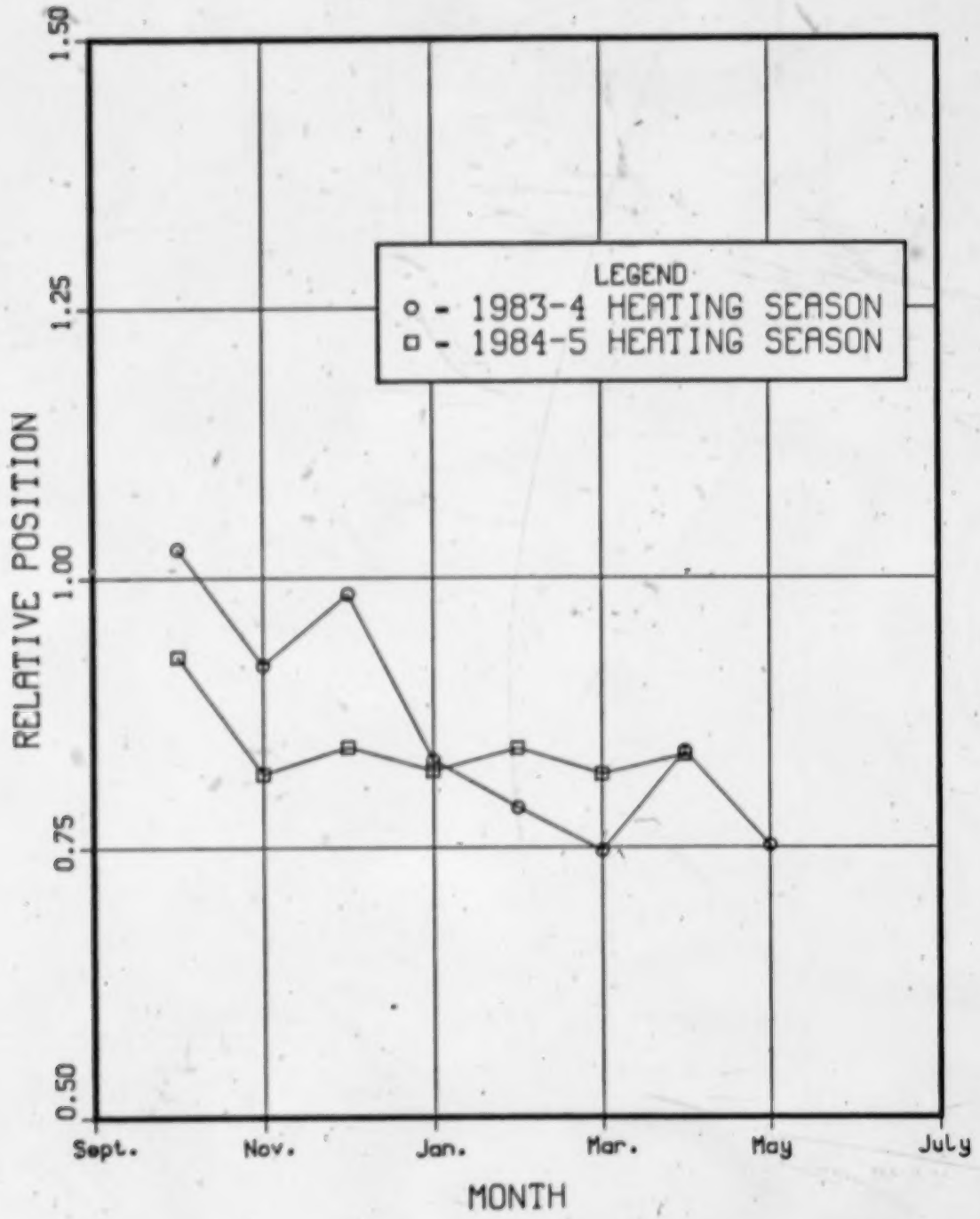

Figure 2.6 Relative Overall Transmission Coefficient (UA) for Module 1

Other problems did occur in the testing of the modules that could strongly effect these results. Primarily, the relative natural air infiltration rates between Modules 1 and 5 changed from 60% to 75% for much of the 1984-5 heating season (see Section 2.2.3). Some of this increased air infiltration could possibly be attributed to the installation of the windows. Another sources of the increased air infiltration would be the door of Module 1 which became noticeably warped. It is possible to subtract the heating load created by the air infiltration from the total energy consumed by the modules. The energy consumed without the air infiltration would constitute the heat transmission losses from the modules. The effects of the windows could then be evaluated in terms of increasing the module's heat transmission losses. The measured heat transmission losses can also be compared to the predicted UA values for the modules that were presented in Table 2.4.

The cumulative heat transmission losses of Modules 1 and 5 are plotted against each modules own HDD in Figures 2.7 and 2.8, for the 1983-4 and 1984-5 heating seasons, respectively. For the same reasons as before it is necessary to observe the changes between heating seasons in terms of a module's relative position. Figure 2.9 shows the monthly relative heat transmission losses of Module 1. During the 1983-4 heating season the relative transmission losses of Module 1 were 81%, then rose 3% to 84% for the 1984-5 heating season. The effects of the south facing

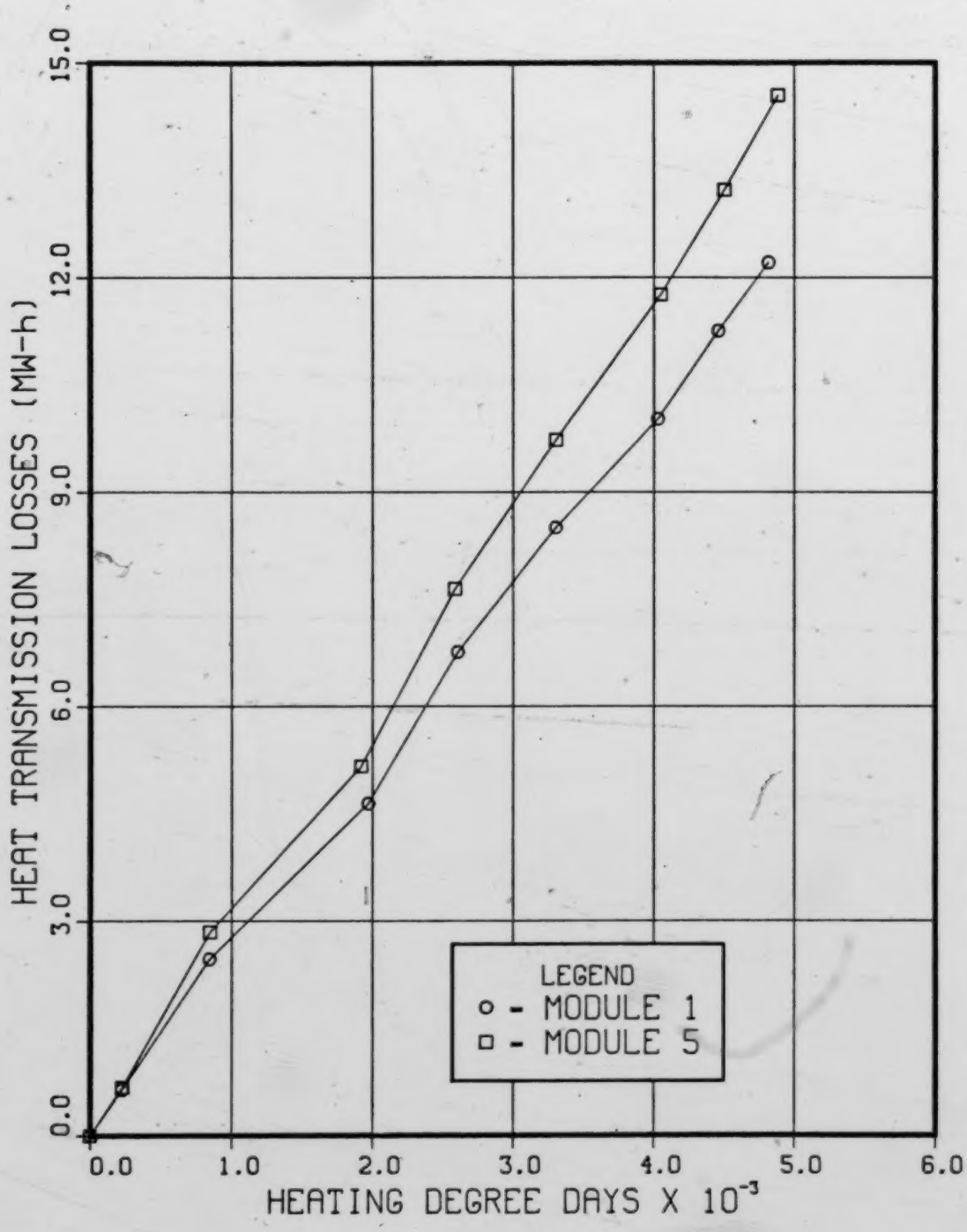

Figure 2.7 Heat Transmission Losses for Modules 1 and 5 for the 1983-4 Heating Season

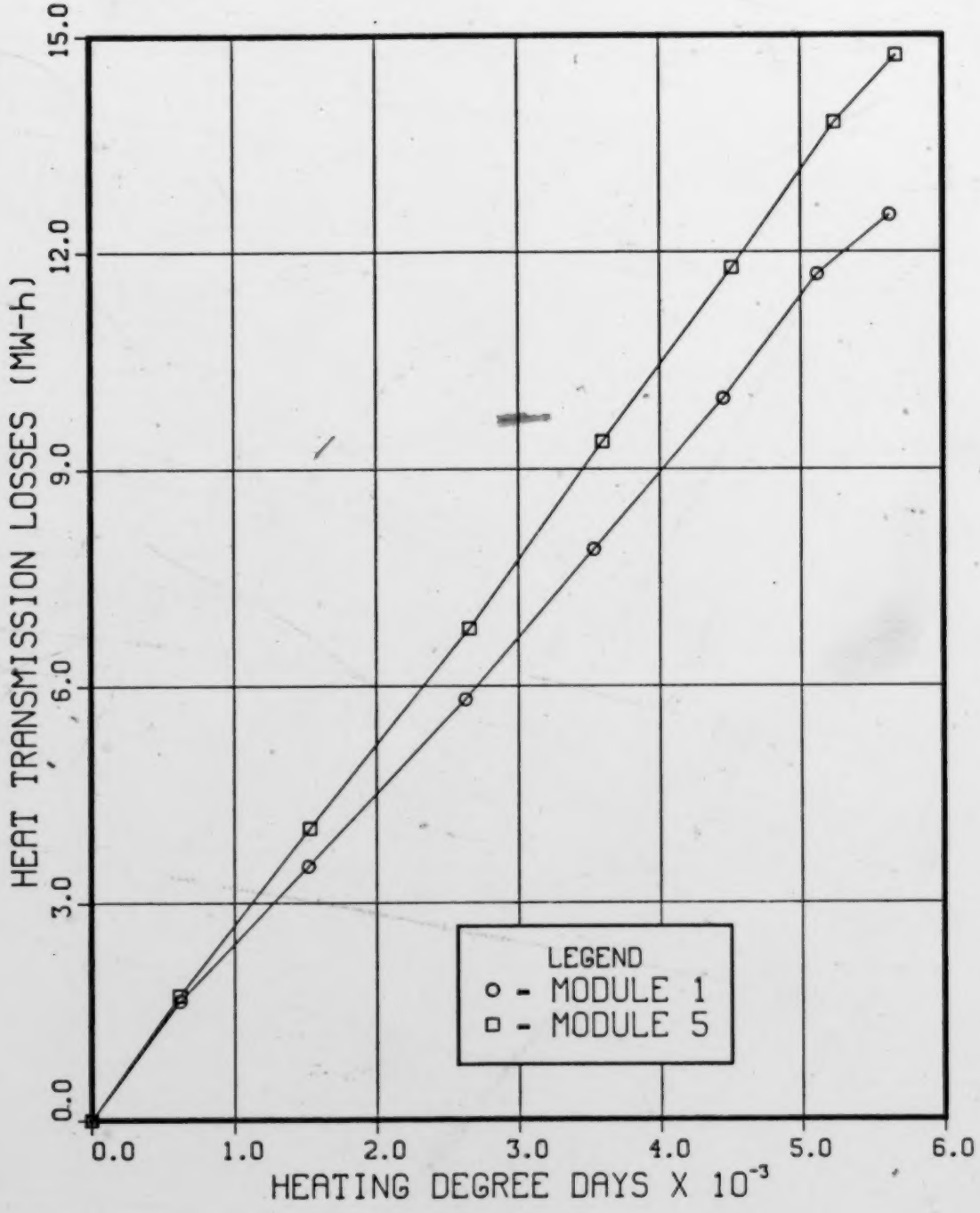

Figure 2.8 Heat Transmission Losses for Modules 1 and 5 for the 1984-5 Heating Season

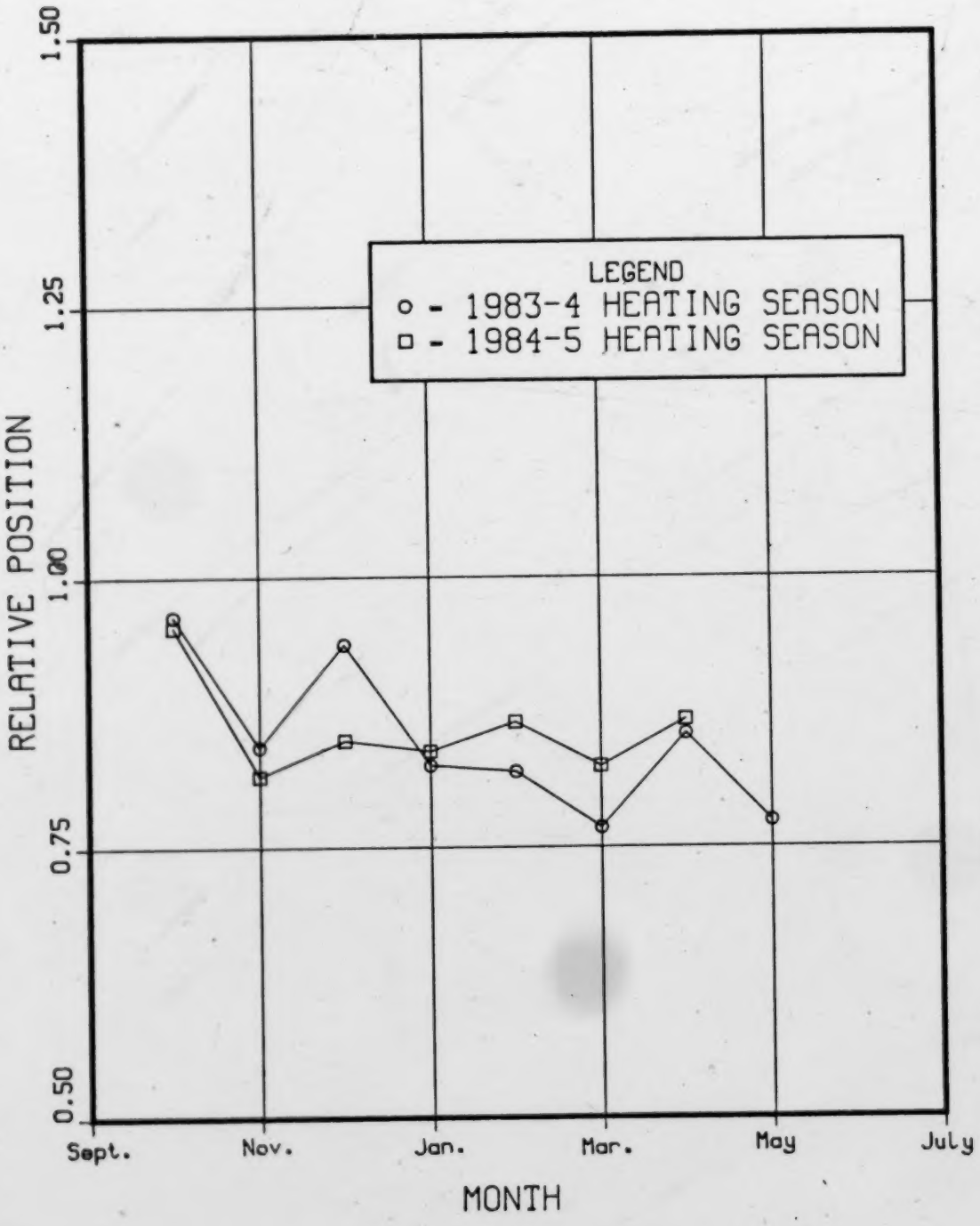

Figure 2.9 Relative Heat Transmission Losses for Module 1

windows would therefore have to be considered a detriment to Module 1's heating energy requirements.

From the slopes of the lines in Figures 2.7 and 2.8 the measured transmission coefficients without air infiltration can be calculated. Comparison of these measured UA values to the predicted values are shown in Table 2.5. Considering Table 2.5, Module 5 shows that there can be a large variation in the measured UA from year to year. This is not to surprising considering that almost half of a module is below ground level, and that the below grade heat loss is not directly a function of the measured HDD. This also stresses the need for basing comparisons between heating seasons on the "relative position" of a module's performance. Table 2.6 shows the measured and predicted relative UA values for Module 1. Note that in both heating seasons the prediction would over estimate the heat transmission losses of Module 1 relative to Module 5.

2.2.2 Measured Component Resistances

In the previous section, the concern was with the measuring of the total energy consumption of the masonry module. No attempt was made to determine the energy loss associated with the module's individual components. In this section, the measured effective thermal resistances of some of the above grade components of the masonry module are calculated. These measured thermal resistances are then compared to their predicted resistances.

Table 2.5
Comparison of Measured and Predicted UA Values for Modules 1 and 5
(W/°C) (not including air infiltration)

Heating Season	Module 1		Module 5	
	Measured	Predicted	Measured	Predicted
1983-4	102.3	98.3	126.0	114.9
1984-5	92.2	106.0	109.4	114.9

Table 2.6
Comparison of Measured and Predicted Relative UA for Module 1
(not including air infiltration)

Heating Season	Measured	Predicted
1983-4	81.0	85.5
1984-5	84.3	92.2

Combining Equations 2.1 and 2.2 together, and rearranging, the thermal resistance can be written in terms of two measurable quantities - temperature difference and heat flux.

$$q = Q / A = \Delta T / R \qquad (2.4)$$

where: Q - rate of heat transfer (W)

A - area (m^2)

q - heat flux (W/m^2)

ΔT - temperature difference (^oC)

R - thermal resistance ($m^2 \cdot ^oC/W$)

Plotting long term averages of heat flux through, and temperature difference across a component of the module, allows one to measure the in-situ thermal resistance of that component. Figures 2.10, 2.12, and 2.13 show the measured relationship between heat flux and temperature difference for four of the masonry modules heat flux transducers. In all the cases shown in these figures the averaging period for each data point was 48 hours. The thermal resistance is the inverse of the least squares regression of the data points. This measured resistance includes the resistance of the heat flux transducer (approximately 0.18 $m^2 \cdot ^oC/W$), and can be subtracted off to give the component's resistance.

Table 2.7 contains the measured thermal resistances of some of the above grade components of the masonry module. For comparison, the predicted thermal resistances of these components are also shown in Table 2.7. The predicted

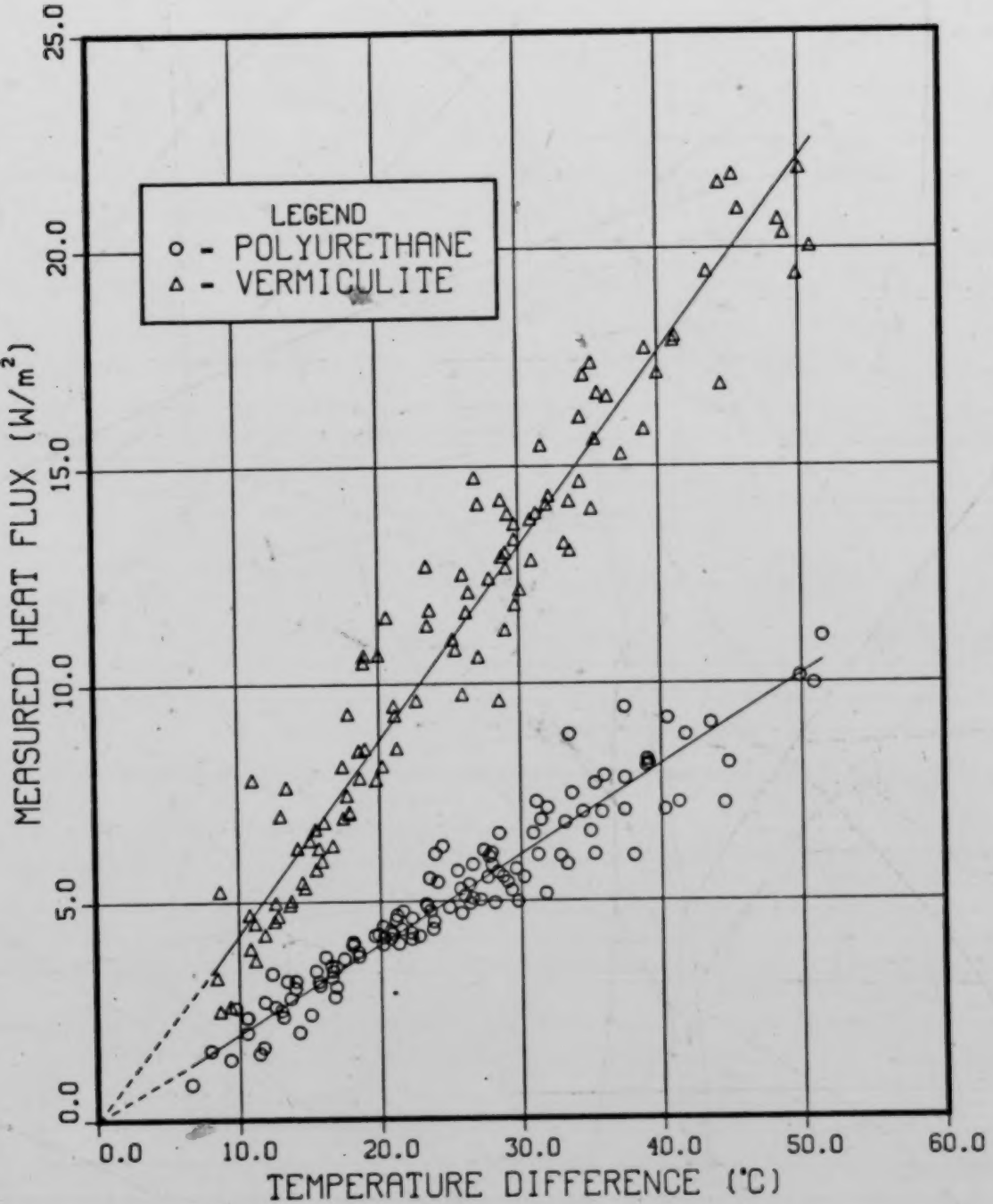

Figure 2.10 Overall Heat Transfer Coefficient for North Wall of Module 1

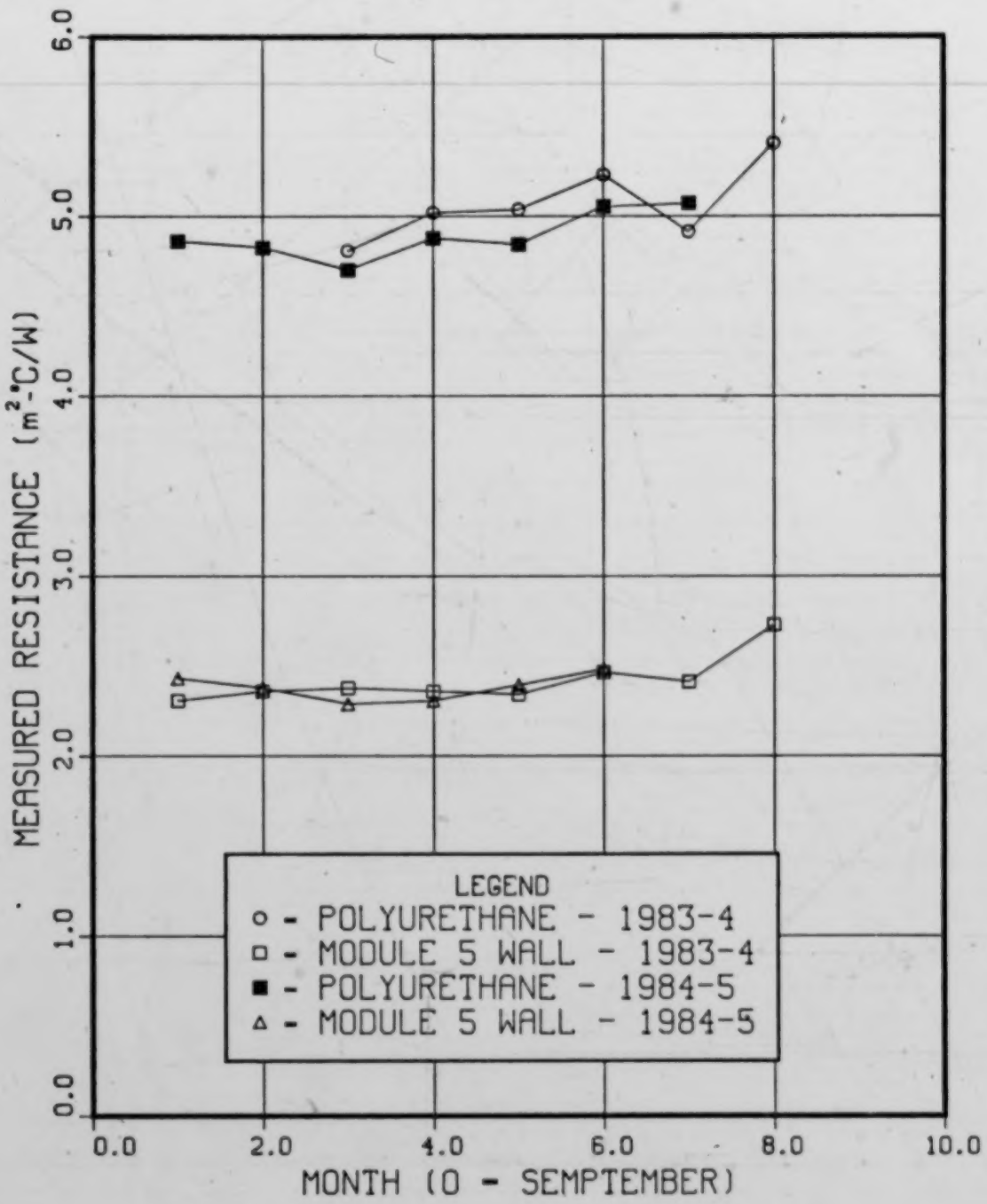

Figure 2.11 Monthly Measured Thermal Resistance of the North Polyurethane Wall Section and the Above Grade Walls of Module 5

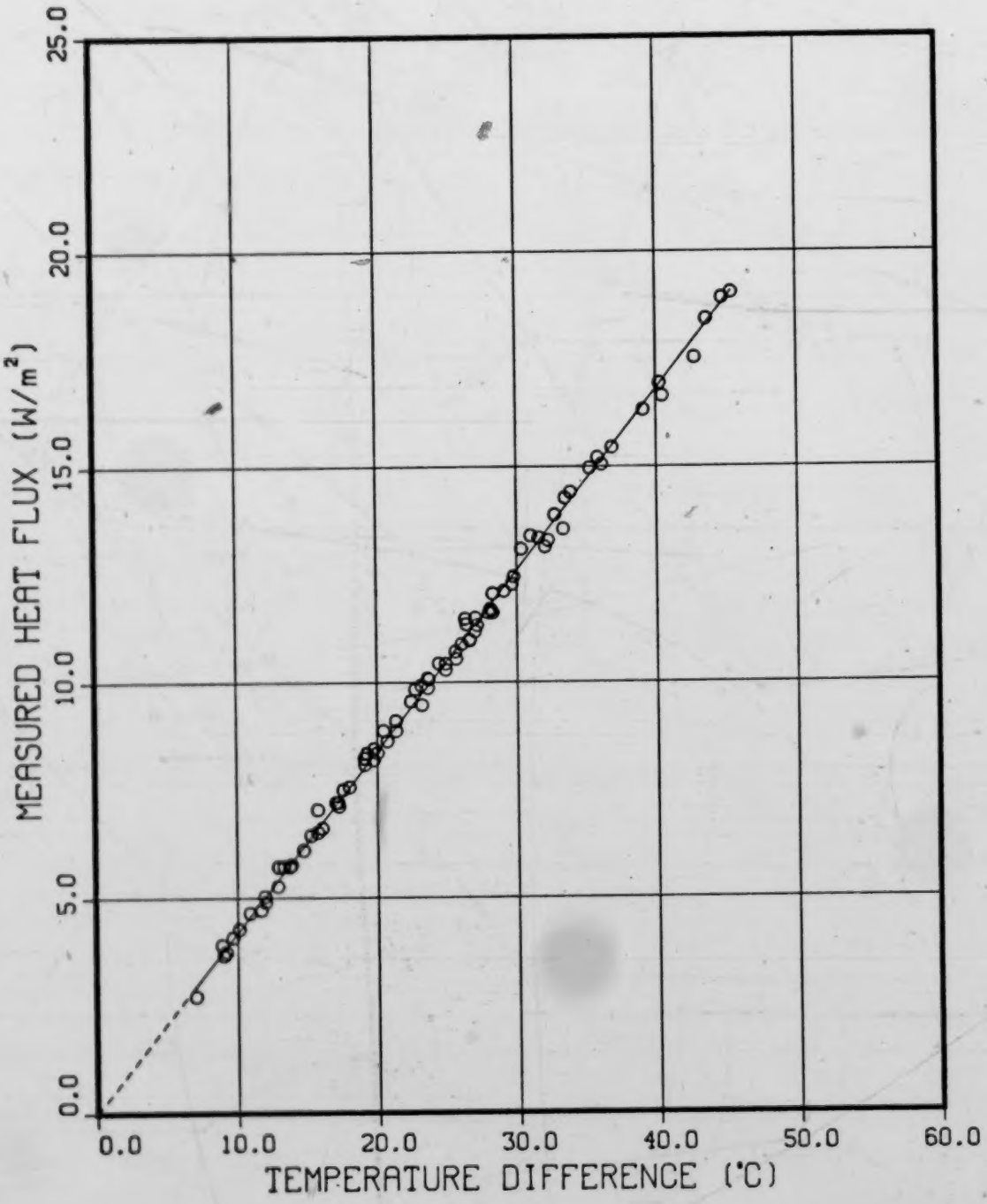

Figure 2.12 Overall Heat Transfer Coefficient for the Ceiling of Module 1

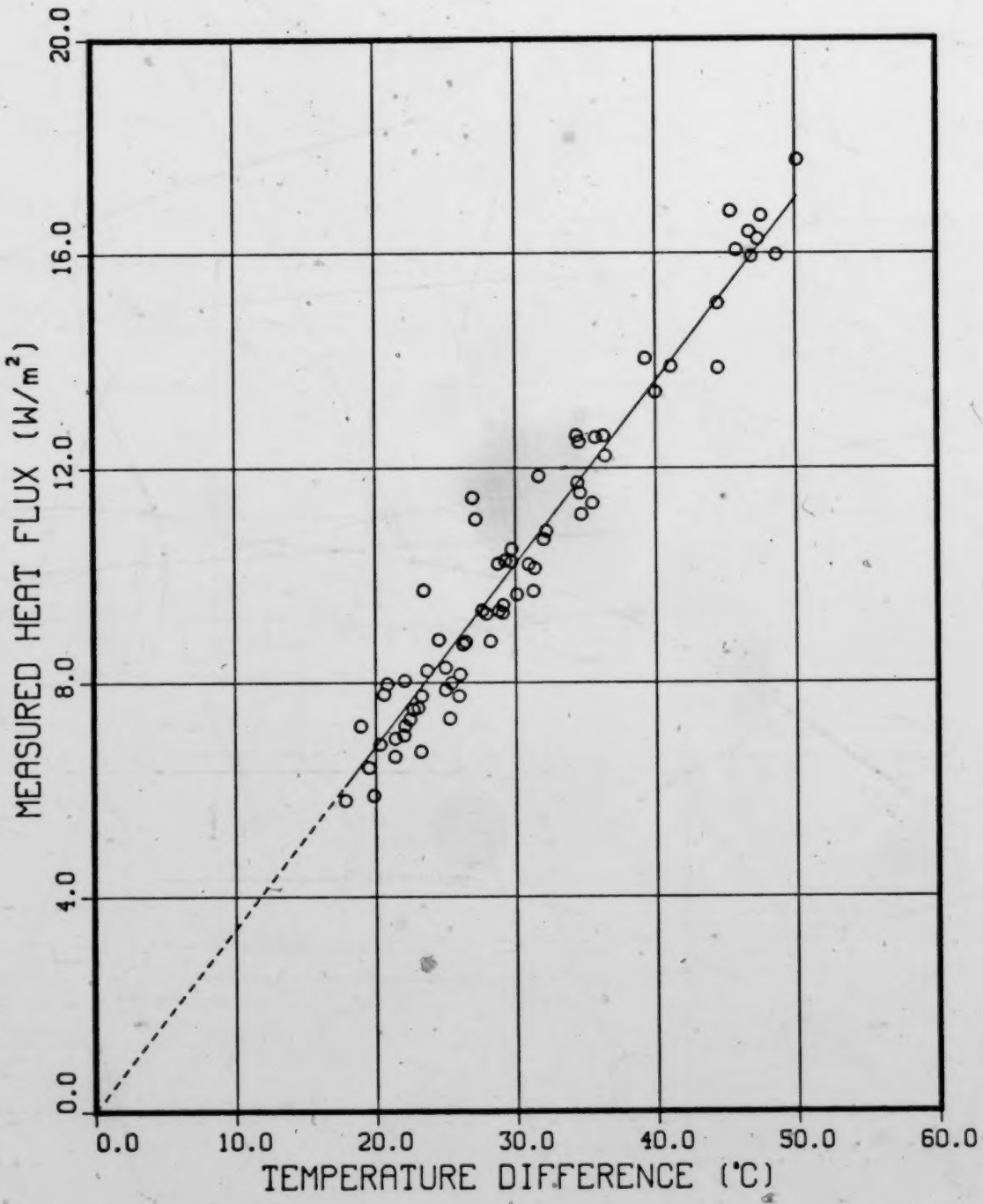

Figure 2.13 Overall Heat Transfer Coefficient for West Wall of Module 1

Table 2.7
Measured and Predicted Thermal Resistances
for Components of Module 1
($m^2 \cdot °C/W$)

Component	Measured	Predicted
Above Grade Walls		
- north polyurethane	4.76	4.62
- south polyurethane	4.81	4.62
- vermiculite	2.10	2.06
- west wall[(a)]	2.77	—
Ceiling	2.20	2.23

resistances of these components were calculated as part of predicting the long term overall heat transfer coefficients shown in Table 2.4.

Main Wall Results - not including West Wall Section

The data used in Figure 2.10 to calculate the thermal resistance of the masonry walls was taken from both heating seasons. This was done because there was essentially no measurable difference in the walls' resistance for the two years. The thermal resistance of the north polyurethane wall section was also calculated on a monthly basis. The monthly measured resistances are presented in Figure 2.11, along with the monthly measured resistances of Module 5's above grade walls. The monthly resistance of the polyurethane varied up to 5% from its mean resistance over both heating seasons. The measured average thermal resistance also decreased 3% from the first to the second heating season. This 3% change in resistance is not considered to be within the accuracy of the measuring system, and therefore cannot be attributed to the aging of the foam. Especially since the tends within each heating season are not of a consistently decreasing thermal resistance of the wall section.

Table 2.7 shows there is good agreement between the measured and predicted resistances for all of the wall sections. This agreement would tend to validate some of the assumptions used in making the predictions of the polyurethane wall sections. That is;

1) The conductivity of the polyurethane foam is close to 0.0159 W/m·°C, the value associated with unaged polyurethane.
2) The effect of the metal ties are not very significant when the wallboard and air gap are present.

By taking advantage of the thermocouples installed within the wall section, the effective resistance of the air gap can be estimated. The resistance of the air gap, wallboard, and interior air film can be calculated from the measured heat flux, and the temperature difference across just those elements. Figure 2.14 is a plot of 48 hour averages of heat flux through the north wall's polyurethane section, and the appropriate temperature difference. From Figure 2.14, the overall resistance of the air gap, wallboard, and air film is 0.52 $m^2 \cdot °C/W$. Subtracting off the thermal resistance of the wallboard and air film, listed in the ASHRAE handbook as 0.079 and 0.03 $m^2 \cdot °C/W$, respectively. The effective thermal resistance of the 25.4 mm air gap is 0.416 $m^2 \cdot °C/W$, which compares well to the estimate made in Section 2.1.2. Further extrapolation of this result would suggest that the emissivity of the polyethelene air-vapor barrier to be approximately 0.5.

Ceiling Results

For the case of the ceiling measurements, shown in Figure 2.12, the temperature difference used was between the room and attic temperatures, not the temperature difference

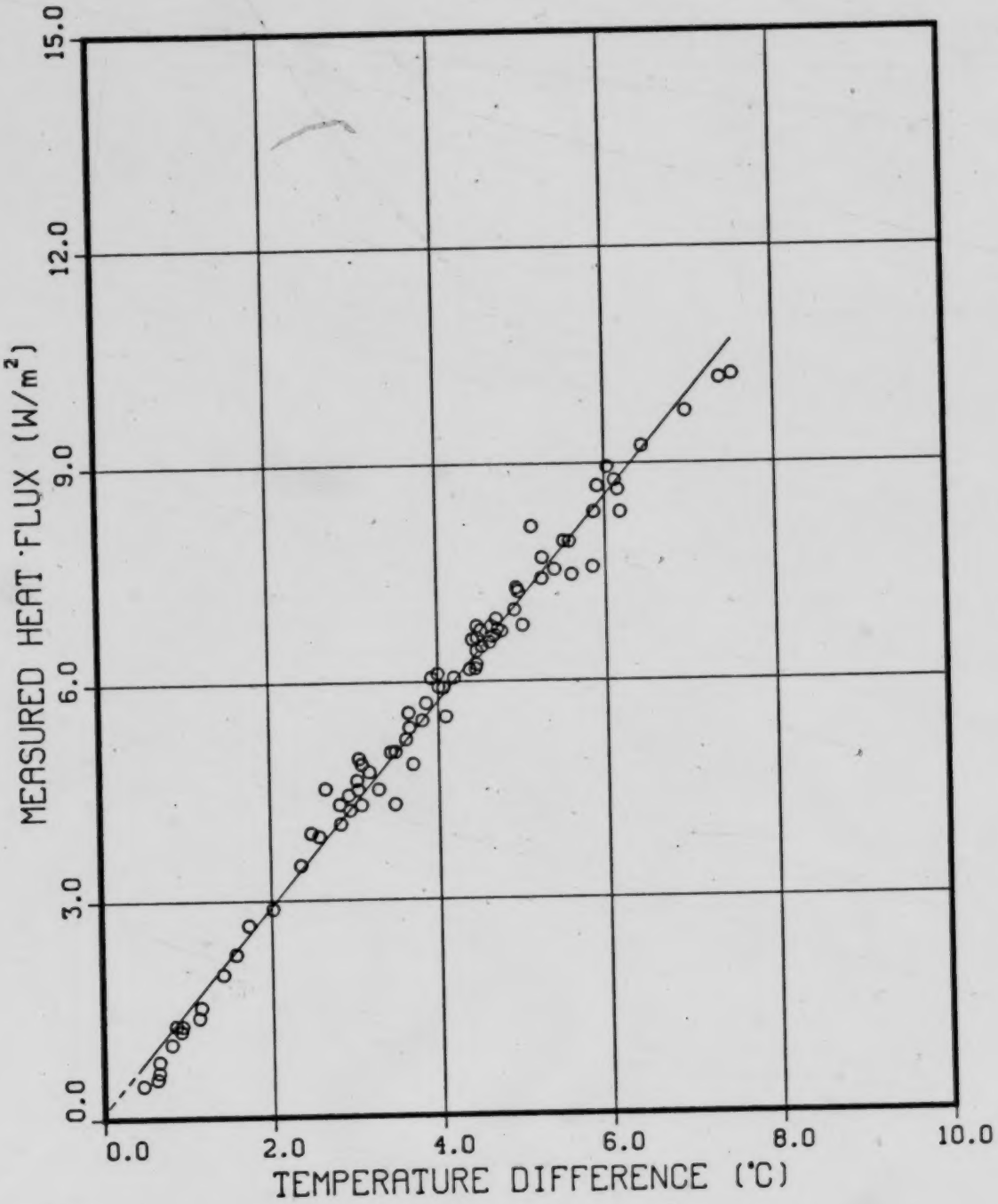

Figure 2.14 Heat Transfer Coefficient for Air Gap, Wallboard, and Interior Air Film of North Wall of Module 1

between the room and ambient temperatures. Therefore, the measured resistance of the ceiling does not include the effects of the roof structure. Table 2.7 shows very good agreement between the measured and predicted thermal resistance for the ceiling.

West Wall Results

A 356 mm wide strip of wallboard was removed from the west wall of the masonry module. In that area a heat flux transducer was mounted directly onto the concrete blocks. The intention of this west wall transducer was to substantiate the effective resistance of the 25.4 mm air gap. Also, if the transducer was fortunate enough to be placed over a metal tie, the finite element model could be tested.

The average measured thermal resistance of the north and south polyurethane wall sections is 4.79 $m^2 \cdot {}^oC/W$. Subtracting off the previously measured resistance of the air gap (0.416 $m^2 \cdot {}^oC/W$), and the resistance of the wallboard, leaves a resistance of 4.29 $m^2 \cdot {}^oC/W$. From Table 2.7, the measured resistance of the west wall was only 2.77 $m^2 \cdot {}^oC/W$, a difference of 55%.

It was necessary to remove some of the concrete blocks inorder to find the location of the metal ties. Suspecting that the metal ties, if located directly under the transducer, would account for some of this discrepancy in wall resistance. Figure 2.15 shows the positioning of the

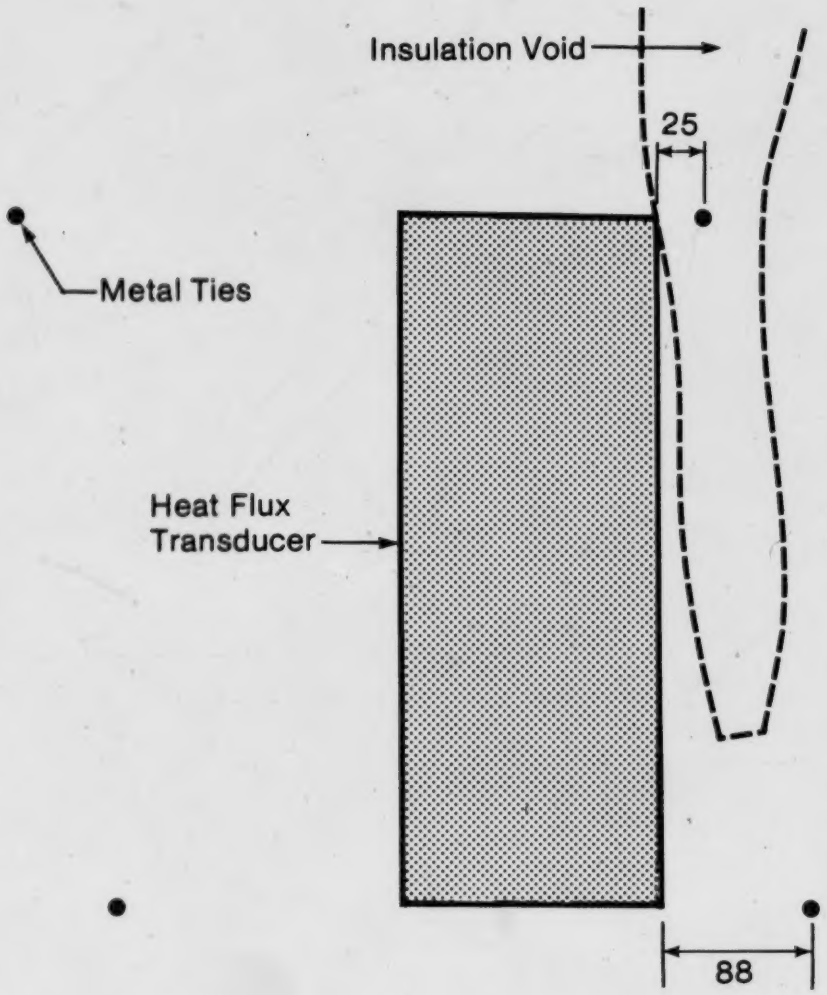

Figure 2.15 Positioning of Metal Ties Relative to Heat Flux Transducer on West Wall

metal ties relative to the heat flux transducer. The location of the ties are too far from the transducer to have any significant influence on the measured heat flux.

After completely removing the concrete blocks, a gap in the polyurethane foam was discovered immediately north of the transducer. Figure 2.15 shows the approximate size and location of the missing insulation. There was essentially no insulation between the facing bricks and the concrete blocks in this area.

This gap in the insulation made any results of the west wall heat flux transducer impossible to interpret. It does though highlight one major problem with the use of foamed-in-place insulations. That is, without being able to visually inspect the placement of the insulation there are no assurances that the wall cavities are completely filled with insulation. It should also be noted that this was not the only gap in the polyurethane insulation that was found. During the removal of the bricks to install the module's south facing windows a similar gap in the insulation was discovered.

2.2.3 Measured Air Infiltration

Weekly average air infiltration rates for Modules 1 and 5 over the 1983-4, and the 1984-5 heating seasons are shown in Figures 2.16 and 2.17, respectively. There can be large variations in infiltration rates from week to week depending on ambient conditions (indoor-outdoor temperature

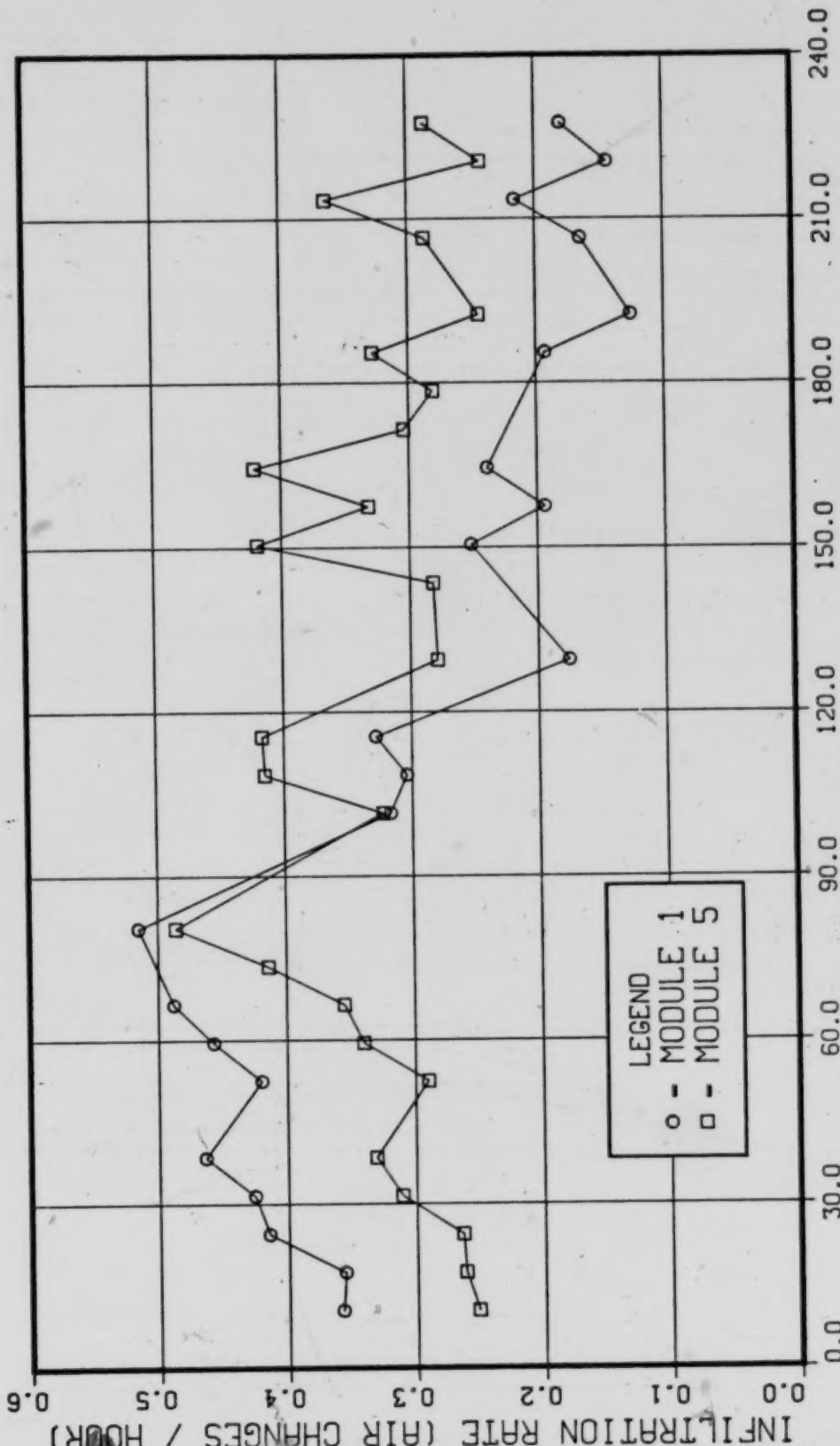

Figure 2.16 Air infiltration Rates for Modules 1 and 5 for the 1983-4 Heating Season

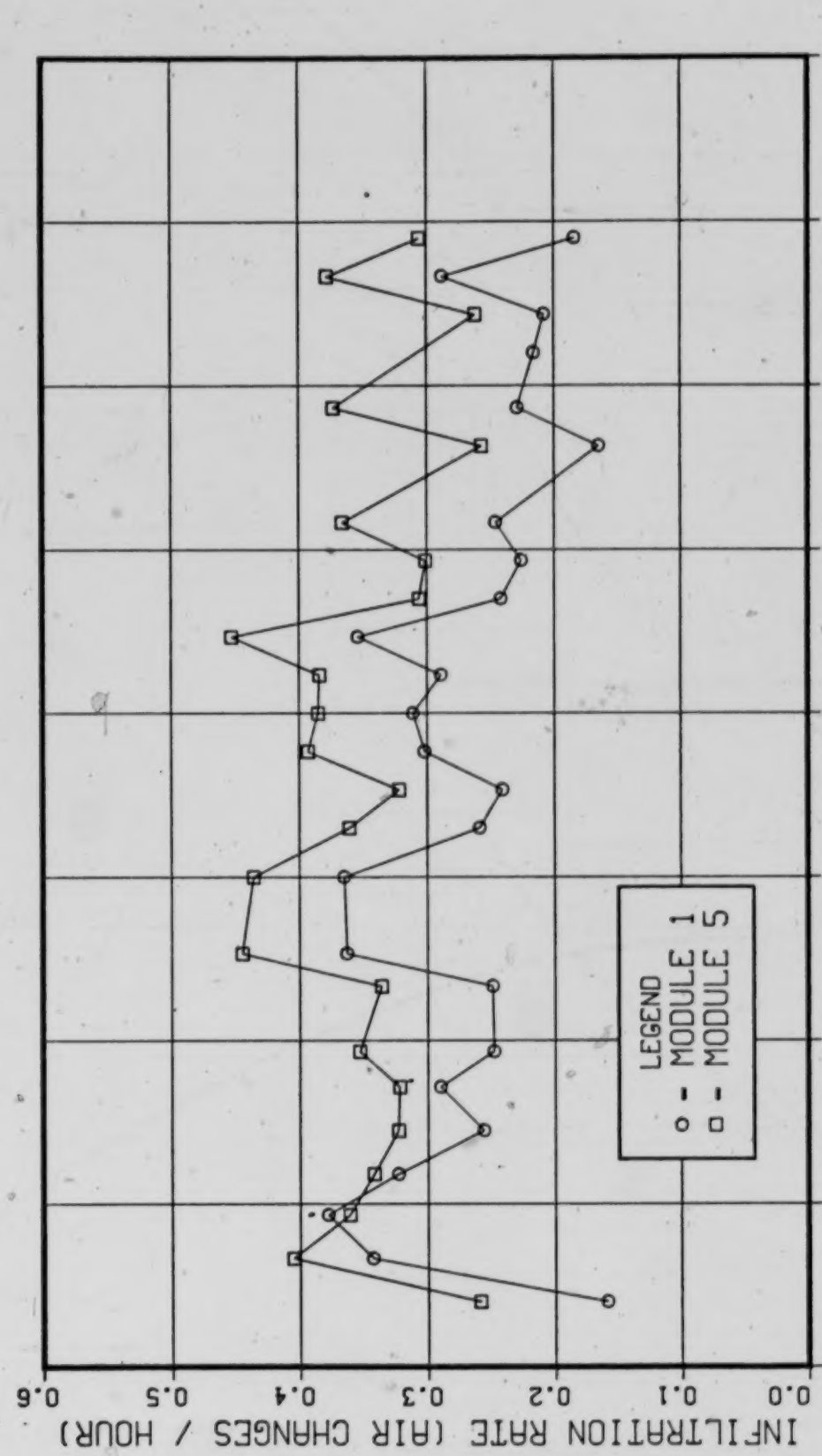

Figure 2.17 Air infiltration Rates for Modules 1 and 5 for the 1984-5 Heating Season

difference, wind speed, wind direction). Therefore, it is common to ratio the infiltration rate of the masonry module to the infiltration rate of the reference module to calculate the "relative" infiltration rate of the masonry module. Figure 2.18 shows the relative weekly air infiltration rate of Module 1 for both heating seasons.

1983-4 Heating Season

Initially the air infiltration rate for Module 1 was substantially higher than the infiltration rate for the reference module. On January 12, 1984 (day 104) it was discovered that the makeup air vent in Module 1 had not been properly sealed following its construction. Once the makeup air vent had been sealed, the average air infiltration rate for Module 1 was cut in half from 0.4 to 0.2 air changes/hour. The relative infiltration rates shows more clearly the effect of sealing the makeup air vent. Originally, the air infiltration rate of Module 1 was 1.6 times that of Module 5, and then dropped sharply to only 0.6 of that of Module 5.

This large change in air infiltration rate was responsible for the 15% change in Module 1's relative overall heat transfer coefficient from the period before sealing the vent to the period after (see Figure 2.6).

1984-5 Heating Season

After installing the two south facing windows in

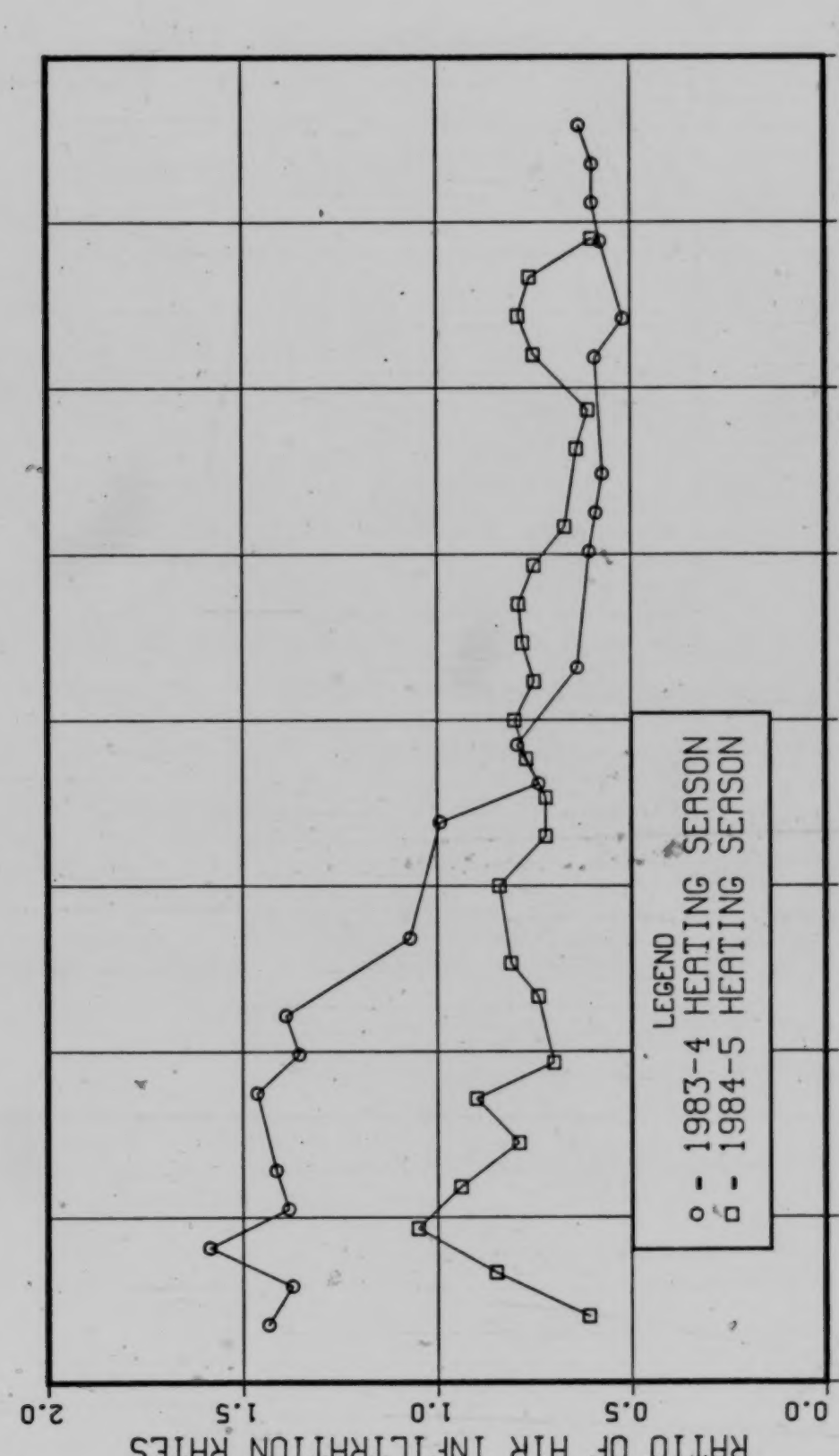

Figure 2.18 Relative Air Infiltration Rate for Module 1

Module 1 the relative air infiltration rate increased substantially, and the windows had to be resealed. The weatherstripping on the door of Module 1 also had to be adjusted periodically because the door was warping. Once these problems had been solved, Module 1's average air infiltration rate was about 0.26 air changes/hour. This is up slightly from the 1983-4 heating season's air change rate. Comparisons between heating seasons should not be made using the absolute value of the air infiltration rates because of their dependency on ambient conditions. Instead comparisons of Module 1's natural air infiltration rate between heating seasons should be based on its relative infiltration with Module 5. Since both modules experience similar climatic conditions the relative infiltration rates are not strongly dependent on ambient conditions. The relative infiltration rate of Module 1 was 0.75 for the 1984-5 heating season, up from 0.6 in the previous heating season. This is a 15% increase in the relative air infiltration rate from the 1983-4 heating season.

The possible sources of air infiltration can be located by depressurizing a module 50 to 100 Pa below atmospheric pressure. With this severe depressurization of a module, outdoor air will be drawn in through holes in the module's envelope, and using a smoke source the location of the holes can be identified.

Below is a listing of the leakage sites detected in

Modules 1 and 5.

Module 5:
- around all windows and window frames
- around door and door frame
- at instrumentation cable conduits
- makeup air vent
- no leakage at the sill plate above the basement walls

Module 1:
- around all windows except the south facing windows
- around door and door frame
- at instrumentation cable conduits
- between the main floor walls and the basement walls in the vermiculite wall section only
- no leakage at makeup air vent

CHAPTER 3

SHORT TERM THERMAL BEHAVIOR OF MASONRY MODULE

In the previous chapter discussion centered around the long term thermal performance of the masonry module. Viewing the masonry module, or any of its components in the long term allowed the analysis to ignore the cyclic or periodic nature of the ambient conditions. In this chapter, analysis will focus primarily on the masonry module's response to the changing ambient conditions.

The first part of this chapter will present an analytical solution to a composite wall's response to a sinusoidally varying ambient temperature. Experimental results from the masonry module will then be presented to show the actual wall response. The masonry wall's response has important implications for the module's overall heating load in the short term. The final part of this chapter presents other short term experimental results that show the effect of the south facing windows, and the results of temperature decay tests.

3.1 Steady Periodic Heat Transfer

In general, the heat transfer through the above grade portion of a building is not steady with time. The

temperature inside a building is held almost constant ($20 \pm 1^{o}C$), but the ambient temperature is continually changing. This continually changing, almost random, boundary condition on one side of the wall makes the heat transfer analysis very complex. In order to study the heat transfer through a wall of a building it is necessary to simplify the ambient boundary condition.

Common experience suggests that the ambient temperature is not random, but is somewhat periodic, in a diurnal cycle. To a first approximation the ambient temperature can be assumed to be varying sinusoidally with a period of 24 hours. Using this simplification, the heat transfer through a single component wall is shown in Figure 3.1. The walls of the building are represented by an infinite slab of thickness L. The boundary conditions applied to the two surfaces of the slab represent the building interior conditions, and the simplified ambient conditions.

The important quantity in terms of building heating load is the heat flux at the wall's interior surface. Figure 3.2 shows qualitatively the response of a wall section in terms of the interior heat flux when subjected to the boundary conditions stated previously. There are two different wall responses shown in Figure 3.2 - one the "potential" heat flux and the other the "actual" heat flux. The "potential" heat flux is the idealized maximum limit to the heat flux through the wall for a given temperature

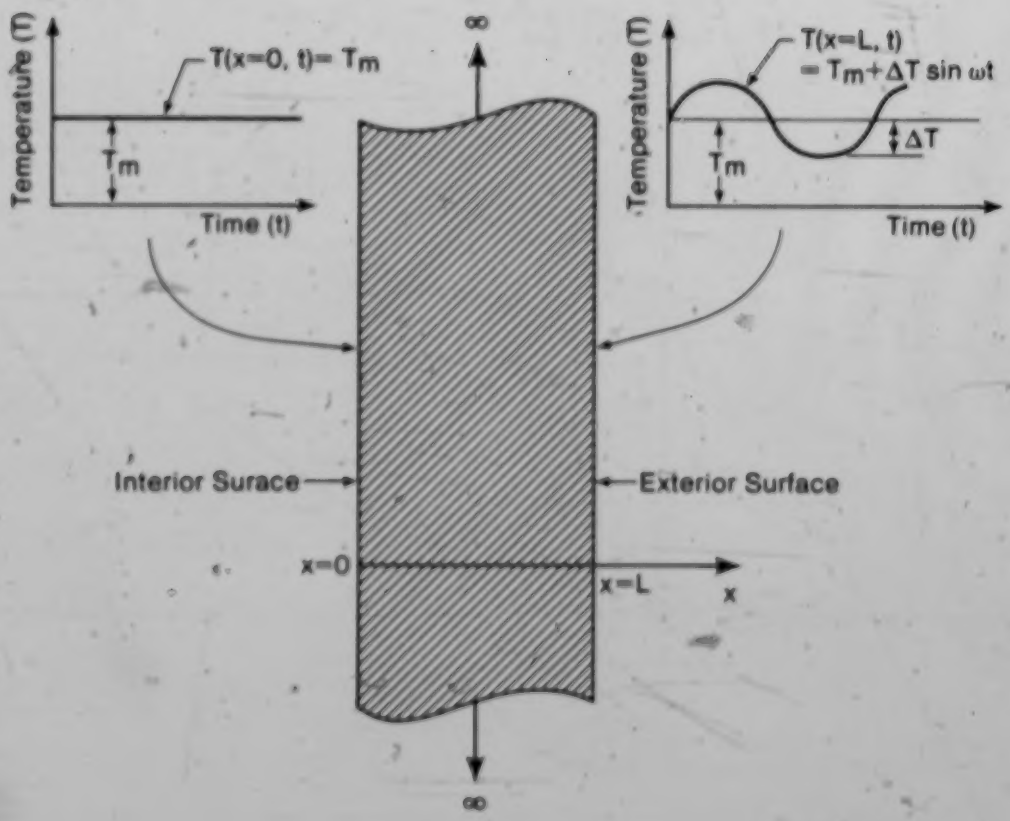

Figure 3.1 Steady Periodic Heat Conduction through a Finite Slab

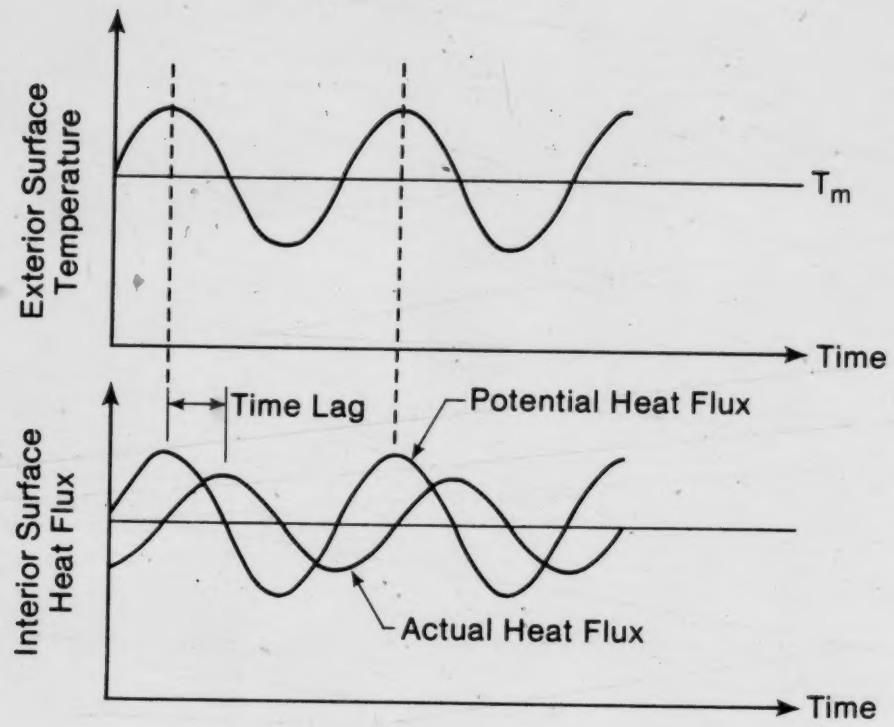

Figure 3.2 Potential and Actual Heat Flux Response to Steady Periodic Heat Conduction

difference. The "potential" heat flux can be calculated from the instantaneous interior-exterior temperature difference and the wall's thermal resistance, assuming the wall has no energy storage capability and considering the problem to be quasi-steady state. Since the diffusion of heat through the wall section requires a finite amount of time the problem is not quasi-steady state. The actual heat flux lags behind the potential heat flux, and is also somewhat reduced in amplitude. When analyzing the masonry walls in the short term the time lag and the attenuation in heat flux amplitude will be the two quantities used to quantify the wall's response. The definition of the time lag of a wall section is shown in Figure 3.2. The attenuation in heat flux is defined a the ratio of the actual heat flux to the potential heat flux.

The walls of the masonry module are constructed of layers of different materials, and therefore can be considered to be a composite slab. An analytical solution for the steady periodic heat transfer through a composite slab can be found in Carslaw and Jaeger (13). To use this solution the concrete block, facing brick, and the air gap have to be idealized as homogeneous materials that transfer heat only by conduction.

A computer program has been written based on Carslaw and Jaeger's solution and is given in Appendix E. The program was written for the boundary conditions:

1) Specified constant temperature of a medium on the

interior side of the slab.

2) Specified sinusoidal temperature of a medium on the exterior side of the slab.

The output of the program is the amplitude, and time lag of the heat flux at the interior surface of the composite slab. Shown in Appendix E is an example problem for the heat transfer through the idealized form of the polyurethane section of the masonry walls. The predicted time lag for the interior heat flux is 9.9 hours, and the attenuation from the potential heat flux is 0.15. A similar prediction for the vermiculite wall section shows a time lag of 8.8 hours, and an attenuation of about 0.21.

An interesting result from the use of the analytical solution is the response of a composite slab is dependent on the order of the layers. That is, both the time lag and amplitude of interior heat flux can be changed by simply exchanging the position of the different materials. Another result exemplified by the use of this solution is that the time lag is a function of a material's thermal diffusivity, and not just its thermal capacitance.

3.2 Short Term Experimental Results

3.2.1 Response of Masonry Walls

The actual response of the masonry walls to changing ambient temperatures can be observed by using the thermocouples inside the wall section. Figures 3.3, 3.4,

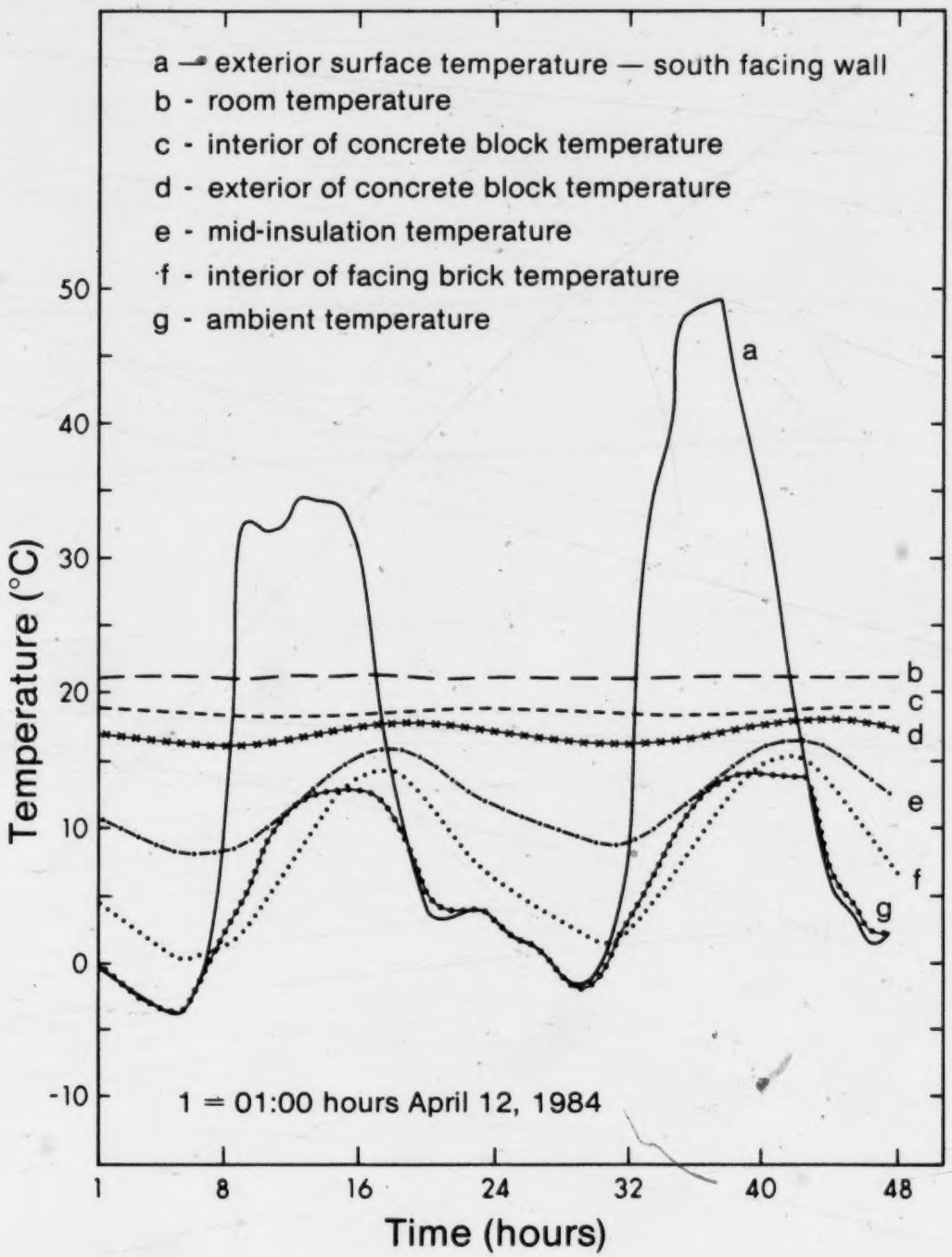

Figure 3.3 Internal Wall Temperatures for North Polyurethane Wall Section

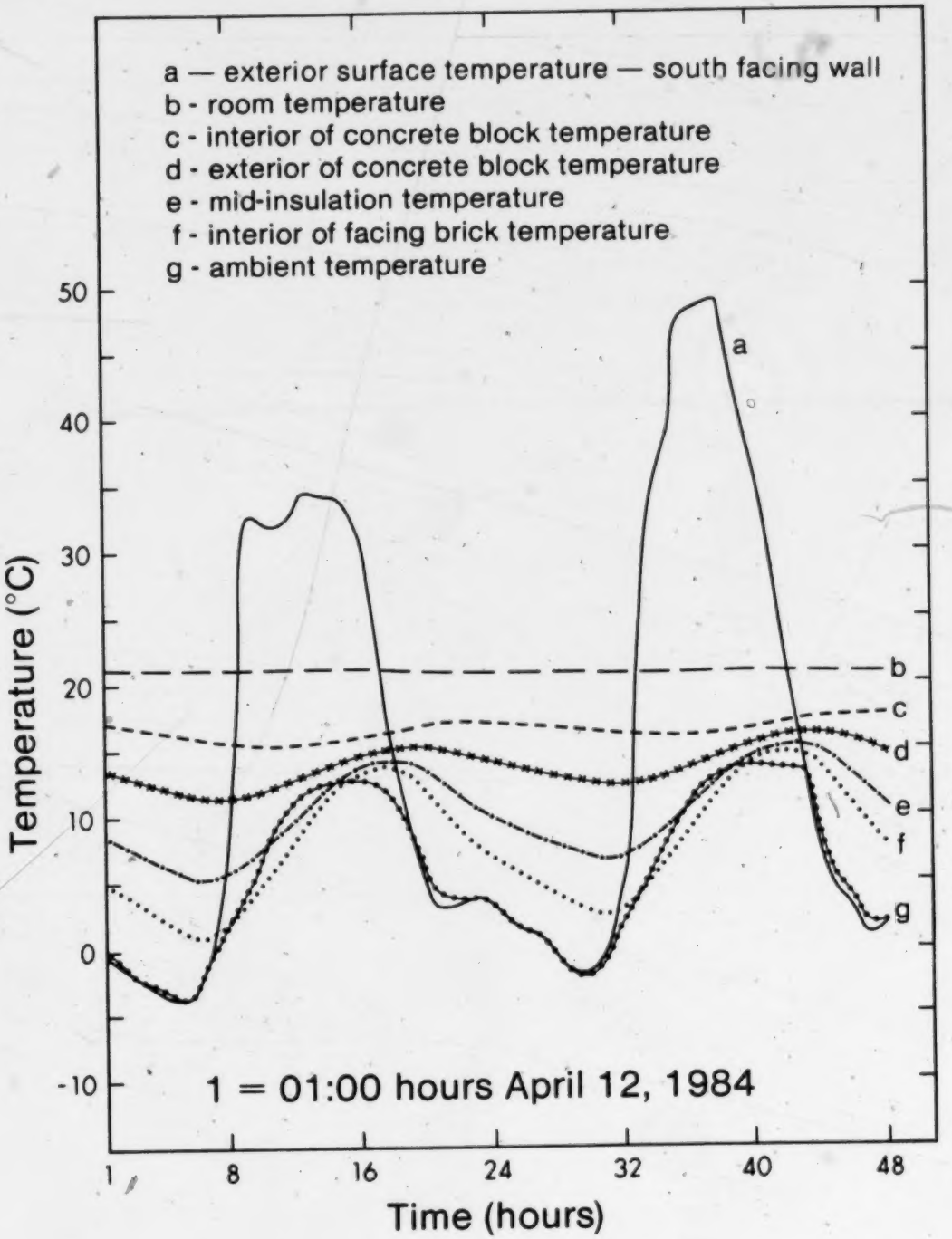

Figure 3.4 Internal Wall Temperatures for North Vermiculite Wall Section

and 3.5 show the hour by hour temperature reading across the wall section at three different locations. Figures 3.3 and 3.4 are the measured temperatures in the north polyurethane wall and the north vermiculite wall sections, respectively. Figure 3.5 is the measured temperatures across the the south wall section. Plotted concurrently on all these figures are the ambient and room air temperatures, and the temperature on the exterior surface of the south wall of Module 2. Though this exterior temperature is not directly applicable to the masonry module, due to different material properties of the wood frame walls of Module 2, it does give a good indication of the temperatures experienced by south facing walls.

In Section 3.1 the assumption was made that the ambient boundary condition could be approximated as a sinusoid. For the two days of April 12 and 13, 1984 shown in Figures 3.3 through 3.5, the ambient temperature is roughly a sinusoid. Figure 3.5 shows that the heat transfer through the south facing wall section is strongly influenced by solar radiation. The temperatures inside the south wall follows the exterior surface temperature, and not the ambient air temperature. The exterior surface temperature is also roughly sinusoidal in shape but with a larger amplitude then the ambient temperature. By comparing the time that peaks (or troughs) occur in the different temperature lines the development of the time lag within the walls can be followed.

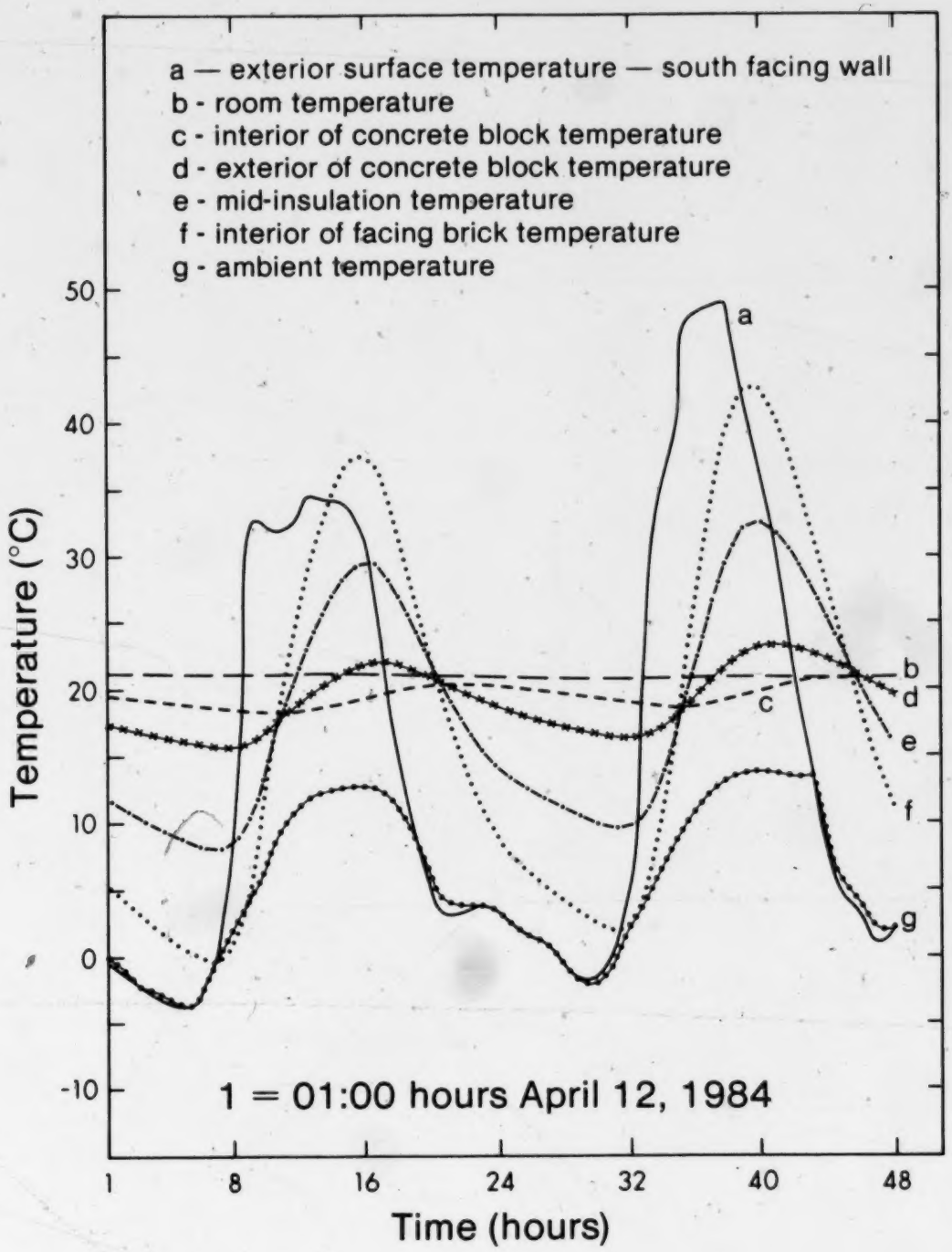

Figure 3.5 Internal Wall Temperatures for South Polyurethane Wall Section

In Section 3.1 the time lag of a wall was defined in terms of the heat flux at the interior surface lagging behind the outdoor temperature changes. Figure 3.6 shows the measured hour by hour heat flux at the interior surface of the masonry module for April 12 and 13, 1984. The time lag can be measured by comparing the time that the largest indoor-outdoor temperature difference occurs (Figures 3.3 - 3.5) to the time the largest heat flux occurs (Figure 3.6). The time lag between the interior heat flux and the ambient temperature is approximately 8 hours for the vermiculite and the south polyurethane wall sections. The time lag of the north polyurethane wall section appears to be slightly longer at about 10 hours. The faster response of the south polyurethane wall compared to the north polyurethane wall section is believed to caused by the rapid changes in exterior surface temperature of the south wall during certain times of the day. These rapid changes no longer represent a sinusoid of a 24 hour period, but having a period somewhat shorter, and therefore making the wall's response faster. Comparing the measured and predicted time lags for the two north wall section shows good agreement. The attenuation in the amplitude of the heat flux could not be estimated from the experimentally measured heat flux.

As a result of this time lag, the time of the largest wall heat losses and the coldest ambient temperatures no longer coincide. For the two day period shown here the largest wall heat loss from the north polyurethane section

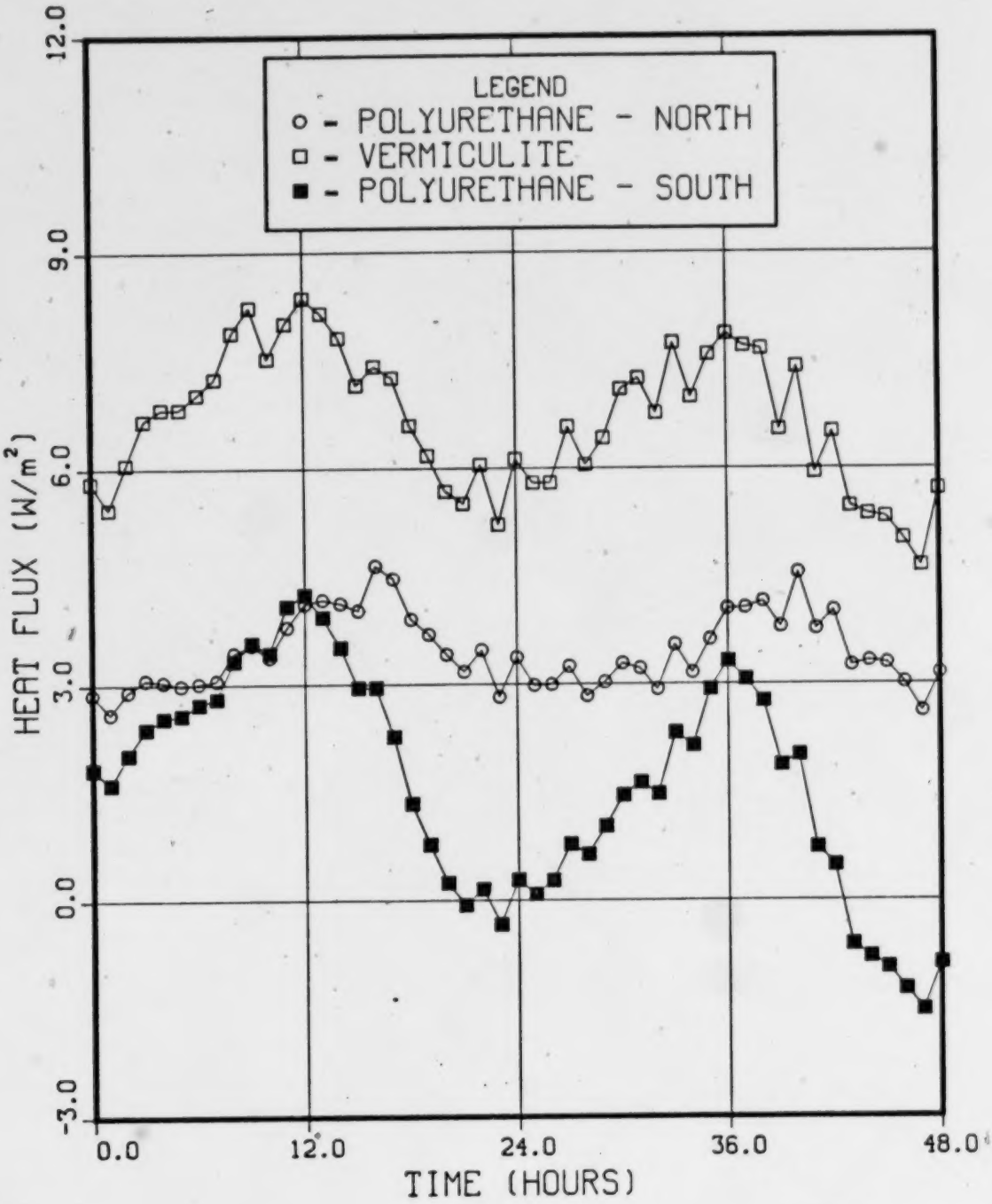

Figure 3.6 Wall Heat Flux for April 12-13, 1984

occurs at approximately 16:00 MST (The smallest heat loss from the walls occur at 04:00 MST.)

Another result of the wall's time lag can be seen by observing the interaction of the wall's heating load with the rest of the module's load. The overall module heating load can be separated into walls, ceiling, basement, and air infiltration loads. The basement can be considered to be a type of base load that remains constant on a daily basis. All other component loads vary periodically, but not necessarily in-phase with changes in the ambient temperature. The air infiltration load is in-phase with the ambient temperature changes because the infiltration rate,and the energy contained in the air, are related directly to the indoor-outdoor temperature. The heating loads for the ceilings of the modules, as well as for standard wood frame walls, are almost in-phase with respect to changing ambient temperature. The masonry walls because of their thickness, and overall low thermal diffusivity are out-of-phase with the other loads by several hours.

Summing the component loads together will give the overall heating energy requirement for the module. In the case of a standard wood frame module all the components of the module would have their peak loads coincide, creating large diurnal swings in heating energy requirements. In the case of a masonry module not all the component loads are in-phase with each other, and consequently the heating load is more balanced. For both cases, the sum of the energy

transferred would be the same when integrated over one complete cycle (given that the component thermal resistances is the same). These points are confirmed in Figures 3.7 and 3.8 where Module 5 shows a much larger day-night variation in power consumption than Module 1. Therefore, the effect of the masonry walls is to balance the overall heating requirements of the module more evenly over the day. (The lower mean power consumption of Module 1 shown in Figure 3.7 is due to higher thermal resistance of the walls and lower natural air infiltration rates than Module 5.)

Taking these arguments one step further, there exist a time of year when real energy saving become possible simply because of the wall's lagging response. Consider a time of year when the daily ambient temperature creates a situation of alternate heating and cooling loads for the module. The masonry walls, because of their load balancing effect, would not allow extreme nighttime heating loads or extreme daytime cooling loads to develop. Therefore, less energy would be required for both heating and cooling in order to maintain constant room temperature in a masonry module.

To quantify the magnitude of this time lag effect, the relative overall heat transfer coefficient (UA) can be split into "day" and "night" values. Using only data during the 1983-4 heating season (no south facing windows) after the air infiltration rates of Module 1 had stabilized, the relative UA of Module 1 was 79%. The "day" relative UA was 87%, while the "night" value was only 72%. That is, if the

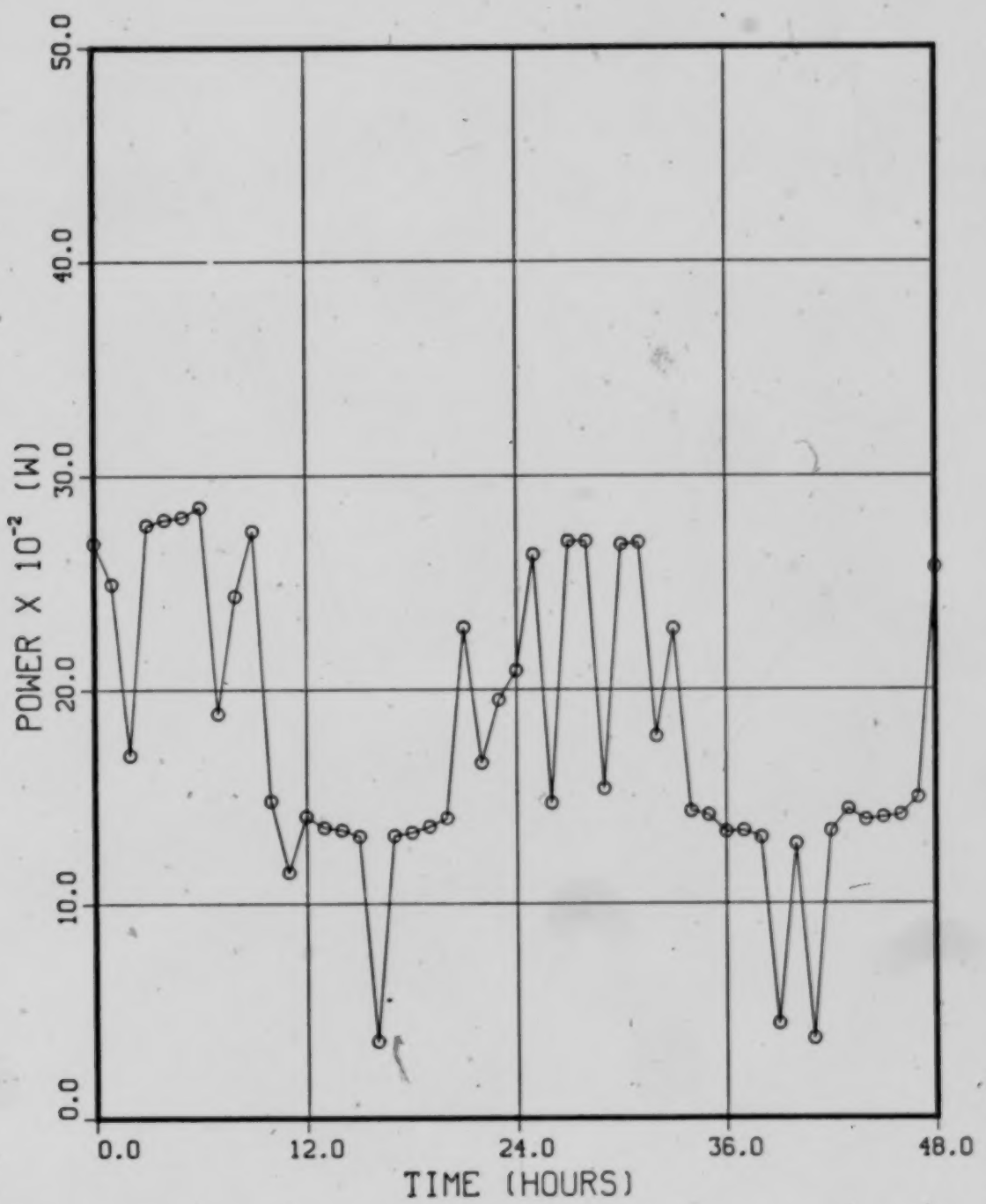

Figure 3.7 Measured Power Consumption for Module 1 for April 12-13, 1984

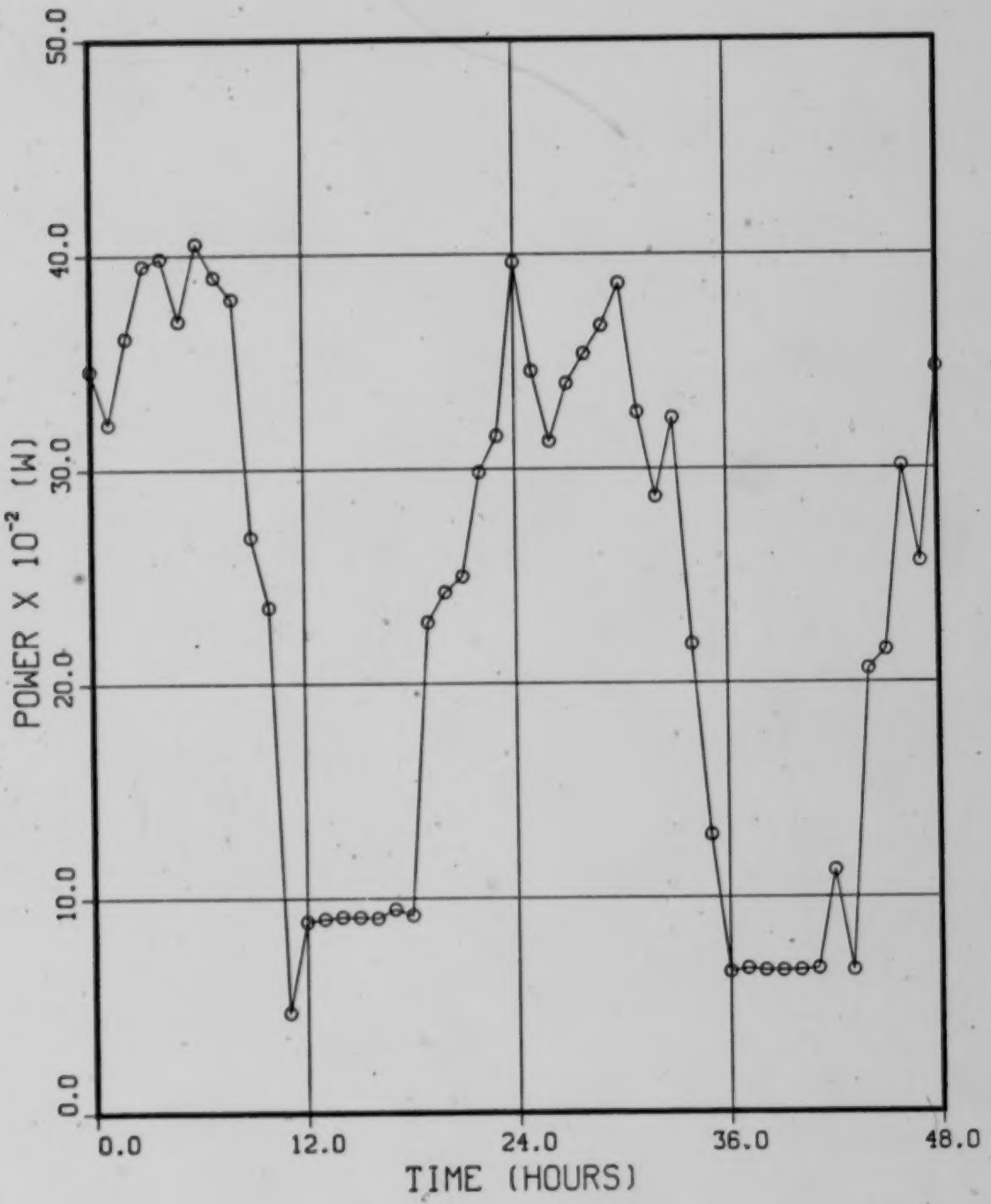

Figure 3.8 Measured Power Consumption for Module 5 for April 12-13, 1984

indoor-outdoor temperature difference were the same for Modules 1 and 5, the energy consumption in Module 1 would have been 87% of Module 5's during the "day", and 72% during the "night". "Day" is defined as periods when the total horizontal radiation is greater than 5 W/m^2. All other times of the day are defined as "night".

3.2.2 Short Term Effect of South Facing Window

During certain times of the day the south facing windows allow solar radiation to enter directly into the masonry module. This solar radiation can offset some of the heating energy normally required from the furnace to maintain the module at a constant temperature. In some cases, when the heating load of the module is relatively low, and the rate of incoming solar radiation is high, the module cannot adequately store the incoming radiation without overheating.

In the previous section, the masonry module was shown to have a more balanced heating load than the reference module. Proof of this more balanced heating load was based on calculating the relative UA of the masonry module during the "day" and "night" separately. Over the 1983-4 heating season the masonry module's relative UA during the "day" was 87%. During the "night" period, when a modules heating energy requirements increases dramatically (see Figures 3.7 and 3.8), the masonry module's relative UA was only 72%. During the 1984-5 heating season the "day" relative UA of

Module 1 was 79%, and the "night" relative UA was 86%. The "day" relative UA fell 8% because of solar gains offsetting the module's furnace load. The "night" relative UA increased 14% because of the higher transmission losses from the masonry module's windows. It should be noted again that during the 1984-5 heating season Module 5 had no south facing windows as did Module 1, and one must be cautious when interpreting these results.

The short term effect of the south facing windows is therefore to destabilize the heating load of the masonry module relative to the previous heating season. That is, the diurnal variation in Module 1's power consumption has became larger after the installation of the south facing windows. Figures 3.9 and 3.10 show hour by hour power consumption of Modules 1 and 5 over a two day period in the 1984-5 heating season. There is very little difference in the amplitude of the daily power consumption between Modules 1 and 5. The destabilizing effect of the windows can be seen by comparing Figures 3.9 and 3.10 from 1984-5, to Figures 3.7 and 3.8 from 1983-4. Note the smoother hourly power consumption for Module 1 in 1984-5 compared to 1983-4. This is a result of installing a proportional controller on Module 1's furnace to prevent on-off cycling of the heating system.

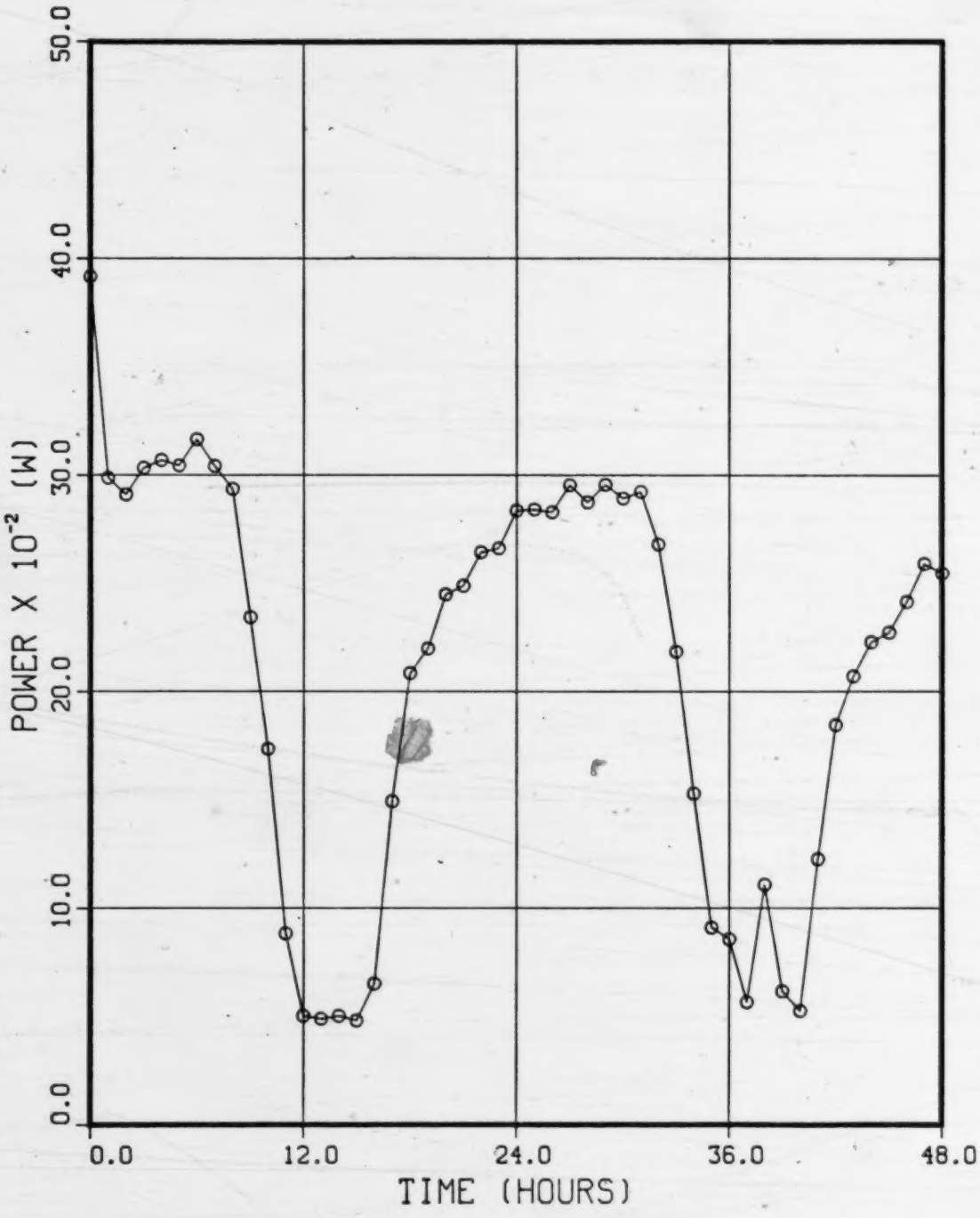

Figure 3.9 Measured Power Consumption for Module 1 for March 31 - April 1, 1985

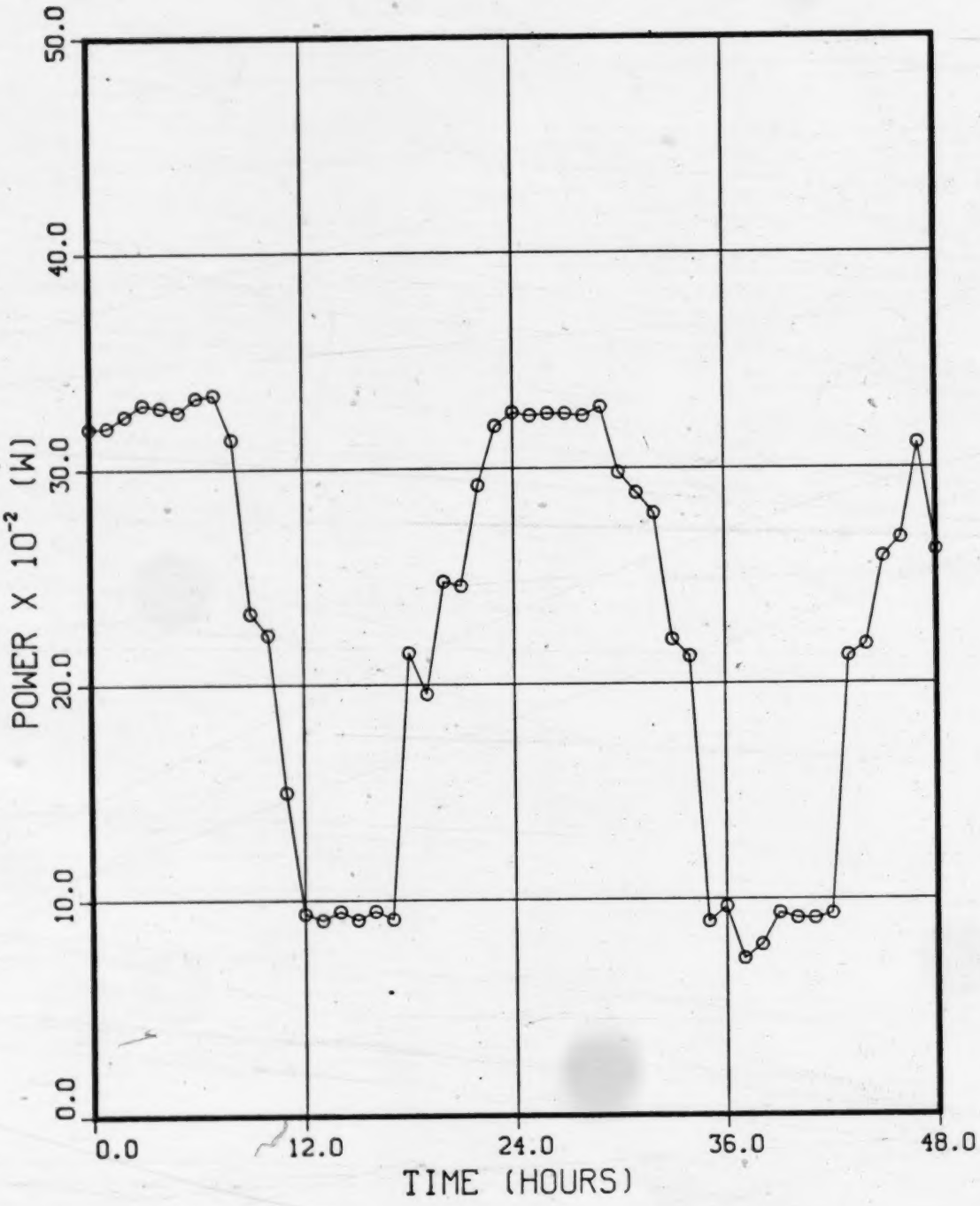

Figure 3.10 Measured Power Consumption for Module 5 for March 31 - April 1, 1985

3.2.3 Temperature Decay Test

Temperature decay tests are used to determine the effective thermal capacitances of the modules. The decay tests are done simply by shutting off the modules' heating system, and measuring the decay in interior temperature with time. The circulation fans are left on to maintain uniform air temperature throughout the modules. The tests last about eight hours during the night, when the ambient conditions are most stable.

To help interpret the results of the temperature decay tests a simplified model of the modules has been created. The model treats the modules as lumped masses with an internal energy source (the circulation fan). It is necessary to include the fan power in the model because in some modules the fan power can be large portion of its auxiliary heating requirements.

An electrical analogy to this model is shown in Figure 3.11. At the bottom of Figure 3.11 is a list of the analogous quantities used in the model. Using Kirchhoff's current law the differential equation for the electrical analogy can be formulated:

$$\frac{dV(t)}{dt} + \frac{1}{RC} V(t) = \frac{1}{C} \left(\frac{V_\infty}{R} + Q \right) \qquad (3.1)$$

where: V(t) - node voltage (V)

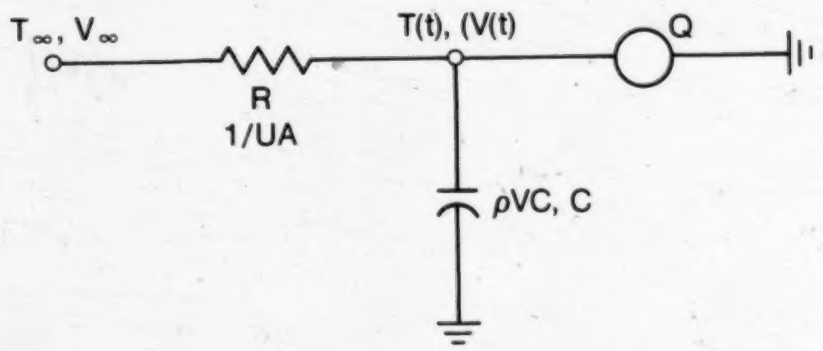

Heat Transfer - Electrical Analogy

Heat Transfer Quantity	Electrical Quantity
UA - overall heat transfer coefficient of module	R - resistance
ρVC - effective thermal capacitance of module	C - capacitance
Q - fan energy	Q - current source
T (t) - room temperature of module	V (t) - node voltage
T_∞ - ambient temperature	V_∞ - node voltage

Figure 3.11 Electrical Analogy of Modules during Temperature Decay Tests

V - node voltage (V)

Q - current source (A)

C - electrical capacitance (F)

R - electrical resistance (Ω)

t - time (s)

Substituting in the analogous quantities for heat transfer results in a first order differential equation representing the modules. Specifying the initial temperature of the module as T_o allows the differential equation to be solved. Giving;

$$T(t) = T_\infty + Q_f/UA + (T_o - T_\infty - Q_f/UA)e^{\frac{-tUA}{\rho VC}} \qquad (3.2)$$

where: T(t) - interior temperature (°C)

T_∞ - ambient temperature (°C)

Q_f - fan power (W)

T_o - initial interior temperature (°C)

ρVC - effective thermal capacitance (J/°C)

t - time (s)

UA - overall transmission coefficient (W/oC)

Rearranging equation 3.2 to a more useful form;

$$\ln\left[\frac{T(t) - T_\infty - Q_f/UA}{T_o - T_\infty - Q_f/UA}\right] = -\frac{tUA}{\rho VC} \qquad (3.3)$$

where: t - time (s)

$\frac{\rho VC}{UA}$ - time constant (s)

$$\ln\left[\frac{T(t) - T_\infty - Q_f/UA}{T_o - T_\infty - Q_f/UA}\right]$$ - non-dimensional temperature difference

The UA and Q_f are measured quantities for each of the modules. The UA of a module is calculated similarly to that shown in Section 2.2.1 from a module's measured energy consumption and indoor-outdoor temperature difference. For the purpose of the temperature decay tests the UA for a module is based only on the nighttime data from the month that the test was conducted (not including the nights of the tests). The fan power, Q_f, includes all the internal electric gains of the module, not just the circulation fan (examples: computer system, vacuum pump, sump pump, etc.). Table 3.1 lists the measured UA and Q_f for the modules.

Figure 3.12 shows the non-dimensional temperature difference plotted against time for a typical temperature decay test. The inverse of the slopes of the lines in Figure 3.12 are the time constants for the modules. The lines in Figure 3.12 are not straight, indicating that the "time constant" of a module is not a constant. "Time constants" are therefore calculated near the start of a test (t = 1/2 hour), and near the end of the test (t = 6 hours). Table 3.2 lists the average values of the measured time

Table 3.1
Measured UA and Q_f for Modules 1 and 5
during March 1984

Module	UA (W/°C)	Q_f (W)
1	127	385
5	176	875

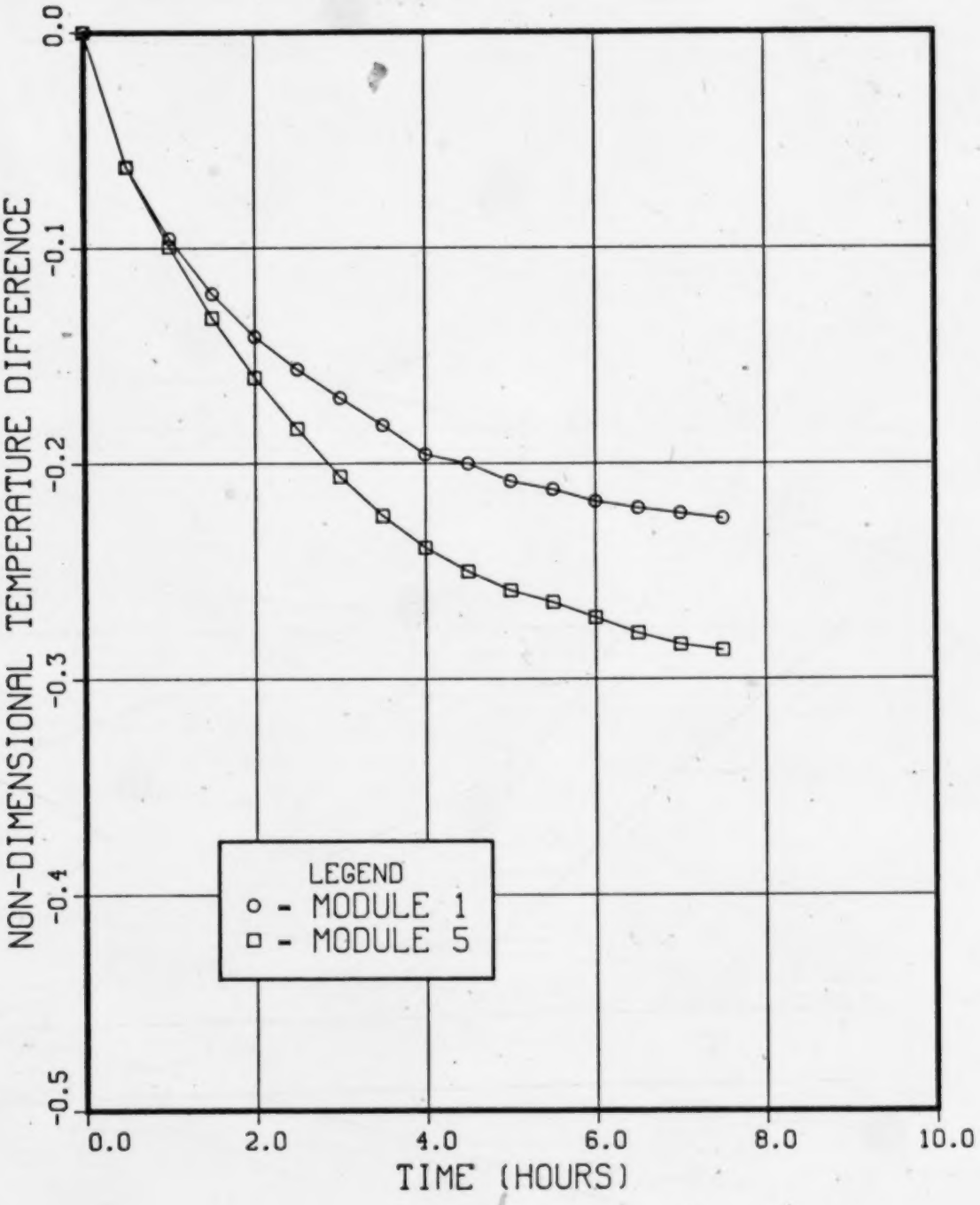

Figure 3.12 Typical Temperature Decay Test

Table 3.2
Measured Time Constants for Modules 1 and 5
with Flue Pipes Open (hours)

Module	1/2 Hour Time Constant	6 Hour Time Constant
1	15.3	58.3
5	11.1	38.7

constants for the modules. These results are based on 1983-4 tests when the modules underwent the temperature decay test simultaneously. The tests were performed simultaneously so that all the modules would experience the same ambient conditions. One interpretation of the rapid initial decay is that the lower thermal capacitance elements of the module are losing their stored energy first (example, air), while the slower decay after 6 hours is due to the larger thermal capacitance elements losing their energy.

The time constant of a module is a function of both its overall heat transfer coefficient and effective thermal capacitance. The effective thermal capacitance of a module can be calculated by multiplying the measured time constant (Table 3.2) by the modules measured UA (Table 3.1).

The effective thermal capacitance of the modules over the first 1/2 hour are more important than the thermal capacitance after several hours. During normal operation of a building in the heating season a standard thermostat would seldom allow the building to cool down for several hours. Instead the building is cycled through a series of short term cool downs, and the effective thermal capacitance during that period is important to the operation of the furnace. The effective thermal capacitance for the modules, based on the 1/2 hour time constant, are listed in Table 3.3. Note the very similar effective thermal capacitance for Modules 1, and 5 during the first 1/2 hour of the temperature decay tests. This would suggest that in

Table 3.3
Measured Effective Capacitance at 1/2 Hour of Temperature Decay (MJ/°C)

Module	Effective Capacitance
1	7.0
5	7.0

the short term Modules 1, and 5 respond almost the same, and the large thermal capacitance elements in the masonry walls are essentially decoupled from the module's interior.

A closer analysis of the masonry walls can be made by observing the changes in internal wall temperatures during a temperature decay test. Figure 3.13 shows the approximate hour by hour temperature profile across the north wall of the masonry module during the December 26, 1984 test. The locations of the thermocouples used to approximate the temperature profile are shown in Figure 1.4. Two points can be made about Figure 3.13. Firstly, the temperature profile is such that the direction of heat flow is always outward. And secondly, the thermocouple measuring the interior block temperature is unaware of the module cooling down for over two hours. The implication of these results are that no energy can be recovered back from the masonry to the room air during any part of an eight hour cool down of the module. Two reasons for this are:

1) The natural air infiltration rate of the masonry module is so low that the room air temperature does not decrease fast enough to reverse the flow of heat in the walls.
2) The wallboard and air gap have decoupled the masonry elements of the walls from the module's interior.

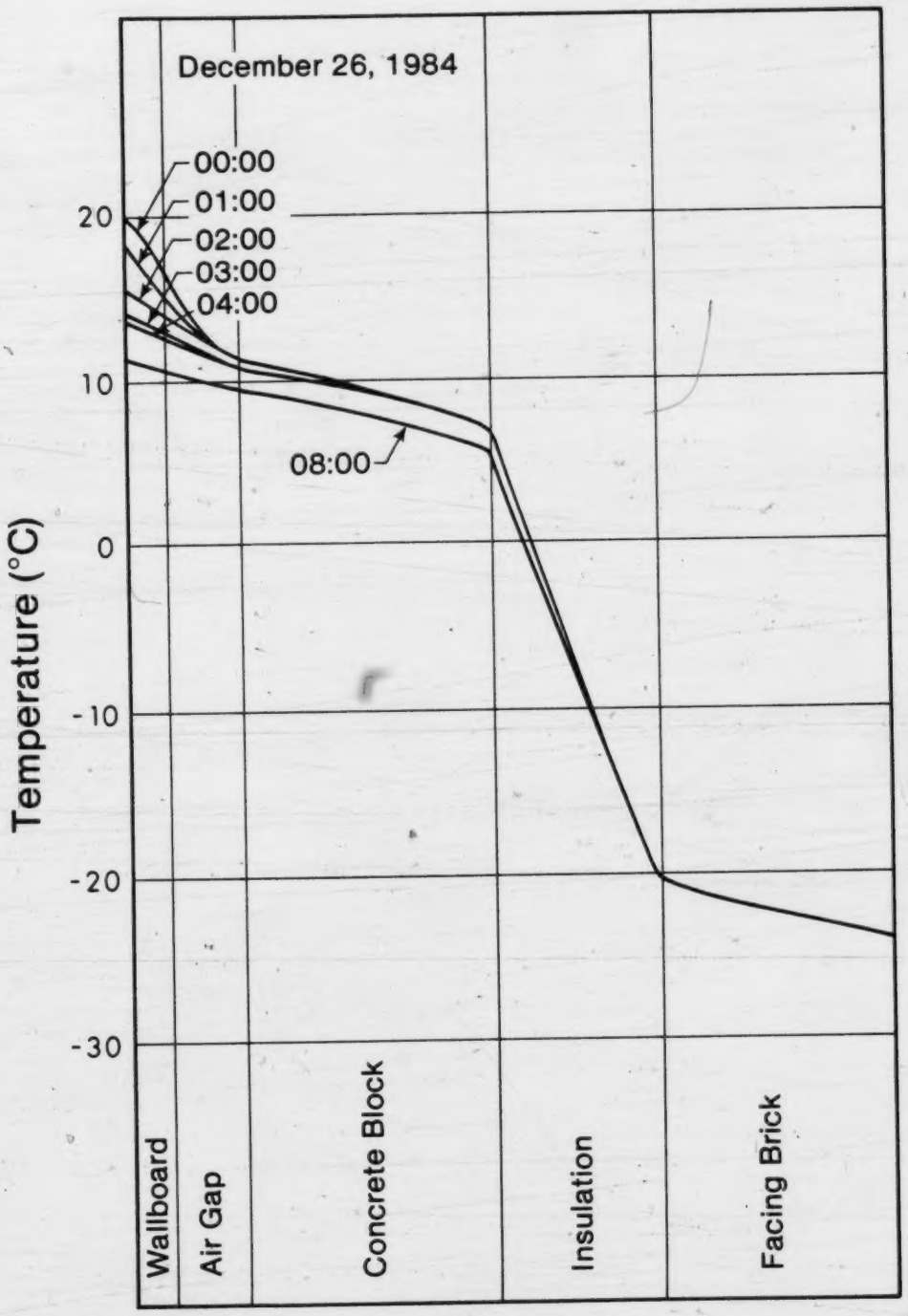

Figure 3.13 Internal Wall Temperatures during Temperature Decay Test

CHAPTER 4

CONCLUSIONS

Based on a two year study of a masonry module with double wythe walls and foamed-in-place insulation several conclusions have been drawn. The conclusions are grouped in three categories: 1983-4 heating season, 1984-5 heating season, and general conclusions. In the 1983-4 heating season the masonry module had no south facing windows. In the 1984-5 heating season the masonry module had two south facing windows.

1983-4 Heating Season

1) The overall energy loss of the masonry module including air infiltration was 79% of the reference module. The reference module is a wood framed unit on the same site, and the only significant difference between the masonry and reference modules during the 1983-4 heating season were their above grade walls.
2) The reasons for the lower overall energy loss for the masonry module was due to higher insulation levels in the walls and a lower natural air infiltration rate.
3) The average rate of natural air infiltration for

the masonry module after sealing the make up air vent was 0.2 air changes/hour. This rate was about 60% of the reference module's air change rate.

4) Subtracting off the energy loss from air infiltration the masonry and reference module were compared on their heat transmission losses. The heat transmission losses of the masonry module were 81% of the reference module, accounting for differences in the heating degree days between the modules. The predicted heat transmission losses of the masonry module were 84% of the reference module.

1984-5 Heating Season

5) The overall energy loss of the masonry module including air infiltration was 83% of the reference module. During the 1984-5 heating season the masonry module had south facing windows which did not exist in the reference module.

6) The south facing windows of the masonry module increased its relative overall energy loss 4% over the heating season from 79% to 83% of the reference module.

7) The heat transmission losses of the masonry module were 86% of the the reference module. The south facing windows of the masonry module increased the relative transmission losses 5% over the heating

season. The predicted transmission losses of the masonry module were 92% of the reference module.

8) The average rate of natural air infiltration for the masonry module was 0.26 air changes/hour. This rate was about 75% of the reference module's air change rate. This is a 15% increase in the relative air infiltration rate from the 1983-4 heating season.

9) The addition of the south facing windows in the masonry module destabilized its daily auxiliary heating requirements. The windows increased the nighttime auxiliary heating requirements, but decreased the daytime auxiliary heating requirements by introducing solar gains.

General Conclusions

10) The measured overall thermal resistance for the masonry walls were:

North Wall - Polyurethane 4.76 $m^2{}^oC/W$

North Wall - Vermiculite 2.10 $m^2{}^oC/W$

South Wall - Polyurethane 4.81 $m^2{}^oC/W$

11) The measured thermal resistance of the walls suggest that the conductivity of the polyurethane is close to the value of unaged polyurethane (0.0159 W/m^oC), and the effects of the metal reinforcing ties are not very significant when the wallboard and air gap are present. No aging of the

polyurethane foam was detected over the two heating seasons.

12) The measured effective thermal resistance of the 25.4 mm air gap was 0.416 m^2-$^oC/W$.

13) A finite element approximation of the heat transfer through the masonry walls not including the wallboard estimates the metal ties increase the overall heat transfer through the walls by 10%.

14) Based on steady periodic heat transfer theory through composite slabs the time lag introduced by the masonry walls was predicted to be:

Polyurethane Section - 9.9 hours

Vermiculite Section - 8.8 hours

The time lag is defined as the time for heat flux at the interior surface to respond to changes in the exterior temperature.

15) The measured time lag of the two north wall section are:

Polyurethane Section - 10 hours

Vermiculite Section - 8 hours

16) The time lag created by the double wythe walls was shown to balance the heating energy requirements of the masonry module relative to the reference module.

17) The use of temperature decay tests allowed the effective thermal capacitance of the modules to be calculated. The results shows the masonry module

to respond the same as the reference module in a short term (1/2 hour) cool down. The large quantities of high thermal capacitance elements of the masonry module were shown to be effectively decoupled from the module's interior.

REFERENCES

1. Latta, J.K., "Canadian Energy Consumption and Conservation Programs Related to Buildings", Division of Building Research, National Research Council of Canada, DBR Paper No. 1102, Ottawa.
2. Ackerman, M., "A Study of Residential Housing Envelope Heat Loss", Department of Mechanical Engineering Report No. 35, University of Alberta, Edmonton, Alberta, Canada, 1983.
3. Flanders, S.N., "Time Constraints on Measuring Building R-Values", The Northern Engineer, Vol. 11, No. 1, Spring, 1979, pp 11-18.
4. Handbook of Fundamentals, American Society of Heating, Refrigerating, and Air Conditioning Engineers, 1791 Tullie Circle, N.E., Atlanta, GA 30329, 1981.
5. Knox, R.E., "Insulating Properties of Fluorocarbon Expanded Rigid Urethane Foam", ASHRAE Journal, Vol. 4, October 1962, pp 43-49.
6. Bomberg, M., "Problems in Predicting the Thermal Properties of Faced Polyurethane Foams", Division of Building Research, National Research Council of Canada, DBR Paper No. 973, Ottawa.
7. Holman, J.P., "Heat Transfer", Fifth Edition, New York, McGraw-Hill, 1981.
8. Chapman, A.J., "Heat Transfer", Fourth Edition, New York, Macmillian, 1984.

9. Eckert, E.R.G., and Carlson, W.O., "Natural Convection in an Air Layer Enclosed Between Two Vertical Plates with Different Temperatures", International Journal of Heat and Mass Transfer, Vol. 2, 1961, pp 106-109.

10. Robinson, H.E., Powlitch, F.J., and Dill, R.S., "The Thermal Insulating Value of Airspaces", Housing and Home Finance Agency, Office of the Administrator, Division of Housing Research, Paper No. 32, Washington, D.C., 1954.

11. "Guide to Energy Efficiency in Masonry and Concrete Buildings", The Masonry Council of Canada, 201 - 10113 Wilson Avenue, Downsview, Ontario, M3K 1G1, 1982.

12. Ackerman, M.Y., Dale, J.D., Forest, T.W., Sadler, G.W., Wilson, D.J., and Zaheerudden, M., "Final Report on the Alberta Home Heating Research Facility", Department of Mechanical Engineering Report No. 34, University of Alberta, Edmonton, Alberta, Canada, February, 1983.

13. Carslaw, H.S., and Jaeger, J.C., "Conduction of Heat in Solids", Second Edition, New York, Oxford U.P., 1959.

14. Huebner, K.H., and Thornton, E.A., "The Finite Element Method for Engineers", Second Edition, New York, John Wiley and Sons, 1982.

15. Myers, G.E., "Analytical Methods in Conduction Heat Transfer", New York, McGraw-Hill, 1971.

APPENDIX A

CONSTRUCTION DETAILS OF REFERENCE MODULE

Table A.1

SPECIFICATIONS - MODULE 5 - REFERENCE MODULE (SI units)

Exterior Dimensions	6700 x 7300 mm
Interior Dimensions	6500 x 7100 mm
Main Floor Wall Height	2440 mm
Basement: Wall Height	2440 mm
Wall Thickness	200 mm
Floor Thickness	100 mm

Ceiling Construction
- standard truss with 610 mm bobtail
- 38 x 89 mm rafters, 610 mm on center
- fiberglass insulation, RSI = 2.11
- 0.102 mm polyethelene air-vapor barrier
- 13 mm gypsum wallboard

Wall Construction
- 10 mm prestained plywood exterior finish
- 38 x 89 mm framing, 410 mm on center
- fiberglass insulation, RSI = 1.76
- 0.102 mm polyethelene air-vapor barrier
- 13 mm gypsum wallboard

Windows
North Wall - 1000 x 1950 mm sealed unit (double glazed)
South Wall - none
East Wall - 1000 x 1950 mm horizontal slider (vinyl frame)
West Wall - 1000 x 1950 mm horizontal slider (vinyl frame)

Door
- 910 x 2030 mm urethane foam core

Basement Insulation
- 51 mm polystyrene extending 610 mm below grade, RSI = 1.76
- 13 mm pressure treated plywood covering

Auxiliary Heating
- 7.5 kW electric duct heater

Interior Finish
- painted walls
- carpeted floor

Table A.2

SPECIFICATIONS - MODULE 5 - REFERENCE MODULE (English units)

Exterior Dimensions	22.0 x 24.0 feet
Interior Dimensions	21.3 x 23.3 feet
Main Floor Wall Height	8 feet
Basement: Wall Height	8 feet
Wall Thickness	8 inches
Floor Thickness	4 inches

Ceiling Construction
- standard truss with 2 foot bobtail
- 2 x 4 inch rafters 24 inch on center
- fiberglass insulation, R-12
- 4 mil polyethelene air-vapor barrier
- 1/2 inch gypsum wallboard

Wall Construction
- 3/8 inch prestained plywood exterior finish
- 2 x 4 inch framing, 16 inch on center
- fiberglass insulation, R-10
- 4 mil polyethelene air-vapor barrier
- 1/2 inch gypsum wallboard

Windows
North Wall - 40 x 76 inch sealed unit (double glazed)
South Wall - none
East Wall - 40 x 76 inch horizontal slider (vinyl frame)
West Wall - 40 x 76 inch horizontal slider (vinyl frame)

Door
- 3.0 x 6.7 feet urethane foam core

Basement Insulation
- 2 inch polystyrene extending 2 feet below grade, R-10
- 1/2 inch pressure treated plywood insulation covering

Auxiliary Heating
- 7.5 kW electric duct heater

Interior Finish
- painted walls
- carpeted floor

APPENDIX B

ENVIRONMENTAL AND MODULE MEASUREMENTS

ENVIRONMENTAL MEASUREMENTS

Temperature

All temperatures at the Facility are measured using copper-constantan thermocouples with cold junction compensation provided by an ice point cell (Omega - model TRC-III).

The ambient air temperature is measured in a shaded location just to the north of Module 2 in order to negate direct solar radiation effects on the thermocouple.

Many ground temperatures are measured at the site in order to evaluate methods used in calculating the heat loss from the below grade portion of structures. To measure ground temperatures, metal probes with thermocouples attached were driven into the ground on the north sides of Modules 2 and 4. The thermocouples are attached with 667 mm spacing along a 2000 mm probe. The probes are centered on the north sides of the modules at a distance of 300, 1840, and 6150 mm away from the basements. Figure B.1 shows the thermocouples' location in the ground. The ground probes have their temperatures read manually on a weekly basis.

The exterior surface temperature of the south wall of

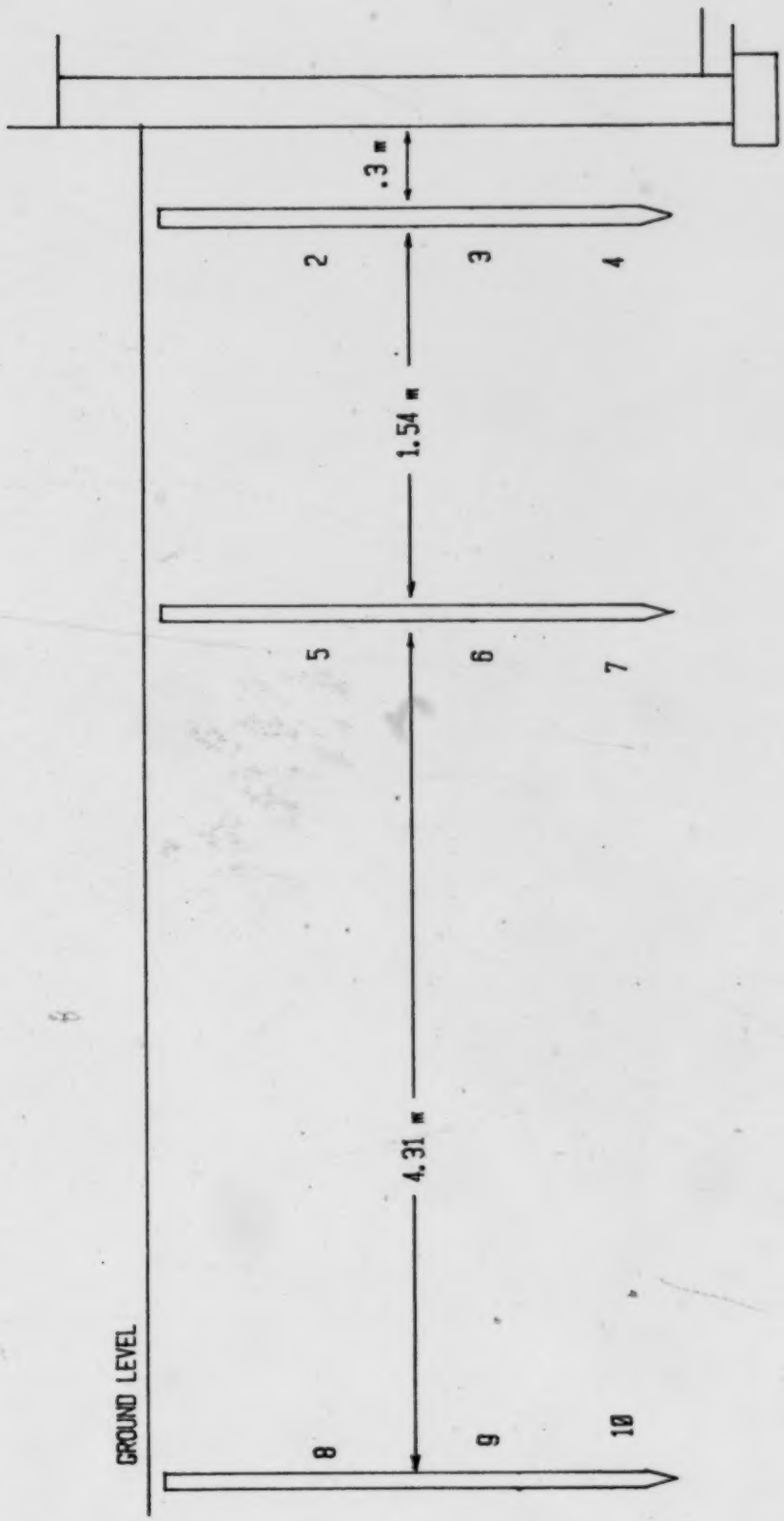

Figure B.1 Ground Probe Thermocouple Location

Module 2 is measured with a thermocouple embedded in the plywood exterior.

Solar Radiation

Five solar radiation levels are measured at the Facility using Eppley pyranometers. Total vertical radiation, diffuse radiation, and total vertical radiation transmitted through a south facing window are measured by Eppley model 8-48 black and white pyranometers. Total horizontal radiation and total radiation falling on the active solar collectors are measured by Eppley model PSP precision pyranometers.

Wind Speed and Direction

Towers for measuring wind speed and direction at a 10000 mm height were installed at two locations - one 30000 mm north and the other 30000 mm south of the modules approximately mid distance along the row of modules. Monitoring at these two locations was required to give a measure of "up wind" conditions. The sensing heads used on the towers are the Athabasca Research model-540.

MODULE MEASUREMENTS

Electrical Power Input

At the onset of the project it was decided to electrically heat the modules so their energy input could be accurately measured. Also, since the modules have lights and fan motors, the electrical energy they contribute would have to be determined. Measurements of energy input to each module is done by using calibrated Sangramo residential watt meters modified to be read remotely. As of the 1983-4 heating season, Modules 3 and 4 have been heated alternately with electric or natural gas furnaces.

Interior Temperatures

Each of the modules had three thermocouples installed to record attic, room, and basement air temperatures. The attic air temperatures are needed to aid in the modelling of the modules' ceiling heat losses. Attic temperatures are normally somewhat higher than ambient temperatures and significantly affect the predicted heat loss through the ceilings. The basement air temperatures are monitored to check the uniformity of interior temperatures.

Component Heat Flux

Measurements of actual heat flux through walls, ceilings, and basements are needed to breakdown the overall energy load of a module into its component heat losses.

Heat flux transducers designed and built at the University of Alberta are used at the Facility. The transducers consist of a cork resistance element, 6.35 mm thick, laminated between two layers of 3.18 mm thick plexiglass. Fourteen pairs of copper - constantan thermocouples measure the temperature difference across the plexiglass surfaces - a measurement which is related to the heat flux. The transducers cover a rectangular area of 152 x 406 mm. The 406 mm dimension was chosen so that the transducer would average heat flux over a width of wall equal to standard stud spacing. In the design of the transducers there was a trade off to be made between sensitivity and resistance. The transducers, as built, have a resistance value of RSI = 0.18. This resistance value can significantly effect the heat flow through low resistance elements, such as an uninsulated concrete basement wall.

Each transducer was calibrated against a "standard" commercial transducer which was provided with National Bureau of Standards traceable calibration.

Air Infiltration

The final component of heat loss to be accounted for is air infiltration. That is, the energy loss due to the natural exchanging of cold ambient air with warm interior air. Measurement of air infiltration rates were done on a continuous basis in all the modules, and recorded as an average rate over one hour. A schematic diagram of the

system used is shown in Figure B.2. The system functions by injecting discrete volumes of Sulphur Hexafloride (SF6) into a module to maintain its inside air concentration of SF6 at a constant level of 5 ppm. This constant concentration is maintained using an Hewlett-Packard HP-85 computer data acquisition system monitoring a Wilks-Miran 103 infrared concentration detector. Using two concentration detectors allows each of the modules to be sampled eight times per hour throughout the day.

Knowing, N, the number of injections of SF6 per hour and, V_i, the volume of each injection required to maintain the constant concentration level, C, allows one to easily calculate the air infiltration rate by

$$Q_v = C\ V_i\ N$$

where Q_v is the flow rate in units volume/hour. Dividing Q_v by the module volume produces the air change rate per hour.

To compliment the continuous air infiltration measurements all of the modules periodically undergo blowerdoor tests. All of the modules have been fitted with special blowerdoor vents on the inside of their east windows. This allows the blowerdoor fan assemble and pressure probes to be easily hooked up. The blowerdoor unit itself was constructed at the University of Alberta, designed especially for research applications.

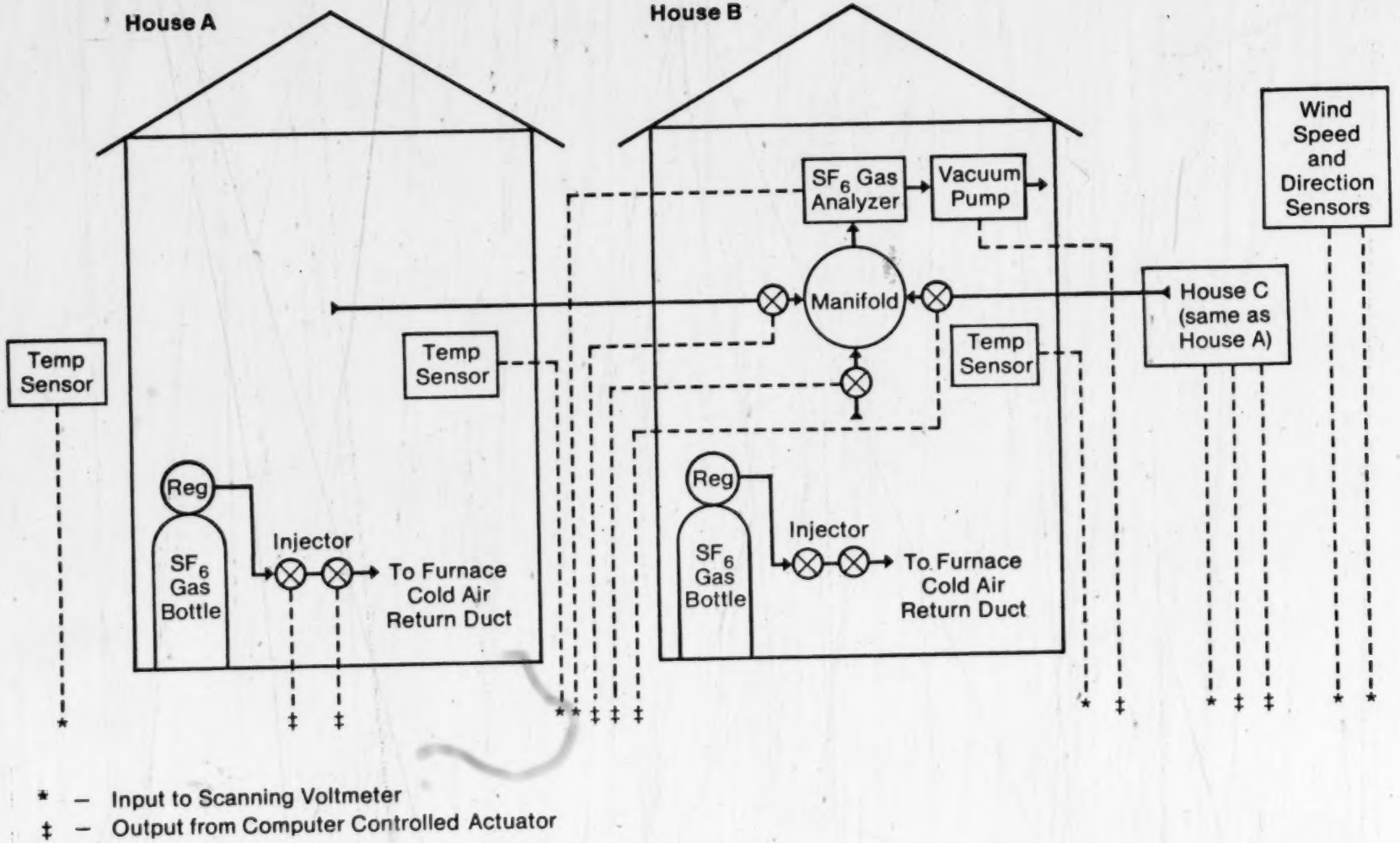

Figure B.2 Air Infiltration Measurement System Schematic

APPENDIX C

ASHRAE PREDICTION

A prediction of the overall heat transfer coefficient for Modules 1 and 5 by the method proposed in the ASHRAE Fundamentals Handbook is presented in this Appendix. The uncertainty and variability of some material properties suggests that a single prediction would not be appropriate. Instead the ASHRAE prediction is done for the range of possible material properties. This results in an upper and lower bound for the ASHRAE prediction. Shown in the calculations is the ASHRAE prediction using the least resistive properties for the modules' materials. Shown beside, in brackets, is the result using the most resistive properties.

MODULE 1 - no south facing windows

A) Ceiling

- Ceiling Area = 42.8 m^2
  percent framing - 6.25 %
  percent insulation - 93.75 %

- Thermal Resistance of Materials ($m^2 \cdot ^oC/W$)
  fibreglass insulation - 2.114
  wood studs - 0.766
  wall board - 0.079

- Surface Resistances ($m^2 \cdot ^oC/W$)
  interior - 0.107
  exterior - 0.107

1) Path 1 - Through Framing

$A_1 = 0.0625 \times 42.8 = 2.675\ m^2$

$R_1 = 1/h_i + R_a + R_b + 1/h_e$

$= 0.107 + 0.079 + 0.766 + 0.107$

$R_1 = 1.06$

$U_1 = 1/R_1 = 0.944 \text{ W/m}^2\cdot^\circ\text{C}$

2) Path 2 - Through Insulation

$A_2 = 0.9375 \times 42.8 = 40.125 \text{ m}^2$

$R_2 = 1/h_i + R_a + R_b + 1/h_e$

$= 0.107 + 0.079 + 2.114 + 0.107$

$R_2 = 2.407$

$U_2 = 0.415 \text{ W/m}^2\cdot^\circ\text{C}$

$UA_{total} = U_1A_1 + U_2A_2$

$= 0.944 \times 2.675 + 0.415 \times 40.125$

$UA_{total} = 19.2 \text{ W/}^\circ\text{C}$

B) Main Floor Walls and Joist Space

- Wall Area = 61.4 m^2
  polyurethane section - 54.8 m^2
  vermiculite section - 6.6 m^2

- Joist Space Area = 7.2 m^2
  polyurethane section - 6.5 m^2
  vermiculite section - 0.7 m^2
  - the joist space is calculated as part of the main floor walls because the double wythe walls extend down below the floor level to the basement walls.

- Thermal Resistance of Materials ($m^2\cdot^\circ C/W$)
  facing brick - 0.058
  vermiculite - 1.100
  polyurethane - 2.447 (4.00)
  concrete block - 0.244
  air gap - 0.178 (0.615)
  wallboard - 0.079

- Surface Resistances ($m^2\cdot^\circ C/W$)
  interior - 0.120
  exterior - 0.030

The main walls have steel reinforces ties that bridges

the insulation layer, as shown in Figure C.1. The steel ties have a diameter of 3.2 mm, and are placed between every second layer of concrete block. To try to account for the steel ties the 'zone method' described in ASHRAE will be applied.

Diameter of zone A (W)

$$W = m + 2d$$

m - diameter of metal (3.2 mm)
d - distance from end of tie to wall surface (88.9 mm)

$$W = 3.2 + 2 \times 88.9 = 181 \text{ mm} = 0.18 \text{ m}$$

Total Area = 0.165 m^2

Area of Zone A = 0.026 m^2

Area of Zone B = 0.139 m^2

1) Path 1 - Polyurethane
- see Table C.1

$UA_{zone\ A} = A/R = 0.00938$ W/°C (0.00600)

Zone B

$$R_B = 1/h_i + R_a + R_b + R_c + R_d + R_e + 1/h_e$$

$$R_B = 0.12 + 0.079 + 0.178 + 0.244 + 2.447 + 0.058 + 0.03$$

$R_B = 3.156$ (5.146)

$UA_{zone\ B} = 0.0440$ W/°C (0.027)

$UA_{A+B} = 0.0533$ W/°C (0.0330)

$U_{A+B} = 0.324$ W/m^2·°C (0.20)

For the entire polyurethane wall section

$UA_{poly} = 17.76$ W/°C (11.0)

2) Path 2 - Vermiculite Section

- using the same procedure as above

$UA_{zone\ A} = 0.0151$ W/°C (0.012)

$UA_{zone\ B} = 0.0713$ W/°C (0.0570)

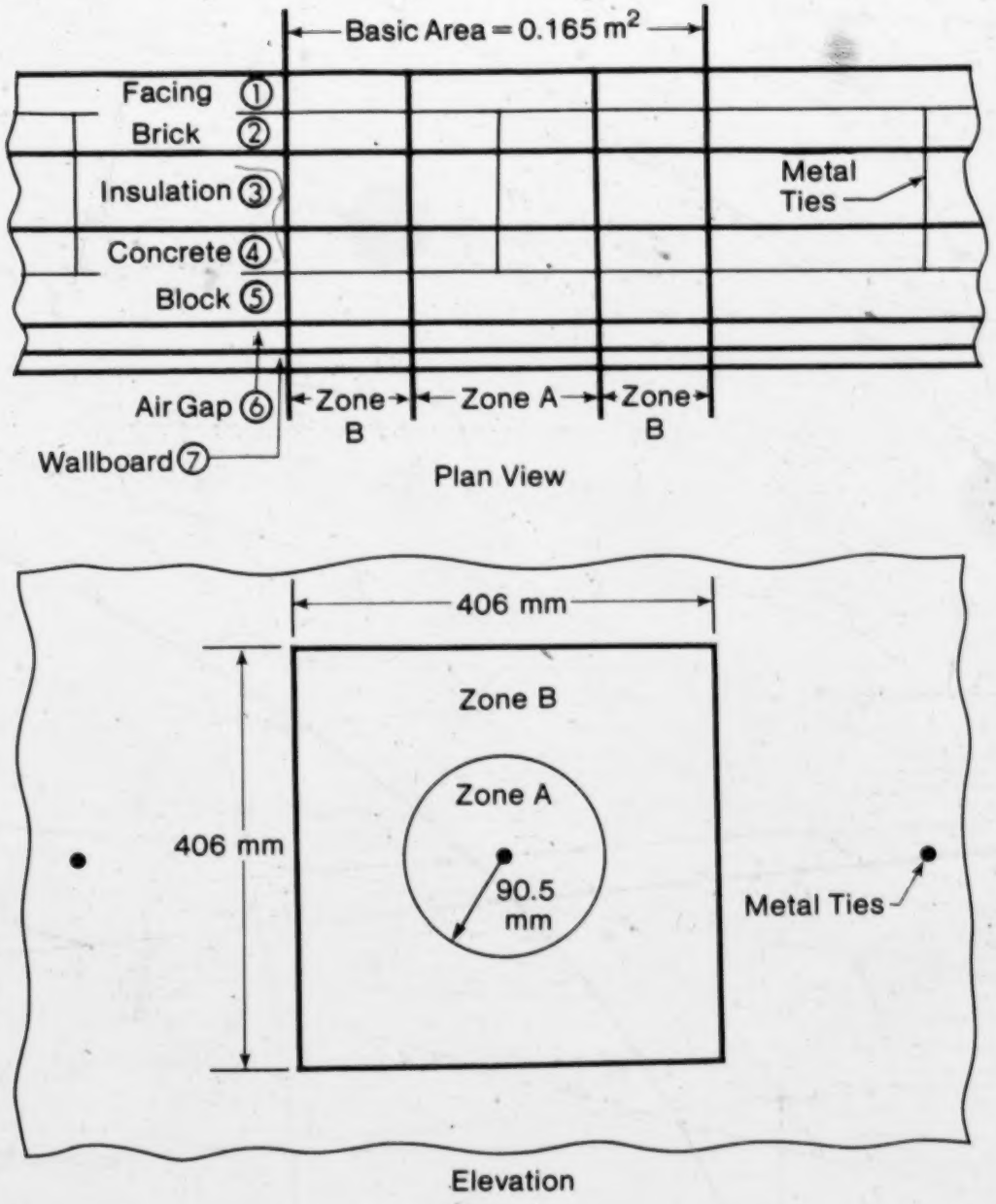

Figure C.1 Wall Cross Section for 'Zone Method' Calculation

Table C.1
Resistance Calculation For Zone A of Wall Section
by ASHRAE's 'Zone Method'

Section	Area x Conductance (W/°C)	A x C (W/°C)	R/A (°C/W)
Air	.026 x 33.3	0.867	1.153
1	0.26 x 34.5	0.897	1.115
2 Steel	8.04×10^{-6} x (15/.045)	0.00271	} 1.111
2 Brick	.026 x 34.5	0.897	
3 Steel	8.04×10^{-6} x (15/.064)	0.00190	} 79.37
3 Insulation	.026 x 0.41	0.0107	
4 Steel	8.04×10^{-6} x (15/.051)	0.00237	} 4.64
4 Block	.026 x 8.2	0.2132	
5	.026 x 8.2	0.2132	4.69
6	.026 x 5.62	0.1461	6.84
7	.026 x 12.6	0.3276	3.05
Air	.026 x 8.3	0.2158	4.63

Total = 106.6 °C/W

For the entire vermiculite wall section

UA_{verm} = 3.68 W/°C (2.96)

$UA_{walls} = UA_{poly} + UA_{verm}$

UA_{walls} = 21.4 W/°C (13.9)

3) Path 3 - Joist Space (Polyurethane)

A_3 = 6.5 m^2

$R_3 = 1/h_i + R_a + R_b + R_c + 1/h_e$

$= 0.12 + 0.244 + 2.447 + 0.058 + 0.03$

R_3 = 2.9 (4.45)

U_3 = 0.345 W/m^2·°C (0.225)

U_3A_3 = 2.24 W/°C (1.46)

neglect vermiculite joist space because of small area

$UA_{total} = UA_{walls} + U_3A_3$

UA_{total} = 23.64 W/°C (15.4)

C) Windows - no south facing windows

- Window Area = 5.85 m^2
  aluminum frame, horizontal slider - 3.9 m^2
  sealed unit - 1.95 m^2

- Thermal Resistance of Materials (m^2·°C/W)
  aluminum frame, horizontal slider - 0.30
  sealed unit - 0.359

1) Horizontal slider

$U_1 = 1/R_1$ = 3.35 W/m^2·°C

2) Sealed unit

$U_2 = 1/R_2$ = 2.78 W/m^2·°C

$UA_{total} = U_1A_1 + U_2A_2$

$UA_{total} = 3.35 \times 3.9 + 2.78 \times 1.95$

UA_{total} = 18.5 W/°C

D) Door

- Door Area = 1.85 m^2

- Thermal Resistance of Materials ($m^2 \cdot ^oC/W$)
  solid core fir - 0.359

UA_{total} = 5.15 $W/^oC$

E) Basement Walls - based on path length method, see Figure C.2

Basement perimeter = 26420 mm
width of path 1 - 400 mm
width of paths 2 through 7 - 310 mm

Thermal Resistance of Materials ($m^2 \cdot ^oC/W$)
51 mm styrofoam - 1.76
13 mm plywood - 0.11
concrete - 0.12
soil, concrete, air films:
path 2 - 0.43
path 3 - 0.79
path 4 - 1.14
path 5 - 1.48
path 6 - 1.83
path 7 - 2.23

Surface Resistances ($m^2 \cdot ^oC/W$)
interior - 0.12
exterior - 0.03

1) Path 1 - above grade

$A_1 = 10.57\ m^2$

$R_1 = 1/h_i + R_a + R_b + R_c + 1/h_e$

$= 0.12 + 0.12 + 1.76 + 0.11 + 0.03$

$R_1 = 2.14$

$U_1 = 0.467\ W/m^2 \cdot ^oC$

$U_1A_1 = 4.94\ W/^oC$

2) Path 2 - (grade - 0.31 m)

$A_2 = 8.19\ m^2$

$R_2 = R_a + R_b + R_c$

$= 1.76 + 0.11 + 0.43$

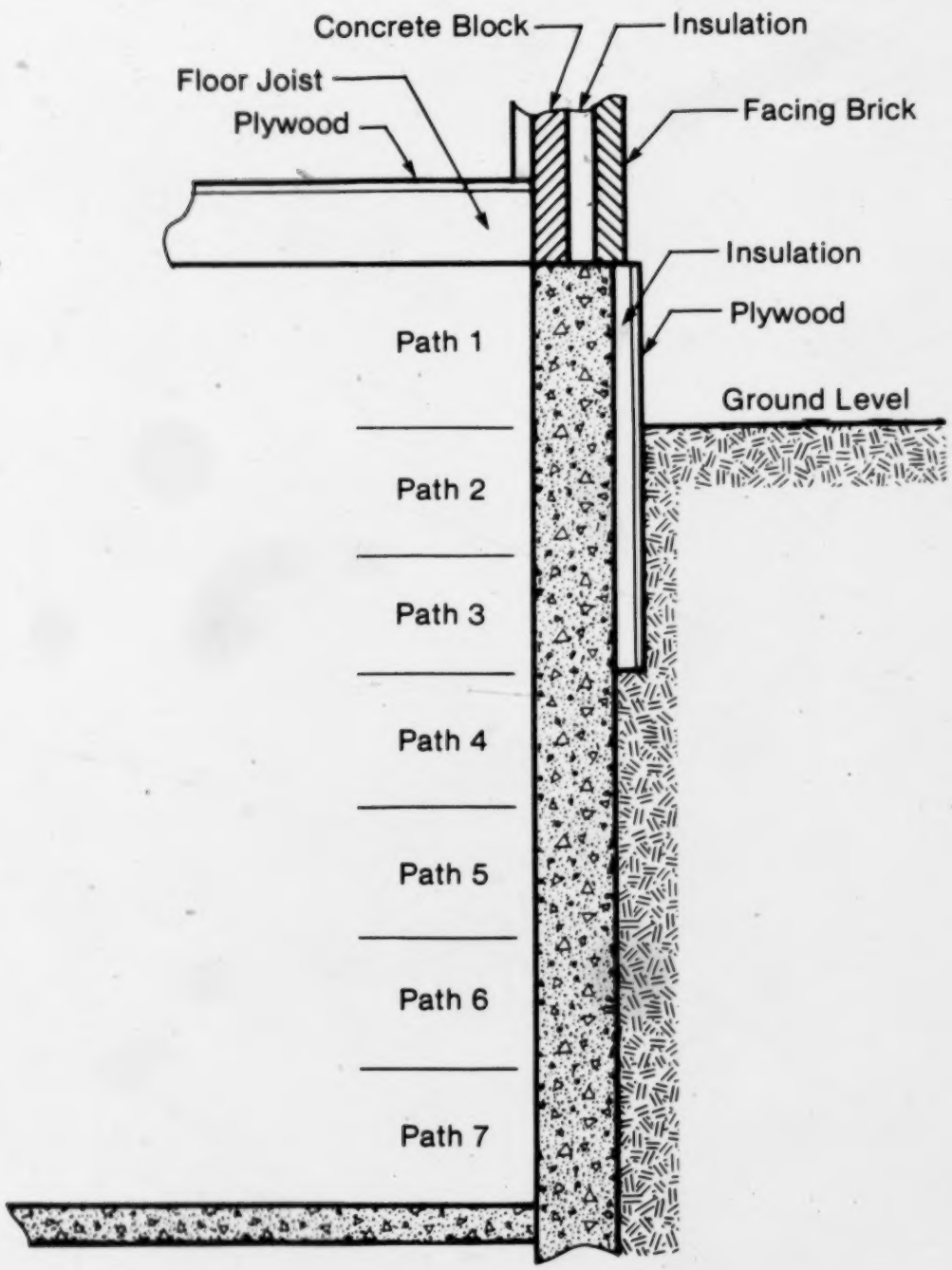

Figure C.2 Basement of Module 1

$R_2 = 2.3$

$U_2 = .435\ W/m^2.{}^oC$

$U_2A_2 = 3.56\ W/{}^oC$

similarly for paths 3 through 7

$U_3A_3 = 3.08\ W/{}^oC$

$U_4A_4 = 7.18\ W/{}^oC$

$U_5A_5 = 5.54\ W/{}^oC$

$U_6A_6 = 4.47\ W/{}^oC$

$U_7A_7 = 3.67\ W/{}^oC$

$UA_{total} = 32.44\ W/{}^oC$

F) Basement Floor

Foundations are approximately 1900 mm below grade

Width of module - 6800 mm

$A = 43.5\ m^2$

$U = 0.157\ W/m^2.{}^oC$

$UA_{total} = 6.82\ W/{}^oC$

MODULE 5

A) Ceiling

- same as ceiling in Module 1 except area larger by $6.3\ m^2$, therefore

$UA_{total} = 22.0\ W/{}^oC$

B) Main Floor Walls

- Wall Area = $60.6\ m^2$
  percent framing - 13.6 %
  percent insulation - 86.4 %

- Thermal Resistance of Materials ($m^2.{}^oC/W$)
  fibreglass insulation - 1.76

wood studs - 0.766
wallboard - 0.079
plywood - 0.083

- Surface Resistances ($m^2.^oC/W$)
interior - 0.12
exterior - 0.03

1) Path 1 - Through Framing

$A_1 = 0.136 \times 60.6 = 8.24\ m^2$

$R_1 = 1/h_i + R_a + R_b + R_c + 1/h_e$

$= 0.12 + 0.079 + 0.766 + 0.083 + 0.03$

$R_1 = 1.078$

$U_1 = 0.928\ W/m^2.^oC$

$U_1A_1 = 7.64\ W/^oC$

2) Path 2 - Through Insulation

$A_2 = 0.864 \times 60.6 = 52.4\ m^2$

$R_2 = 1/h_i + R_a + R_b + R_c + 1/h_e$

$= 0.12 + 0.079 + 1.76 + 0.083 + 0.03$

$R_2 = 2.072$

$U_2 = 0.483\ W/m^2.^oC$

$U_2A_2 = 25.3\ W/^oC$

$UA_{total} = 32.9\ W/^oC$

C) Windows

- Window Area = $5.85\ m^2$
vinyl frame, horizontal slider - $3.9\ m^2$
sealed unit - $1.95\ m^2$

- Thermal Resistance of Materials ($m^2.^oC/W$)
vinyl frame, horizontal slider - 0.374
sealed unit - 0.359

1) Horizontal slider

$U_1 = 1/R_1 = 2.67\ W/m^2.^oC$

2) Sealed unit

$U_2 = 1/R_2 = 2.78\ W/m^2.{}^oC$

$UA_{total} = U_1A_1 + U_2A_2$

$UA_{total} = 2.67 \times 3.9 + 2.78 \times 1.95$

$UA_{total} = 15.8\ W/{}^oC$

D) Door

- Door Area = $1.85\ m^2$
- Thermal Resistance of Materials ($m^2.{}^oC/W$)
  urethane foam core - 0.927

$UA_{total} = 2.0\ W/{}^oC$

E) Basement Walls

- same as Module 1 except includes the floor joist space
- Joist Space Area = $7.2\ m^2$
- Thermal Resistance of Materials ($m^2.{}^oC/W$)
  38 mm softwood - 0.33
  51 mm styrofoam - 1.76
  plywood - 0.11
- Surface Resistances ($m^2.{}^oC/W$)
  interior - 0.12
  exterior - 0.03

$R = 1/h_i + R_a + R_b + R_c + 1/h_e$

$= 0.12 + 0\ 33 + 1.76 + 0.11 + 0.03$

$R = 2.35$

$U = .426\ W/m^2.{}^oC$

$UA = 3.03\ W/{}^oC$

$UA_{total} = 35.47\ W/{}^oC$

F) Basement Floor

- same as Module 1

Table C.2
Summary of ASHRAE Predicted Overall Transmission Coefficients (W/°C)
(not including air infiltration)

Component	Module 1 Without South Facing Windows	Module 1 With South Facing Windows	Module 5
Ceiling	19.2	19.2	22.0
Main Walls	23.6[a] (15.4)[a]	22.7[a] (14.9)[a]	32.9
Doors	5.2	5.2	2.0
Windows	18.5	26.8	15.8
Basement Walls	32.4	32.4	35.4[a]
Basement Walls	6.8	6.8	6.8
Total	105.7 (97.5)	113.1 (105.5)	114.9

(a) Includes joist space

APPENDIX D

Finite Element Model of Simplified Wall Section

With no analytical solution available to calculate the multidimensional heat transfer around the metal ties a numerical approach was taken. The masonry walls were simplified to include only the concrete blocks, the insulation layer, and the facing bricks. Figure 2.1 shows the region modelled by the finite element method. This appendix will describe the assumptions made in modelling the wall section, the finite element model itself, the testing of the model, and the results predicted for the masonry walls. The last part of this appendix contains a listing of the finite element program.

Assumptions:

1) The metal ties are sufficiently isolated from each other that it is only necessary to model the region around one of the ties.
2) All the materials are homogeneous and isotropic. The internal air spaces in the blocks and bricks were neglected.
3) The heat transfer around a metal tie is independent of the angular coordinate when viewed in the cylindrical coordinate system.

The Finite Element Model

The elements used to model the temperature field were two dimensional triangular elements. Each element having three nodes, the nodes were located at the vertices of the triangles. At each node there is only one degree of freedom, the field variable temperature. The interpolation function used within each element was linear. The approach taken to derive the element equations for two dimensional heat conduction was the method of weighted residuals or Galerkin's method. The derivation of the element equations, their assembly, and the application of boundary conditions can be found in any standard text on the finite element method (14,15).

The assembled mesh of elements used to model the wall section is shown in Figure 2.1. The mesh around the metal tie is very fine because the temperature field was expected to change rapidly with location. Further away from the metal tie, the temperature field was expected to be almost uniform and a coarse mesh of elements was used. Altogether there are 159 nodes, and 271 elements in the model. The global numbering of the nodes starts at the bottom left hand corner of the mesh shown in Figure 2.1. The numbering increases left to right across the bottom row of nodes. The second row of nodes is then numbered successively left to right starting with node number 24. The material properties used in the finite element model are listed in Table D.1.

The boundary conditions for the model are:

Table D.1
Material Properties used in Finite Element Model

Material	Conductivity (W/m· °C)	Thickness (mm)
Concrete Blocks	0.37	89
Polyurethane	0.01586	63.5
Facing Bricks	1.316	76
Steel Ties	45.0	146

1) Interior Surface - specified temperature
2) Exterior Surface - specified temperature
3) Symmetric Boundary at Metal Tie - adiabatic or zero heat flux
4) Infinite Boundary - adiabatic or zero heat flux

Testing the Finite Element Model

Before the finite element model was used to predict the temperature field within the masonry walls it had to be tested. Two tests were applied to the model:

TEST 1) Without any steel tie in the wall section the heat flux would be predicted using the finite element model, and compare to one dimensional steady heat transfer through a plane composite wall section.

TEST 2) Construct a wall section that could be experimentally tested. Have the wall section instrumented with thermocouples, and compare the measured temperatures to temperatures predicted by the finite element model.

TEST 1

The heat flux through the simplified wall section without any metal ties can be calculated from one dimensional heat transfer theory. Using the material properties in Table D.1 the overall resistance of the wall section is 4.30 $^{o}C \cdot m^2/W$. Assuming a temperature difference of 20^{o}C across the wall section, from Equation 2.4, the heat

flux through the wall section would be 4.65 W/m^2.

The same boundary conditions were applied to the finite element model. Using the nodal temperatures, the temperature gradient at the interior surface of the wall could be approximated. Associating the proper areas to each surface element the rate of heat transfer through the wall section was calculated in Table 2.3. The rate of heat transfer predicted by the finite element model is 0.7675 W. Dividing the rate of heat transfer by the overall area (0.1652 m^2) gives a heat flux through the wall section of 4.65 W/m^2. There is essentially no difference between the heat flux predicted by one dimensional heat transfer theory, and the finite element model.

TEST 2

The physical model tested was a wall 740 x 575 mm made of four layers of styrofoam each 38.1 mm thick compressed between two 13 mm thick plywood covers. The metal tie used in the styrofoam wall was copper to exaggerate any effects on the temperature field. Figure D.1 shows a cross sectional view of the physical model tested. Figure D.1 also shows the positioning and numbering of the thermocouples used to measure the temperature field at discrete points in the wall.

The wall was placed between two environmental chambers so a large temperature difference across the wall could be created. One chamber was left at room temperature, and the

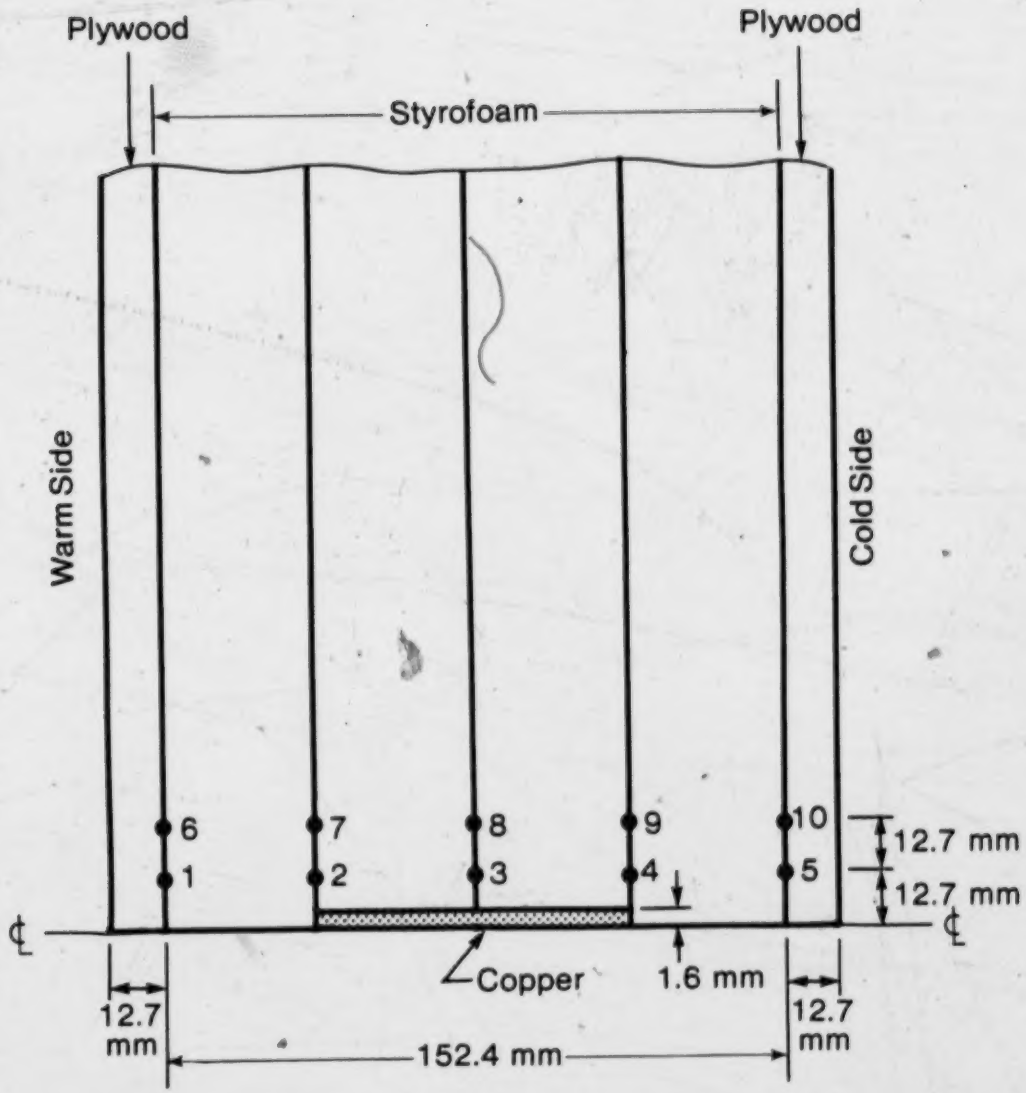

Figure D.1 Cross Section of Experimental Wall

other was set to provide approximately a 50°C temperature difference. The model was then allowed to come to steady state conditions, and the thermocouple voltages were recorded.

The finite element model was then used to predict the temperatures at the locations corresponding to the thermocouples. The finite element model is 1.5 times larger than the physical model. Care was taken to insure that the positioning of all the thermocouples and the copper rod were dimensionally similar between the models. The boundary conditions applied to finite element model were based on the experimental results. The interior surface temperature was set equal to the average reading of thermocouples 1 and 6, the exterior surface temperature was set equal to the average reading of thermocouples 5 and 10.

Table D.2 shows the results of the measured and predicted temperatures at the thermocouple locations in the styrofoam wall. The difference between the measured and predicted is approximately 1°C at all locations when the entire wall section is subjected to a temperature difference of 47.4°C. This was considered good enough to accept the results of the finite element model when predicting the temperature field inside the walls of the masonry module.

Finite Element Model Results for Simplified Wall Section

The boundary conditions at the interior surface were set at 20°C, and the exterior surface at 0°C. The

Table D.2
Measured and Predicted Temperatures Within the Styrofoam Wall (°C)

Thermocouple Number	Measured Temperature	Predicted Temperature
1	18.5	18.45
2	5.6	4.6
3	- 4.1	- 5.3
4	- 14.0	- 15.1
5	- 29.1	- 28.95
6	18.4	18.45
7	6.7	5.7
8	- 4.1	- 5.3
9	- 15.3	- 16.3
10	- 28.8	- 28.95

temperatures predicted for the 159 nodes in the finite element model are listed on the following page. Using the nodal temperatures, the temperature gradient at the interior surface of the wall could be approximated. Associating the proper areas to each of the surface elements (Figure 2.3) the rate of heat transfer through the wall was calculated in Table 2.3. Comparing the rates of heat transfer with and without the metal ties shows a 10% increase in the heat flux due to the ties.

Following the list of node temperatures is a listing of the finite element program and its subroutines.

NODE	TEMPERATURE	NODE	TEMPERATURE	NODE	TEMPERATURE
1	20.00	54	11.58	107	0.0
2	19.73	55	8.73	108	20.00
3	19.44	56	5.88	109	19.87
4	18.83	57	2.98	110	19.62
5	18.38	58	1.47	111	19.35
6	17.80	59	1.20	112	19.09
7	16.96	60	0.70	113	18.81
8	15.74	61	0.39	114	18.46
9	15.00	62	0.22	115	18.26
10	13.73	63	0.12	116	14.65
11	11.14	64	0.03	117	11.07
12	8.54	65	0.0	118	7.55
13	5.92	66	20.00	119	4.00
14	3.30	67	19.86	120	0.45
15	2.01	68	19.58	121	0.39
16	1.52	69	19.22	122	0.32
17	0.79	70	18.75	123	0.23
18	0.42	71	18.52	124	0.15
19	0.30	72	18.03	125	0.07
20	0.22	73	17.45	126	0.0
21	0.12	74	16.93	127	20.00
22	0.03	75	13.61	128	19.68
23	0.0	76	10.47	129	19.26
24	20.00	77	7.38	130	18.61
25	19.86	78	4.27	131	11.28
26	19.59	79	1.03	132	3.99
27	19.21	80	0.76	133	0.34
28	18.37	81	0.47	134	0.23
29	18.11	82	0.28	135	0.12
30	17.43	83	0.16	136	0.0
31	16.41	84	0.08	137	20.00
32	15.02	85	0.0	138	19.58
33	12.44	86	20.00	139	19.18
34	9.84	87	19.73	140	18.80
35	7.23	88	19.43	141	9.53
36	4.61	89	19.09	142	0.28
37	1.99	90	18.92	143	0.14
38	1.09	91	18.55	144	0.0
39	0.57	92	18.17	145	20.00
40	0.29	93	17.82	146	19.61
41	0.16	94	17.70	147	19.22
42	0.08	95	15.91	148	18.84
43	0.0	96	12.47	149	9.56
44	20.00	97	9.12	150	0.27
45	19.73	98	5.79	151	0.18
46	19.42	99	2.41	152	0.09
47	18.91	100	0.68	153	0.0
48	18.57	101	0.63	154	20.00
49	18.04	102	0.48	155	19.42
50	17.35	103	0.33	156	18.85
51	16.46	104	0.21	157	0.27
52	16.03	105	0.12	158	0.13
53	14.50	106	0.03	159	0.0

```
C*****************************************************************
C*****************************************************************
C
C                    PROGRAM NUMBER 1
C
C     PROGRAM TO CALCULATE THE STEADY - STATE TEMPERATURE
C      DISTRIBUTION IN WALL SECTION INCLUDING STEEL TIES
C                APPROIMATED AS 2-D PROBLEM
C
C*****************************************************************
C*****************************************************************
C
      DIMENSION A(159,159),AE(3,3),X(159),Y(159),NGE(271,3)
      DIMENSION XE(3),YE(3),ST(20),NS(20),T(159),R(159)
C
C     A - GLOBAL CONDUCTIVITY MATIX
C     AE - ELEMENT CONDUCTIVITY MATRIX
C     X - X COORDINATES OF NODES
C     Y - Y COORDINATES OF NODES
C     NGE - MATRIX RELATING ELEMENT NUMBERS TO NODE NUMBERS
C     R - LOAD MATRIX CUASED BY IMPOSED TEMPERATURE BC'S
C     XE - ELEMENT X COORDINATES
C     YX - ELEMENT Y COORDINATES
C     ST - SPECIFIED TEMPERATURE BOUNDARY CONDITIONS
C     NS - NODES WITH SPECIFIED BOUNDARY CONDITIONS
C     T - RESULTING TEMPERATURES AT NODES
C
C     CALCULATE COORDINATES OF NODES
C
      CALL NODE(X,Y)
C
C     DEVELOPE NGE MATRIX
C
      CALL PNGE(NGE)
C
C     INITIALIZE VECTORS AND MATRICES
C
      DO 10 I=1,159
      DO 10 J=1,159
   10 A(I,J)=0.0
C
      DO 20 I=1,271
C
C     DEVELOPE ELEMENT CONDUCTIVITY MATRIX
C
      DO 30 J=1,3
      XE(J)=X(NGE(I,J))
   30 YE(J)=Y(NGE(I,J))
      CALL COND(I,XK)
      CALL DEVY(I,XK)
      CALL TRISTF(AE,XE,YE,XK)
C
C     ASSEMBLE GLOBAL CONDUCTIVITY MATRIX
```

```
C
   20 CALL ASSMG(A,AE,3,1,3,159,NGE,1,271)
C
C      SET CONSTRAINTS (BOUNDARY CONDITIONS)
C
       DO 40 I=2,20,2
       ST(I-1)=20.0
   40  ST(I)=0.0
       DATA NS/1,23,24,43,44,65,66,85,86,107,108,126,127,136
      &,137,144,145,153,154,159/
C
C      APPLY BOUNDARY CONDITIONS
C
       CALL SETBC(ST,20,NS,A,R,159)
C
C      SOLVE SYSTEM OF EQATIONS
C
       CALL SOLIN(159,A,R,T)
       WRITE(6,100)(T(I),I=1,159)
  100  FORMAT(3X,F10.5)
       STOP
       END
C*********************************************************************
C*********************************************************************
       SUBROUTINE NODE(X,Y)
       DIMENSION  X(159),Y(159)
C
C      SUBROUTINE THAT GENERATES X AND Y COORIDINATE OF NODES
C
       A=0.5
       DO 1 I=1,4
     1 X(I)=(I-1)*A
       DO 2 I=5,8
     2 X(I)=1.75+(I-5)*A
       X(9)=3.5
       DO 3 I=10,14
     3 X(I)=3.75+(I-10)*A
       X(15)=6.0
       X(16)=6.25
       X(17)=6.75
       X(18)=7.25
       X(19)=7.5
       X(20)=7.75
       X(21)=8.25
       X(22)=8.75
       X(23)=9.0
       X(24)=0.0
       DO 4 I=25,28
     4 X(I)=0.25+(I-25)*A
       DO 5 I=29,43
     5 X(I)=2.0+(I-29)*A
       DO 6 I=44,47
     6 X(I)=(I-44)*A
```

```
      DO 7 I=48,51
    7 X(I)=1.75+(I-48)*A
      X(52)=3.5
      DO 8 I=53,57
    8 X(I)=3.75+(I-53)*A
      X(58)=6.0
      DO 9 I=59,64
    9 X(I)=6.25+(I-59)*A
      X(65)=9.0
      X(66)=0.0
      DO 10 I=67,70
   10 X(I)=0.25+(I-67)*A
      DO 11 I=71,85
   11 X(I)=2.0+(I-71)*A
      DO 12 I=86,89
   12 X(I)=(I-86)*A
      X(90)=1.75
      X(91)=2.25
      X(92)=2.75
      X(93)=3.25
      X(94)=3.5
      DO 13 I=95,99
   13 X(I)=3.75+(I-95)*A
      X(100)=6.0
      DO 14 I=101,106
   14 X(I)=6.25+(I-101)*A
      X(107)=9.0
      X(108)=0.0
      DO 15 I=109,113
   15 X(I)=0.25+(I-109)*A
      DO 16 I=114,126
   16 X(I)=3.0+(I-114)*A
      X(127)=0.0
      X(128)=0.75
      X(129)=1.75
      X(130)=3.5
      X(131)=4.5
      X(132)=5.5
      X(133)=6.0
      X(134)=7.0
      X(135)=8.0
      X(136)=9.0
      X(137)=0.0
      X(138)=3.5/3.0
      X(139)=7.0/3.0
      X(140)=3.5
      X(141)=3.5+2.5/2.0
      X(142)=6.0
      X(143)=7.5
      X(144)=9.0
      X(145)=0.0
      X(146)=3.5/3.0
      X(147)=7.0/3.0
```

```
      X(148)=3.5
      X(149)=4.75
      X(150)=6.0
      X(151)=7.0
      X(152)=8.0
      X(153)=9.0
      X(154)=0.0
      X(155)=3.5/2.0
      X(156)=3.5
      X(157)=6.0
      X(158)=7.5
      X(159)=9.0
      DO 17 I=1,159
      IF(I.GE.1.AND.I.LE.23)Y(I)=0.0
      IF(I.GE.24.AND.I.LE.43)Y(I)=0.0625
      IF(I.GE.44.AND.I.LE.65)Y(I)=0.125
      IF(I.GE.66.AND.I.LE.85)Y(I)=0.25
      IF(I.GE.86.AND.I.LE.107)Y(I)=0.5
      IF(I.GE.108.AND.I.LE.126)Y(I)=1.0
      IF(I.GE.127.AND.I.LE.136)Y(I)=2.0
      IF(I.GE.137.AND.I.LE.144)Y(I)=4.0
      IF(I.GE.145.AND.I.LE.153)Y(I)=6.0
      IF(I.GE.154)Y(I)=8.0
   17 CONTINUE
      RETURN
      END
C*****************************************************************
C*****************************************************************
      SUBROUTINE PNGE(NGE)
      DIMENSION NGE(271,3)
C
C     PROGRAM TO PRODUCE NGE MATRIX
C
C     NGE MATRIX RELATING THE ELEMENT NUMBERING TO THE NODE
C     NUMBERING
C
      NGE(1,1)=1
      NGE(1,3)=25
      CALL SP1(1,25,NGE,1)
      CALL EVEN(7,1,NGE)
      NGE(17,1)=9
      NGE(17,3)=32
      CALL SP2(9,32,NGE,17)
      CALL ODD(4,17,NGE)
      NGE(28,1)=15
      NGE(28,3)=37
      CALL SP2(15,37,NGE,28)
      CALL ODD(2,28,NGE)
      NGE(35,1)=19
      NGE(35,3)=40
      CALL SP2(19,40,NGE,35)
      CALL ODD(2,35,NGE)
      NGE(42,1)=24
```

```
      NGE(42,3)=44
      CALL SP2(24,44,NGE,42)
      CALL EVEN(7,42,NGE)
      NGE(58,1)=32
      NGE(58,3)=53
      CALL SP1(32,53,NGE,58)
      CALL ODD(4,58,NGE)
      NGE(69,1)=37
      NGE(69,3)=59
      CALL SP1(37,59,NGE,69)
      CALL ODD(5,69,NGE)
      NGE(82,1)=44
      NGE(82,3)=67
      CALL SP1(44,67,NGE,82)
      CALL EVEN(7,82,NGE)
      NGE(98,1)=52
      NGE(98,3)=74
      CALL SP2(52,74,NGE,98)
      CALL ODD(4,98,NGE)
      NGE(109,1)=58
      NGE(109,3)=79
      CALL SP2(58,79,NGE,109)
      CALL ODD(5,109,NGE)
      NGE(122,1)=66
      NGE(122,3)=86
      CALL SP2(66,86,NGE,122)
      CALL EVEN(7,122,NGE)
      NGE(138,1)=74
      NGE(138,3)=95
      CALL SP1(74,95,NGE,138)
      CALL ODD(4,138,NGE)
      NGE(149,1)=79
      NGE(149,3)=101
      CALL SP1(79,101,NGE,149)
      CALL ODD(5,149,NGE)
      NGE(162,1)=86
      NGE(162,3)=109
      CALL SP1(86,109,NGE,162)
      CALL EVEN(2,162,NGE)
      NGE(168,1)=89
      NGE(168,3)=111
      CALL SP2(89,111,NGE,168)
      NGE(170,1)=90
      NGE(170,3)=113
      CALL SP1(90,113,NGE,170)
      NGE(172,1)=91
      NGE(172,3)=113
      CALL SP2(91,113,NGE,172)
      CALL ODD(1,172,NGE)
      NGE(177,1)=94
      NGE(177,3)=115
      CALL SP2(94,115,NGE,177)
      CALL ODD(4,177,NGE)
```

```
      NGE(188,1)=100
      NGE(188,3)=120
      CALL SP2(100,120,NGE,188)
      CALL ODD(5,188,NGE)
      NGE(201,1)=108
      NGE(201,3)=128
      CALL SP1(108,128,NGE,201)
      DO 10 I=1,3
      NGE(202+I,1)=NGE(202,1)+I
      NGE(202+I,2)=NGE(202,2)+I
   10 NGE(202+I,3)=NGE(202,3)
      NGE(206,1)=112
      NGE(206,3)=129
      CALL SP1(112,129,NGE,206)
      NGE(208,1)=113
      NGE(208,3)=129
      CALL SP2(113,129,NGE,208)
      NGE(210,1)=114
      NGE(210,2)=115
      NGE(210,3)=130
      NGE(211,1)=115
      NGE(211,2)=116
      NGE(211,3)=130
      NGE(212,1)=116
      NGE(212,3)=130
      CALL SP2(116,130,NGE,212)
      NGE(214,1)=117
      NGE(214,2)=118
      NGE(214,3)=131
      NGE(215,1)=118
      NGE(215,3)=131
      CALL SP2(118,131,NGE,215)
      CALL ODD(1,215,NGE)
      NGE(220,1)=121
      NGE(220,3)=133
      CALL SP2(121,133,NGE,220)
      NGE(222,1)=122
      NGE(222,2)=123
      NGE(222,3)=134
      NGE(223,1)=123
      NGE(223,3)=134
      CALL SP2(123,134,NGE,223)
      NGE(225,1)=124
      NGE(225,2)=125
      NGE(225,3)=135
      NGE(226,1)=125
      NGE(226,3)=135
      CALL SP2(125,135,NGE,226)
      NGE(228,1)=127
      NGE(228,3)=137
      CALL SP2(127,137,NGE,228)
      CALL ODD(4,228,NGE)
      NGE(239,1)=133
```

```
      NGE(239,3)=142
      CALL SP2(133,142,NGE,239)
      CALL ODD(1,239,NGE)
      NGE(244,1)=137
      NGE(244,3)=146
      CALL SP1(137,146,NGE,244)
      CALL EVEN(2,244,NGE)
      NGE(250,1)=140
      NGE(250,3)=148
      CALL SP2(140,148,NGE,250)
      NGE(252,1)=141
      NGE(252,3)=149
      CALL SP2(141,149,NGE,252)
      NGE(254,1)=142
      NGE(254,3)=151
      CALL SP1(142,151,NGE,254)
      CALL ODD(1,254,NGE)
      NGE(259,1)=145
      NGE(259,3)=154
      CALL SP2(145,154,NGE,259)
      CALL ODD(1,259,NGE)
      NGE(264,1)=148
      NGE(264,3)=156
      CALL SP2(148,156,NGE,264)
      NGE(266,1)=149
      NGE(266,2)=150
      NGE(266,3)=157
      NGE(267,1)=150
      NGE(267,3)=157
      CALL SP2(150,157,NGE,267)
      CALL ODD(1,267,NGE)
      RETURN
      END
C*********************************************************************
C*********************************************************************
      SUBROUTINE COND(NEL,XK)
C
C     SUBROUTINE TO PROVIDE THE PROPER CONDUCTIVITY OF
C     MATERIAL TO EACH ELEMENT
C
C     NEL - ELEMENT NUMBER
C     XK - CONDUCTIVITY (WATTS/METER*DEG.CEL)
C
C     XK1 - CONCRETE BLOCK =.37
C     XK2 - STEEL =45.0
C     XK3 - FACING BRICK = 1.316
C     XK4 - INSULATION = 0.01586
C
      XK1=0.37
      XK2=45.0
      XK3=1.316
      XK4=0.01586
      IF(NEL.LE.8) GO TO 10
```

```
      IF(NEL.LE.34) GO TO 20
      IF(NEL.LE.41) GO TO 30
      IF(NEL.LE.57) GO TO 10
      IF(NEL.LE.68) GO TO 40
      IF(NEL.LE.81) GO TO 30
      IF(NEL.LE.97) GO TO 10
      IF(NEL.LE.108) GO TO 40
      IF(NEL.LE.121) GO TO 30
      IF(NEL.LE.137) GO TO 10
      IF(NEL.LE.148) GO TO 40
      IF(NEL.LE.161) GO TO 30
      IF(NEL.LE.176) GO TO 10
      IF(NEL.LE.187) GO TO 40
      IF(NEL.LE.200) GO TO 30
      IF(NEL.LE.210) GO TO 10
      IF(NEL.LE.218) GO TO 40
      IF(NEL.LE.227) GO TO 30
      IF(NEL.LE.233) GO TO 10
      IF(NEL.LE.238) GO TO 40
      IF(NEL.LE.243) GO TO 30
      IF(NEL.LE.249) GO TO 10
      IF(NEL.LE.253) GO TO 40
      IF(NEL.LE.258) GO TO 30
      IF(NEL.LE.263) GO TO 10
      IF(NEL.LE.266) GO TO 40
      IF(NEL.LE.271) GO TO 30
   10 XK=XK1
      GO TO 999
   20 XK=XK2
      GO TO 999
   30 XK=XK3
      GO TO 999
   40 XK=XK4
  999 RETURN
      END
C*********************************************************************
C*********************************************************************
      SUBROUTINE DEVY(I,XK)
C
C     SUBROUTINE TO MODIFY CONDUCTIVITY OF MATRIALS
C     FOR CYLINDERICAL COORDINATES
C
C     MODIFICATION INCREASES THE CONDUCTIVITY AS
C     A FUNCTION OF THE DISTANCE FROM THE ROD.
C
C     XK - CONDUCTIVITY
C     I - ELEMENT NUMBER
C
      IF(I.LE.41) XK=XK*0.03125
      IF(I.GT.41.AND.I.LE.81) XK=XK*0.09375
      IF(I.GT.81.AND.I.LE.121) XK=XK*0.1875
      IF(I.GT.121.AND.I.LE.161) XK=XK*0.375
      IF(I.GT.161.AND.I.LE.200) XK=XK*0.75
```

```
      IF(I.GT.200.AND.I.LE.227) XK=XK*1.5
      IF(I.GT.227.AND.I.LE.243) XK=XK*3.0
      IF(I.GT.243.AND.I.LE.258) XK=XK*5.0
      IF(I.GT.258) XK=XK*7.0
      RETURN
      END
C*****************************************************************
C*****************************************************************
      SUBROUTINE TRISTF(AE,XE,YE,P)
      DIMENSION AE(3,3),XE(3),YE(3),T(3,3),TINV(3,3)
      DIMENSION CX(3,3),C(3,3),TINVT(3,3)
C
C     SUBROUTINE FORMS THE ELEMENT STIFFNESS MATRIX FOR A
C     TRIANGULAR ELEMENT
C
C     AE - ELEMENT MATRIX
C     XE - X - COORDINATES
C     YE - Y - COORDINATES
C
C     EQUATION OF THE FORM AE=AREA*(TINVT)*(C)*(TINV)
C

C     T - TRANSFORMATION MATRIX
C     TINV - INVERSE OF T
C     TINVT - TRANSPOSE OF TINV
C
      DO 1 I=1,3
      DO 1 J=1,3
    1 CX(I,J)=0.0
      CX(2,2)=1.0
      CX(3,3)=1.0
      DO 10 I=1,3
      T(I,1)=1.0
      T(I,2)=XE(I)
      T(I,3)=YE(I)
   10 CONTINUE
      CALL INVERS(T,TINV)
      CALL TRANPO(TINV,TINVT,3)
      CALL COORDT(TINV,TINVT,CX,AE,C,3)
      CALL TRIAR(XE,YE,XA)
      DO 20 I=1,3
      DO 20 J=1,3
   20 AE(I,J)=P*XA*AE(I,J)
      RETURN
      END
C*****************************************************************
C*****************************************************************
      SUBROUTINE ASSMG(A,AE,NCORN,NUN,IEX,IOX,NGE,K,NEL)
      REAL A(IOX,IOX),AE(IEX,IEX)
      INTEGER NGE(NEL,NCORN)
C
C     GENERAL SUBROUTINE TO ASSEMBLE ELEMENT MATRIX INTO
C     GLOBAL MATRIX
```

```
C
C     A - GLOBAL MATRIX
C     AE - ELEMENT MATRIX
C     NCORN - NUMBER OF NODES PER ELEMENT
C     NUN - NUMBER OF UNKNOWNS PER.NODE
C     IEX - NUMBER OF ELEMENT DEGREES OF FREEDOM
C     IOX - NUMBER OF GLOBAL DEGREES OF FREEDOM
C     NGE - NODE NUMBERS OF ELEMENTS TO BE ASSEMBLED
C     K - ELEMENT NUMBER
C     NEL - TOTAL NUMBER OF ELEMENTS
C
      DO 10 NR=1,NCORN
      DO 10 NC=1,NCORN
      DO 10 J=1,NUN
      DO 10 I=1,NUN
      A(I+NUN*(NGE(K,NR)-1),J+NUN*(NGE(K,NC)-1))=
     1A(I+NUN*(NGE(K,NR)-1),J+NUN*(NGE(K,NC)-1))+
     2AE(I+NUN*(NR-1),J+NUN*(NC-1))
   10 CONTINUE
      RETURN
      END
C*************************************************************
C*************************************************************
      SUBROUTINE SETBC(ST,NNS,NS,A,R,NGDF)
      DIMENSION A(NGDF,NGDF),R(NGDF),ST(NNS),NS(NNS)
C
C     SUBROUTINE TO APPLY TEMPERATURE SPECIFIED BOUNDARY
C     CONDITIONS TO TWO DIMENSIONAL STEADY STATE PROBLEM
C
C     FORM OF EQUATION BEFORE APPLYING BC'S      A*T=0
C
C     FORM OF EQUATION AFTER APPLYING BC'S       A*T=R
C
C     A - CONDUCTIVITY MATRIX
C     ST - VECTOR CONTAINIG SPECIFIED NODAL TEMPERATURE
C     NS - VECTOR CONTAINING NODE NUMBERS WITH SPECIFIED
C          TEMPERATURES
C     NNS - NUMBER OF NODES WITH SPECIFIED TEMPERATURES
C     R - LOAD VECTOR CREATED BY SPECIFYING TEMPERATURES
C
      DO 1 I=1,NGDF
    1 R(I)=0.0
      DO 10 I=1,NNS
      A(NS(I),NS(I))=1.0
      DO 20 J=1,NGDF
   20 R(J)=R(J)-A(J,NS(I))*ST(I)
      DO 10 L=1,NGDF
      IF(L.EQ.NS(I)) GO TO 10
      A(L,NS(I))=0.0
      A(NS(I),L)=0.0
   10 CONTINUE
      DO 30 I=1,NNS
   30 R(NS(I))=ST(I)
```

```
      RETURN
      END
C*****************************************************************
C*****************************************************************
      SUBROUTINE SOLIN(N,A,F,X)
      DIMENSION A(N,N),F(N),X(N)
C     A - INPUT MATRIX
C     F - INPUT VECTOR
C     X - OUTPUT VECTOR
C     THIS SUBROUTINE SOLVES FOR X BY GAUSS-ELIMINATION FOR
C     THE MATRIX EQUATION OF THE FORM A*X=F
C
      DO 10 J=1,N
      B=A(J,J)
      DO 20 I=J,N
      A(J,I)=A(J,I)/B
   20 CONTINUE
      F(J)=F(J)/B
      IF(N-J.EQ.0) GO TO 50
      K=N-J
      DO 30 II=1,K
      B=A(J+II,J)
      DO 40 I=J,N
      A(J+II,I)=B*A(J,I)-A(J+II,I)
   40 CONTINUE
      F(J+II)=B*F(J)-F(J+II)
   30 CONTINUE
   10 CONTINUE
C
C     BACK SUBSTITUTE TO FIND X
C
   50 X(N)=F(N)
      KK=N-1
      DO 60 J=1,KK
      B=0.0
      DO 70 I=1,J
      B=B+A(N-J,N-I+1)*X(N-I+1)
   70 CONTINUE
      X(N-J)=F(N-J)-B
   60 CONTINUE
      RETURN
      END
C*****************************************************************
C*****************************************************************
      SUBROUTINE SP1(K,M,NGE,NN)
      DIMENSION NGE(271,3)
C
C     K=NGE(NN,1)
C     M=NGE(NN,3)
C
      NGE(NN,2)=M-1
      NGE(NN+1,1)=K
      NGE(NN+1,2)=K+1
```

```
      NGE(NN+1,3)=M
      RETURN
      END
C*****************************************************************
C*****************************************************************
      SUBROUTINE EVEN(N,L,NGE)
      DIMENSION NGE(271,3)
C
C     N- NUMBER OF ELEMENT IN PATTERN
C     L - ELEMENT NUMBER THAT STARTS PATTERN
C
      DO 10 I=1,N
      DO 10 J=1,3
      NGE(I*2+L,J)=NGE(L,J)+I
   10 NGE(I*2+L+1,J)=NGE(L+1,J)+I
      RETURN
      END
C*****************************************************************
C*****************************************************************
      SUBROUTINE SP2(K,M,NGE,NN)
      DIMENSION NGE(271,3)
C
C     K,M,NN - SEE SP1
C
      NGE(NN,2)=K+1
      NGE(NN+1,1)=K+1
      NGE(NN+1,2)=M
      NGE(NN+1,3)=M+1
      RETURN
      END
C*****************************************************************
C*****************************************************************
      SUBROUTINE ODD(N,L,NGE)
      DIMENSION NGE(271,3)
C
C     N , L - SEE SUBROUTINE EVEN
C
      DO 10 I=1,N
      DO 10 J=1,3
      NGE(I*2+L,J)=NGE(L,J)+I
   10 NGE(I*2+L+1,J)=NGE(L+1,J)+I
      DO 20 J=1,3
   20 NGE(I*2+L+2,J)=NGE(L,J)+I+1
      RETURN
      END
C*****************************************************************
C*****************************************************************
      SUBROUTINE INVERS(T,TINV)
      DIMENSION T(3,3),TINV(3,3)
C
C     SUBROUTINE TO CALCULATE THE INVERSE OF A 3X3 MATRIX
C
C     T - MATRIX
```

```
C     TINV - INVERSE OF T
C
      CALL DET(T,DETT)
      TINV(1,1)=T(2,2)*T(3,3)-T(3,2)*T(2,3)
      TINV(2,1)=T(3,1)*T(2,3)-T(2,1)*T(3,3)
      TINV(3,1)=T(2,1)*T(3,2)-T(3,1)*T(2,2)
      TINV(1,2)=T(3,2)*T(1,3)-T(1,2)*T(3,3)
      TINV(2,2)=T(1,1)*T(3,3)-T(3,1)*T(1,3)
      TINV(3,2)=T(3,1)*T(1,2)-T(1,1)*T(3,2)
      TINV(1,3)=T(1,2)*T(2,3)-T(2,2)*T(1,3)
      TINV(2,3)=T(2,1)*T(1,3)-T(1,1)*T(2,3)
      TINV(3,3)=T(1,1)*T(2,2)-T(2,1)*T(1,2)
      DO 10 I=1,3
      DO 10 J=1,3
      TINV(I,J)=TINV(I,J)/DETT
   10 CONTINUE
      RETURN
      END
C*****************************************************************
C*****************************************************************
      SUBROUTINE TRANPO(D,DT,M)
      DIMENSION D(M,M),DT(M,M)
C
C     SUBROUTINE TO TRANSPOSE SQUARE MATRIX
C     DT - TRANSPOSE OF D
C
      DO 1 I=1,M
      DO 1 J=1,M
    1 DT(J,I)=D(I,J)
      RETURN
      END
C*****************************************************************
C*****************************************************************
      SUBROUTINE COORDT(XLAM,XLAMT,AE,AET,C,N)
      DIMENSION XLAM(N,N),XLAMT(N,N),AE(N,N),AET(N,N),C(N,N)
C
C     SUBROUTINE TO PERFORM THE COORDINATE TRANSFORMATION
C     OF THE FORM AET=XLAMT*AE*XLAM
C
C     XLAM - LAMDA MATRIX
C     XLAMT - LAMDA TRANSPOSE
C     AE - ELEMENT STIFFNESS MATRIX
C     AET - ELEMENT STIFFNESS MATRIX IN GLOBAL COORDINATES
C
      DO 1 I=1,N
      DO 1 J=1,N
    1 C(I,J)=0.0
      CALL MATMUL(AE,XLAM,C,N,N,N)
      CALL MATMUL(XLAMT,C,AET,N,N,N)
      RETURN
      END
C*****************************************************************
C*****************************************************************
```

```
      SUBROUTINE TRIAR(X,Y,XA)
      DIMENSION X(3),Y(3)
C
C     SUBROUTINE CALCULATES AREA OF A TRIANGLE FROM ITS S
C     VERTICES
C
C     X(I) - X COORDINATES
C     Y(I) - Y COORDINATES
C
      A=X(2)*Y(3)-X(3)*Y(2)
      B=X(1)*Y(3)-X(3)*Y(1)
      C=X(1)*Y(2)-X(2)*Y(1)
      XA=ABS(0.5*(A-B+C))
      RETURN
      END
C*********************************************************************
C*********************************************************************
      SUBROUTINE DET(A,DETA)
      DIMENSION A(3,3)
C
C     SUBROUTINE  TO CALCULATE THE DETERMINATE OF A 3X3
C     MATRIX
C
C     A - MATRIX
C     DETA - DETERMINATE OF MATRIX A
C
      DETA=A(1,1)*A(2,2)*A(3,3)+A(1,2)*A(2,3)*A(3,1)+A(1,3)
     &*A(3,2)*A(2,1)-A(1,3)*A(2,2)*A(3,1)-A(2,3)*A(3,2)*A(1
     &,1)-A(3,3)*A(2,1)*A(1,2)
      RETURN
      END
C*********************************************************************
C*********************************************************************
```

APPENDIX E

Steady Periodic Heat Conduction through a Composite Slab

The general solution to steady periodic heat transfer through a composite slab is presented in Carslaw and Jaeger (13). The solution relates the temperature and heat flux at one surface to the temperature and heat flux at the other surface by a matrix equation. This matrix equation is of the form (omitting a time factor):

$$\begin{bmatrix} T \\ q \end{bmatrix}_{x=L} = \begin{bmatrix} A & B \\ C & D \end{bmatrix} \begin{bmatrix} T \\ q \end{bmatrix}_{x=0}$$

where: T - temperature
q - heat flux
A,B,C,D - complex quantities that are calculated from material properties and the angular frequency of the heat transfer.

By specifying any two of T(x=L), Q(x=L), T(x=0), or Q(x=0) boundary conditions, the remaining two can be calculated.

For the problem of steady heat transfer through a wall section the boundary conditions are shown in Figure E.1. In terms of Carslaw and Jaeger's solution these boundary conditions are (omitting the time factor): T(x=L) = T, and T(x=0) = 0. The heat flux at either surface can then be calculated. A computer program that solves this problem is

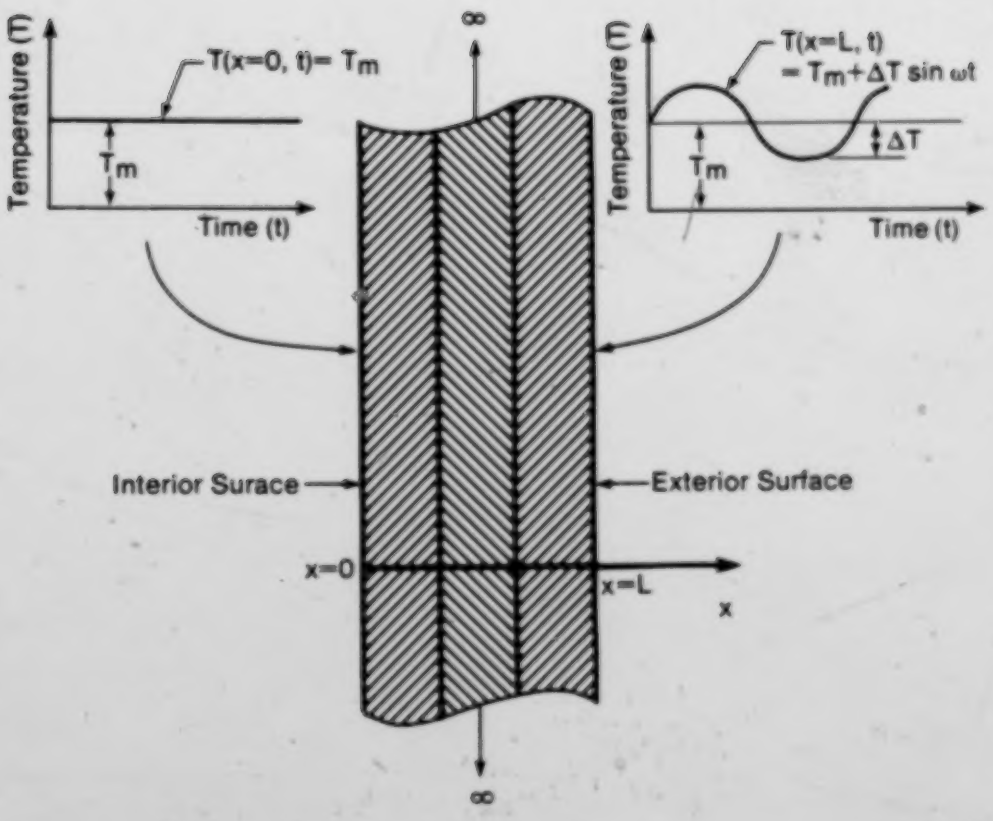

Figure E.1 Steady Periodic Heat Conduction in a Composite Slab

presented at the end of this appendix.

Example Problem

Calculate the amplitude and time lag of the heat flux at the interior surface of the masonry module walls when

Interior Temperature = 20°C
Ambient Temperature = 10sin(wt)
w = 7.272×10^{-5} 1/s (period of one day)

surface resistances ($m^2 \cdot °C/W$)
interior - 0.120
exterior - 0.030

layer	thermal diffusivity (m^2/s)	thickness (mm)	conductivity ($W/m \cdot °C$)
wallboard	1.837×10^{-7}	12.7	0.1602
air gap*	6.0×10^{-5}	25.4	0.0721
concrete block	2.3×10^{-7}	88.9	0.3643
polyurethane	2.5×10^{-7}	63.5	0.0159
facing brick	7.9×10^{-7}	76.2	1.3100

* Air gap is not solely a conduction element, but also transfers heat by convection and radiation. Therefore, it was necessary to approximate some effective properties for the air gap.

a) The long term measured resistance of the air gap is 0.416 $m^2 \cdot °C/W$ (from Section 2.2.2). Dividing the thickness of the air gap by the measured resistance gives an effective conductivity of 0.0721 $W/m \cdot °C$.

b) Calculate the thermal diffusivity of the air gap using the effective conductivity of the air gap, and

the density and specific heat of air. The effective thermal diffusivity of the air gap is approximately 6.0×10^{-5} m^2/s.

Solution

Solve by superposition of two problems

1) Steady state heat transfer across the wall with the exterior temperature equal to 0°C, and the interior temperature equal to 20°C.
2) Steady periodic heat transfer across the wall with the interior temperature equal to 0°C, and the exterior temperature equal to 10sin(wt).

1) Steady State Solution, q_{ss}

Total resistance of wall (R) = 4.88 $m^2.°C/W$

$q_{ss} = T/R = 20/4.88 = 4.1$ W/m^2

2) Steady Periodic Heat Transfer, q_{sp} - from computer program

$q_{sp} = 0.31\sin(wt-2.438)$

Therefore, the total heat transfer, q_T, at the wall's interior surface is

$q_T = q_{ss} + q_{sp}$

$q_T = 4.1 + 0.31\sin(wt-2.438)$

Amplitude of the interior heat flux = 0.31 W/m^2

Time lag of the interior heat flux = 9.9 hours

If the "potential" periodic heat transfer was calculated, considering the problem to be quasi-steady state, amplitude of the heat flux would be 2.05 W/m^2. Therefore, the attenuation of the heat flux is 0.15.

```
C*****************************************************************
C*                                                               *
C*                     PROGRAM NUMBER 2                          *
C*                                                               *
C*    LINEAR FLOW OF HEAT IN A SOLID BOUNDED BY TWO PARALLEL     *
C*      PLANES - STEADY PERIODIC TEMPERATURES IN COMPOSITE       *
C*                          SLABS                                *
C*                                                               *
C*****************************************************************
C
C
C     PROGRAM SIMULATES COMPOSITE WALL SECTION OF A BIULDING
C     SUBJECT TO THE FOLLOWING BOUNDARY CONDITIONS:
C           1) INTERIOR ROOM TEMPERATURE IS HELD CONSTANT
C           2) EXTERIOR TEMPERATURE VARIES AS A SINUSOID AND
C              WHOSE MEAN VALUE EQUAL TO THE ROOM TEMPERATURE
C
C     PROGRAM CALCULATES THE AMPLITUDE AND PHASE LAG OF THE
C     INTERIOR HEAT FLUX WITH RESPECT TO THE EXTERIOR TEMP.
C
C     INPUTS REQUIRED ARE:
C        1) AMPLITUDE OF EXTERIOR TEMPERATURE
C        2) PERIODIC FREQUENCY OF THE EXTERIOR TEMPERATURE
C        3) MATERIAL PROPERTIES OF EACH LAYER OF THE SLAB
C                 - THERMAL DIFFUSIVITY
C                 - THICKNESS
C                 - THERMAL CONDUCTIVITY
C        4) SURFACE HEAT TRANSFER COEFFICENTS AND CONTACT
C           RESISTANCES BETWEEN LAYERS
C
C
C
C     DEFINITIONS AND UNITS
C
C     INPUTS: AL=THERMAL DIFFUSIVITY (M**2/S)
C             XL=LAYER THICHNESS (M)
C             XK=THERMAL CONDUCTIVY (W/MC)
C             T=TEMPERATURE AMPLITUDE (C)
C             W=PERIODIC FREQUNCY (RADS/S)
C             N=NUMBER OF LAYERS, UP TO 5
C             R=CONTACT OR CONVECTIVE RESISTANCES (M**2C/W)
C             RO=INTERIOR SURFACE HEAT TRANSFER COEFF.
C             R(1)-R(N-1)=CONTACT RESISTANCES
C             R(N)=EXTERIOR SURFACE HEAT TRANSFER COEFF.
C
C     OUTPUT: Q=HEAT FLUX AMPLITUDE (W/M**2)
C             PL=TIME LAG (HOURS/DAYS/MONTHS)
C
```

```
C*****************************************************************
C*                                                               *
C*                    FORMAT OF INPUT FILE                       *
C*       FREE FORMAT DATA - DATA SEPARATED BY BLANKS             *
C*                                                               *
C*    ROW 1 :                                                    *
C*      NUMBER OF LAYERS , PERIODIC FREQUENCY OF HEAT            *
C*      FLUX, AMPLITUDE OF TEMPERATURE                           *
C*                                                               *
C*    ROWS 2 THRU 6 (IF NECESSARY)                               *
C*          - LAYER MATERIAL PROPERTIES ; START WITH             *
C*            INTERIOR MOST LAYER AND WORK TO EXTERIOR           *
C*            MOST LAYER                                         *
C*      THERMAL DIFFUSIVITY , THICKNESS , CONDUCTIVITY           *
C*         "          "           "          "                  *
C*         "          "           "          "                  *
C*                                                               *
C*    LAST ROW :                                                 *
C*      INTERIOR HEAT TRANSFER COEFFICENT , CONTACT              *
C*      RESISTANCES IN ORDER OF INTERIOR TO EXTERIOR ,           *
C*      EXTERIOR HEAT TRANSFER COEFFICENT                        *
C*                                                               *
C*****************************************************************
C
      LOGICAL*1 FREE(1)/'*'/
      DIMENSION AL(5),XL(5),XK(5),R(5),CX(5),CL(5)
C
C     READ NUMBER OF LAYERS, FREQUENCY AND AMPLITUDE
C     OF TEMPERATURE
C
      READ(11,FREE) N,W,T
      COMPLEX A(5),B(5),C(5),D(5),XM(2,2),XXM(2,2),G,CMPLX
C
C     READ MATERIAL PROPERTIES
C
      DO 50 I=1,N
      READ(11,FREE) AL(I),XL(I),XK(I)
   50 CONTINUE
C
C     CALCULATE MATRIX ELEMENTS FOR EACH WALL LAYER
C
      DO 10 I=1,N
      CX(I)=SQRT(W/(2.0*AL(I)))
      CL(I)=CX(I)*XL(I)
      A(I)=CMPLX(COSH(CL(I))*COS(CL(I)),SINH(CL(I))*SIN(CL(I
     &)))
      TT=-1.0/(2.0*XK(I)*CX(I))
      Y=TT*(SINH(CL(I))*COS(CL(I))+COSH(CL(I))*SIN(CL(I)))
      Z=TT*(COSH(CL(I))*SIN(CL(I))-SINH(CL(I))*COS(CL(I)))
      B(I)=CMPLX(Y,Z)
      AA=-1.0*XK(I)*CX(I)
      U=AA*(SINH(CL(I))*COS(CL(I))-COSH(CL(I))*SIN(CL(I)))
      V=AA*(SINH(CL(I))*COS(CL(I))+COSH(CL(I))*SIN(CL(I)))
```

```
      C(I)=CMPLX(U,V)
      D(I)=A(I)
   10 CONTINUE
C
C     READ CONVECTIVE AND CONTACT RESISTANCES
C
      READ(11,FREE)R0,R(1),R(2),R(3),R(4),R(5)
C
C     ECHO INPUT DATA
C
      WRITE(6,101)
  101 FORMAT(10X,'Number of Layers     Angular Frequency (ra
     &ds/sec)        Temperature Amplitude',/)
      WRITE(6,102) N,W,T
  102 FORMAT(18X,I1,22X,E8.3,25X,F4.1,///)
      WRITE(6,103)
  103 FORMAT(30X,'Layer Data',//)
      WRITE(6,104)
  104 FORMAT(10X,'Diffusivity     Thickness     Conductivity
     &',/)
      DO 70 I=1,N
      WRITE(6,105) AL(I),XL(I),XK(I)
   70 CONTINUE
  105 FORMAT(12X,E8.3,8X,F6.4,8X,F6.4)
      WRITE(6,106) R0,R(N)
  106 FORMAT(///,10X,'Surface Heat Transfer Coeff.- Interior
     &=',F6.3,'        Outside=',F6.3,//)
      IF (N.EQ.1) GO TO 33
      WRITE(6,107)
  107 FORMAT(10X,'Contact Resistances - inside to outside',/)
      NN=N-1
      DO 80 I=1,NN
      WRITE(6,108) R(I)
   80 CONTINUE
  108 FORMAT(16X,F6.3)
   33 CONTINUE
C
C     CALCULATE THE TRANSFER MATRIX ACROSS ALL LAYERS
C
      XM(1,1)=CMPLX(1.0,0.0)
      XM(1,2)=CMPLX((-1.0)*R0,0.0)
      XM(2,1)=CMPLX(0.0,0.0)
      XM(2,2)=XM(1,1)
      DO 20 I=1,N
      XXM(1,1)=XM(1,1)*A(I)+XM(2,1)*B(I)
      XXM(1,2)=XM(1,2)*A(I)+XM(2,2)*B(I)
      XXM(2,1)=XM(1,1)*C(I)+XM(2,1)*D(I)
      XXM(2,2)=XM(1,2)*C(I)+XM(2,2)*D(I)
      XM(1,1)=XXM(1,1)-R(I)*XXM(2,1)
      XM(1,2)=XXM(1,2)-R(I)*XXM(2,2)
      XM(2,1)=XXM(2,1)
   20 XM(2,2)=XXM(2,2)
```

```
C
C     CALCULATE INTERIOR HEAT FLUX (NOT INCLUDING
C     TIME FACTOR)
C
C     BY DEFINITION HEAT FLUX IS GIVEN BY q=-K*dt/dx. THAT
C     IS,HEAT FLOW IS IN THE DIRECTION OPPOSITE TO THE SLOPE
C     OF THE TEMPERATURE GRADIENT. THEREFORE TO ACCOUNT FOR
C     THIS APPARENT 180 DEGREES PHASE SHIFT THE HEAT FLUX
C     MUST BE MULTPLIED BY NEGATIVE ONE.
C
      G=(-1.0)*T/XM(1,2)
C
C     MULTIPLY BY TIME FACTOR AND CALCULATE REAL
      AND IMAGINARY PARTS
C
      H=REAL(G)
      P=AIMAG(G)
C
C     CALCULATE AMPLITUDE OF HEAT FLUX
C
      Q=SQRT(H**2+P**2)
C
C     CALCULATE PHASE LAG OF HEAT FLUX
C
      PL=ACOS(H/Q)
      IF(P.GT.0.) GO TO 12
      PL=PL*(-1.0)
   12 CONTINUE
C
C     WRITE OUTPUT
C
      PRINT 109,Q
  109 FORMAT('////,10X,'AMPLITUDE OF INTERIOR HEAT FLUX =
     &',F10.4,' WATTS/ SQ. METER')
      PL=PL/W/3600.
      PRINT 110
  110 FORMAT(///,10X,'TIME LAG (if negative) OF INTERIOR HEA
     &T FLUX BEHIND THE EXTERIOR TEMPERATURE FLUCTUATION')
      PRINT 111,PL
  111 FORMAT(/,30X,F8.4,' hours')
      PL=PL/24.
      PRINT 112,PL
  112 FORMAT(30X,F7.4,' days')
      PL=PL/30.
      PRINT 113,PL
  113 FORMAT(30X,F7.4,' months')
      STOP
      END
```